



CLASS VI PERMIT

APPLICATION NARRATIVE

40 CFR 146.82(a)

SHELL U.S. POWER AND GAS
ST. HELENA PARISH SITE

Prepared By:
GEOSTOCK SANDIA, LLC

Revision No. 0
November 2022

TABLE OF CONTENTS

1.0	Project Background and Facility Information.....	13
1.1	Facility Information.....	13
1.2	Project Goals	13
1.2.1	Stratigraphic Test Wells.....	17
1.2.2	CO ₂ Stream	18
1.2.3	Injection and Confining Zones.....	18
1.2.4	Injection Wells and Capacity	19
1.2.5	Monitoring Program.....	20
1.2.6	Project CO ₂ Details	20
2.0	Site Characterization.....	22
2.1	Regional Geology.....	22
2.1.1	Regional Maps and Cross Sections.....	26
2.1.2	Regional Stratigraphy	26
2.1.3	Regional Structural Geology.....	45
2.1.4	Regional Groundwater Flow in the Injection Zones	47
2.2	Local Geology of the Shell St. Helena Parish Site.....	48
2.2.1	Data Sets Used for Site Evaluation.....	49
2.2.2	Local Stratigraphy.....	51
2.2.3	Local Structure and Faulting.....	55
2.3	Description of the Confining and Injection Zones	57
2.3.1	Confining Zones.....	58
2.3.2	Injection Zones.....	60
2.4	Geomechanics and Petrophysics	65

2.4.1	Ductility	66
2.4.2	Stresses and Rock Mechanics	71
2.4.3	Pore Pressures of the Injection Zone	74
2.4.4	Calculated Fracture Gradient	77
2.5	Seismicity	79
2.5.1	Regional Seismic Activity	82
2.5.2	Seismic Risk of the Project Site.....	83
2.5.3	Induced Seismicity Analysis at the Project Site	85
2.5.4	Seismic Risk Models for the Project Site	86
2.6	Hydrogeology.....	92
2.6.1	Regional Hydrogeology	93
2.6.2	Local Hydrogeology	98
2.6.3	Determination of the Base of the Lowermost USDW	98
2.6.4	Base of the Lowermost USDW.....	99
2.6.5	Water Well Data Sets.....	100
2.6.6	Local Water Usage.....	101
2.6.7	Injection Depth Waiver.....	102
2.7	Geochemistry	102
2.7.1	Formation Brine Properties.....	103
2.7.2	Compatibility of the CO ₂ with Subsurface Fluids and Minerals	106
2.7.3	Site Specific Geochemical Modeling.....	112
2.8	Site Suitability Summary	114
3.0	AoR and Corrective Action Plan	117
4.0	Financial Responsibility.....	118
5.0	Injection Well Construction	119

5.1	Proposed Stimulation Program [40 cfr 146.82(a)(9)]	119
5.2.1	Casing String Details	120
5.2.2	Centralizers	121
5.2.3	Annular Fluid.....	121
5.2.4	Cementing Details.....	122
5.2.5	Tubing and Packer Details	122
5.3	Proposed Drilling Program	123
5.3.1	Soterra IF 1-1 Injection Well	123
5.3.2	Soterra IT 2-1 Injection Well.....	131
5.3.3	Wellhead Schematics	139
6.0	Pre-Operational Logging and Testing.....	140
7.0	Well Operation.....	141
8.0	Testing and Monitoring.....	142
9.0	Injection Well Plugging	144
10.0	Post injection Site Care (PISC) and Site Closure	145
11.0	Emergency and Remedial Response	146
12.0	Injection Depth Waiver and Aquifer Exemption Expansion	147
13.0	Optional Additional Project Information	148
14.0	Other Relevant Information	149
	REFERENCES	150

LIST OF TABLES

Section 2.0 – Site Characterization

Table 2-1 Listing of Local Geologic Maps in Appendix A

Table 2-2 Minimum Effective Shale Porosity in Gulf Coast Environments (Table 2, *in Porter and Newsom, 1987*)

Table 2-3 Tabulation of Geomechanical Rock Properties - St Helena Parish Site

Table 2-4 Tabulation of data used in Formation Pressure Analysis

Table 2-5 Five Point Prediction

Table 2-6 Fracture Gradient and Operating Pressures – St Helena Parish Site

Table 2-7 Tabulation of Seismic Events in and around Louisiana since 1900 (*search performed in November 2022*)

Table 2-8 Critical Pressure to Induce Seismicity

Table 2-9 Water Well Tabulation and Data

Table 2-10 Aquifer Uses in Parish and Yields (from White and Prakken, 2016)

Table 2-11 Salinity Values from the Schlumberger Gen-9 Interpretation Nomograph.

Table 2-12 Initial Geochemical Modeling Reactions for Injection Zones

Section 4.0 – Financial Demonstration

Table 4-1 Cost Estimates

Section 5.0 – Injection Well Construction

Table 5-1 Casing String Details - Soterra IF 1-1 (Frio Injector)

Table 5-2 Casing String Details - Soterra IT 2-1 (Tuscaloosa Injector)

Table 5-3 Cementing Details

Table 5-4 Tubing and Packer Details- Soterra IF 1-1 (Frio Injector)

Table 5-5 Tubing and Packer Details - Soterra IT 2-1 (Tuscaloosa Injector)

Table 5-6 Proposed Well Fluids - Soterra IF 1-1 (Frio Injector)

Table 5-7 Surface Casing Cement Program - Soterra IF 1-1 (Frio Injector)

Table 5-8 Intermediate Casing Cement Program - Soterra IF 1-1 (Frio Injector)

Table 5-9 Injection Casing Cement Program - Soterra IF 1-1 (Frio Injector)

Table 5-10 Proposed Well Fluids - Soterra IT 2-1 (Tuscaloosa Injector)

Table 5-11 Surface Casing Cement Program - Soterra IT 2-1 (Tuscaloosa Injector)

Table 5-12 Intermediate Casing Cement Program - Soterra IT 2-1 (Tuscaloosa Injector)

Table 5-13 Injection Casing Cement Program - Soterra IT 2-1 (Tuscaloosa Injector)

Section 7.0 – Well Operation

Table 7-1 Proposed Operational Procedures – Soterra IF 1-1 Injection Well

Table 7-2 Proposed Operational Procedures – Soterra IT 2-1 Injection Well

LIST OF FIGURES

Section 1.0 – Facility Information

Figure 1-1 Project location – St. Helena Parish, Louisiana

Section 2.0 – Site Characterization

Figure 2-1 Louisiana Stratigraphic column (from Louisiana Geological Society)

Figure 2-2 Type Log – [REDACTED] (*submitted as CBI*)

Figure 2-3 Schematic northwest-southeast cross sections showing the evolutionary stages in the formation of the northern Gulf of Mexico and East Texas Basin (modified from Jackson and Galloway, 1984)

Figure 2-4 Distribution of Cretaceous and Cenozoic continental margins in the northwestern Gulf of Mexico (modified from Jackson and Galloway, 1984)

Figure 2-5 Principal sediment sources and depositional systems in the northern Gulf of Mexico during the late Oligocene (modified from Galloway et al., 2000) and location of salt diapirs (modified from Ewing and Lopez, 1991; Lopez, 1995, Martin, 1980).

Figure 2-6 Structural Features of the Northern Gulf Coast Region (from Decade of North American Geology, Volume J, Plate 2, 1991)

Figure 2-7 Regional Published N-S Cross Section M-M' from Louisiana Geological Survey (modified from Bebout and Gutierrez, 1983)

Figure 2-8 Regional Published N-S Cross Section N-N' from Louisiana Geological Survey (modified from Bebout and Gutierrez, 1983)

Figure 2-9 Depositional Systems of the Upper Cretaceous for the Gulf of Mexico Region (from Ewing and Galloway, 2019)

Figure 2-10 Regional Extent of the Tuscaloosa Marine Shale across Louisiana and Mississippi (John et al., 1997)

Figure 2-11 Upper Cretaceous-aged Austin Group regional extent and depositional systems (from Ewing and Galloway, 2019)

Figure 2-12 End of Cretaceous-aged Taylor and Navarro Groups depositional systems impacted by shelf extent and the Olmos and Nacatoch Delta Systems (from Ewing and Galloway, 2019)

Figure 2-13 Regional configuration and thickness trends of the Midway Group. (Hosman, 1996 in USGS Report 1416)

Figure 2-14a Principal Depositional Systems for the Late Paleocene Lower Wilcox episode (from Ewing and Galloway, 2019)

Figure 2-14b Principal Depositional Systems for the Late Paleocene Upper Wilcox episode (from Ewing and Galloway, 2019)

Figure 2-15 Regional configuration and thickness trends of the Wilcox Group. (Hosman, 1996 in USGS Report 1416)

Figure 2-16 Regional configuration and thickness trends of the Cane River Formation (Hosman, 1996 in USGS Report 1416)

Figure 2-17 Regional configuration and thickness trends of the Sparta and Equivalent Formations (Hosman, 1996 in USGS Report 1416)

Figure 2-18 Regional configuration and thickness trends of the Cook Mountain Formation (Hosman, 1996 in USGS Report 1416)

Figure 2-19 Regional configuration and thickness trends of the Cockfield and Equivalent Formations (Hosman, 1996 in USGS Report 1416)

Figure 2-20 Regional configuration and thickness trends of the Vicksburg and Jackson Groups (Hosman, 1996 in USGS Report 1416)

Figure 2-21 Paleogeography of the early Frio/Vicksburg and Delta Systems (modified from Ewing and Galloway, 2019)

Figure 2-22 Paleogeography and principal depositional systems of the Lower Miocene depositional episode (from Ewing and Galloway, 2019)

Figure 2-23 Regional configuration and thickness trends of the Miocene Formations (Hosman, 1996 in USGS Report 1416)

Figure 2-24 Regional configuration and thickness trends of the Pliocene Formation (Hosman, 1996 in USGS Report 1416)

Figure 2-25 Surficial Geology Map of Louisiana (Louisiana Geological Survey 2020)

Figure 2-26 Tectonic Map of Southern Louisiana (modified from Gulf Coast Association of Geological Societies, 1972)

Figure 2-27 Topographic Map of the St. Helena Parish Site

Figure 2-28 Locations of Seismic lines used for Site Characterization

Figure 2-29 Cenozoic shelf margin positions at the end of successive depositional episodes (LK – Lower Cretaceous in grey) (modified from Galloway et al., 2000)

Figure 2-30 Wilcox regional study ternary diagram showing the Lower and Upper Wilcox sections within the feldspathic litharenites (Dutton and Loucks, 2014)

Figure 2-31 Density effects on Shale Ductility (from Hoshino et al. 1972)

Figure 2-32 Change in density and ductility of shales with increasing depth (from Hoshino et al. 1972)

Figure 2-33 Three different creep stages illustrated on a Strain vs Time Plot (modified from Brendsdal, 2017)

Figure 2-34 Schematic diagram of stress and strain concepts (from Han, 2021)

Figure 2-35 Principal Horizontal Stresses along the Gulf Coast Region (Nicholson, 2012)

Figure 2-36 Location of data used in the Pore Pressure Analysis

Figure 2-37 Image from the mud log of Weyerhauser SWD No. 2 with gas spike from Tuscaloosa Marine Shale

Figure 2-38 Mud weight analysis from three fields in St. Helena Parish

Figure 2-39 Location of Digital and Sonic Logs used in Fracture gradient analysis

Figure 2-40 Digital Sonic Logs within the area of interest for the St. Helena Parish Site

Figure 2-41 Composite Rock Property Model for Injection Wells

Figure 2-42 Fracture Gradient value ranges for Shmin and Tensile Initiation Point (Figure 6 in Hasuer, 2021)

Figure 2-43 Calculated Sh_{min} , Fracture Gradient and Bore Hole Stability

Figure 2-44 Injection Wells Pore Pressure Fracture Gradient Plot

Figure 2-45 Modified Mercalli Intensity (MMI) Scale (from USGS, 2022)

Figure 2-46 Seismic Risk Map (USGS, 2018)

Figure 2-47 Map of subsurface faults in Louisiana (modified from Louisiana Geological Society, 2001)

Figure 2-48 Regional and Local Seismic Events in and around Louisiana since 1900. Data search compiled in November 2022 from the United States Geological Society (USGS) National Earthquake Database

Figure 2-49 Nearest Seismic event to St. Helena Parish and the Project Site

Figure 2-50 Louisiana Watershed Divisions and Regional River Drainage Basins (from Louisiana Watershed Initiative (2022) and Louisiana Department of Environmental Quality (2007)

Figure 2-51 Principal Aquifer Systems of Louisiana (Louisiana Management of Water Resources, 2020)

Figure 2-52 Major regional aquifers and systems in Louisiana (from USGS, prepared for Louisiana Groundwater Resources Commission, 2009)

Figure 2-53 Hydrostratigraphic Column for the State of Louisiana from the United States Geological Survey

Figure 2-54 Regional Extent of the Sparta Aquifer System within the Mississippi Embayment systems (modified from USGS Fact Sheet 111-02, 2002)

Figure 2-55 Potentiometric surface map of the Sparta Aquifer in north-central Louisiana, March-April 2012 (from McGee and Brantly, 2015)

Figure 2-56 Potentiometric surface map of the MRVA Aquifer (from McGuire et al., 2019)

Figure 2-57 Potentiometric surface map of the massive, upper, and 200-foot sands of the Chicot Aquifer System in southwestern Louisiana, January 2003 (from Lovelace et al., 2004)

Figure 2-58 General Potentiometric Surface of Pleistocene-aged Aquifers - Project Area of Interest in within the Southern Hills Aquifer System (from USGS, 1980)

Figure 2-59 Display of Southern Hills Aquifer System (modified from White, 2017)

Figure 2-60 Localized hydrogeologic stratigraphic column for the Southern Hills Aquifer System for St. Helena Parish (modified from Nyman and Fayard, 1978, Buono, 1983, and Prakken, 2004)

Figure 2-61 North – South Hydrogeologic Cross Section for St. Helena Parish (modified from Tomaszewski, 1988)

Figure 2-62 Display of West – East Hydrogeologic Cross Section I-I' (modified from Griffith, 2003)

Figure 2-63 Potentiometric Map for the Chicot Equivalent Aquifer System in 2009 (from Tomaszewski, 2011 in USGS Scientific Investigations Map 3173)

Figure 2-64 Potentiometric Map for the 1,500-foot and 1,700-Foot (Evangeline Equivalent Aquifer System) in 2003 (from Prakken, 2004 in Scientific Investigations Map 2862)

Figure 2-65 Potentiometric Map for the 2,800-Foot Sand (Jasper Equivalent Aquifer System) in 2006 (from Fendick, 2007 in Scientific Investigations Map 2984)

Figure 2-66 Base of Lowermost USDW map for the St. Helena Parish Site

Figure 2-67 Water Well Map with a 6-mile radius of Investigation

Figure 2-68 Water Wells by depth within 6-miles of the Injection Wells

Figure 2-69 Pie Chart of Water Wells by Usage within 6-miles of the Injection Wells

Figure 2-70 Pie Chart of Active Water Wells by Aquifer Usage within 6-miles of the Injection Wells

Figure 2-71 Bottomhole Temperature Data and Locations from Drumm and Nunn (2012)

Figure 2-72 Max bottomhole pressures corrected for the St. Helena Parish site

Figure 2-73 Resistivity nomograph for NaCL Solutions (Schlumberger, 1979)

Section 5.0 – Injection Well Construction

Figure 5-1 Proposed Well Schematic - Frio Injector, Soterra IF 1-1

Figure 5-2 Proposed Well Schematic - Tuscaloosa Injector, Soterra IT 2-1

Figure 5-3 Wellhead Schematic

LIST OF APPENDICES

Appendix A Local Geologic Maps and Cross sections (*submitted as CBI*)

Appendix B Data from CoreLabs RAPID™ database used in the Injection Zones Studies (*submitted as CBI*)

Appendix C Spontaneous Potential and Resistivity Method for Determination of USDW

Appendix D Well Technical Specifications (*submitted as CBI*)

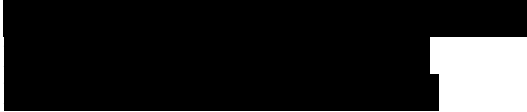
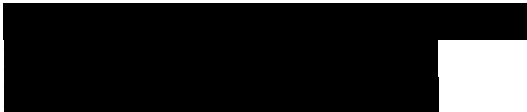
Appendix E Environmental Justice Report (*submitted as CBI*)

INDEX OF SUBMITTED APPLICATION PLANS

GSDT Module	Report Plan Name
Module A - Summary of Requirements	A.1 – Project Narrative
Module B – Area of Review & Corrective Action Plan	B.1 – Area of Review and Corrective Action Plan
Module C – Financial Demonstration	C.1 – Financial Demonstration Plan
Module D – Pre-Operational Testing	D.1 – Pre-Operation Testing Plan
Module E – Project Plan Submission	E.1 – Testing and Monitoring Plan
	E.2 – Injection Plugging Plan
	E.3 – Post-Injection Site Care and Site Closure Plan
	E.4 – Emergency and Remedial Response Plan

1.0 PROJECT BACKGROUND AND FACILITY INFORMATION

1.1 FACILITY INFORMATION

Facility Name:	Shell U.S. Power and Gas – St. Helena Parish Site Two Class VI Injection Wells
Facility Contact:	Jason Dupres/U.S. Environmental and Regulatory Lead 150 N. Dairy Ashford Rd, Houston, Texas 77079 (832) 377-0678 Jason.dupres@shell.com
Well Locations:	SOTERRA IF 1-1  SOTERRA IT 2-1 

1.2 PROJECT GOALS

Global Goals

Shell U.S. Power and Gas (Shell) is assessing the viability of carbon capture and sequestration (CCS) projects in the Gulf Coast to take carbon dioxide (CO₂) from industrial facilities and inject it safely for permanent storage underground. This Class VI permit is the first of its kind for Shell in the United States but is built on Shell's global CCS experience. Shell is actively working CCS projects in its major hubs of Canada, The United Kingdom, The Netherlands, and China – with active CCS operations in Canada.

Shell is committed to net-zero emissions by 2050, and CCS is one of the key pillars in its energy transition efforts. In April 2020, the Shell CEO announced that “By 2050, Shell intends to be a

net-zero emissions energy company.”¹ In line with this goal, Shell is looking at several technological solutions to help it provide more and cleaner energy while lowering its carbon footprint. Virtually all credible climate change scenarios suggest the goals of the Paris Agreement on climate change cannot be met without CCS. Therefore, CCS is one critical piece of Shell’s energy transition plan. Shell has been implementing this technology around the world and is excited to bring its extensive experience and technical expertise to Louisiana.

Shell is investing in multiple projects to capture and store CO₂ around the world – decarbonizing multiple businesses. Shell is actively involved in the entire value chain including operating assets, capturing CO₂, building transport and storage infrastructure, and developing commercial CCS applications. Shell believes that there are multiple value chains that CCS can enable. For example, in the Quest project in Alberta, Canada, Shell is capturing CO₂ from hydrogen units producing lower carbon hydrogen. In the Northern Lights project, Norway, Shell is actively working with its partners to offer CO₂ storage solutions to industrial emitters. In The Netherlands, Shell signed a contract with Porthos, a joint venture between EBN, Gasunie and the Port of Rotterdam Authority, to enable the transport and storage of CO₂ from Shell’s Pernis refinery. Shell is also active in research and development programs advancing technology and supporting project deployment across the globe.

Shell’s flagship CCS project is the Quest project in Alberta, Canada. The Shell Canada Quest project has been in safe and successful operation for over 6 years. Quest captures about one million tons of CO₂ per annum as per design via pre-combustion capture at three hydrogen manufacturing units resulting in over 6 million tons (MT) of CO₂ being captured, transported, and stored to date at a capture unit reliability of 99%. The Quest project stores CO₂ via injection from three wells in a sandstone rock reservoir more than 2 km (1.3 miles) underground. The Quest project has exceeded target storage rates in part due to the excellent reservoir characteristics. The Quest

¹ Additional information about Shell’s Net Zero Ambitions is available at <https://www.shell.com/powering-progress/achieving-net-zero-emissions.html#:~:text=Shell's%20target%20is%20to%20become,levels%20on%20a%20net%20basis>.

development is analogous to the site selected in St. Helena Parish in many ways and the insights that Shell has gained over the last six years of operation will be utilized to replicate the successes seen in Alberta, Canada and even improve upon them in St. Helena, Louisiana.

Shell's Louisiana Position

Shell is assessing the viability of CCS projects that would take carbon dioxide from its Louisiana facilities – and from other companies if capacity allows - and inject it 1 to 3 miles underground where it would be permanently and safely stored. This would both lower carbon emissions from existing facilities and reduce CO₂ emissions from new processes to make low-carbon fuels and other products. Shell has a long history in Louisiana, and we believe CCS is vital to helping build a new energy future and resilient economy for the state. Shell is committed to helping Louisiana transition to a cleaner energy future by reducing emissions and investing in new technologies that will contribute to a vibrant economy.

Shell has a proud and rich heritage in Louisiana, with more than 100 years working with businesses and communities throughout the state. Louisiana is home to many of Shell's businesses ranging from oil and gas exploration and production to refining and chemicals along with pipelines needed for product transportation and trading services to provide products to end customers. The hard work of Shell's employees helps strengthen the state's economy and deliver vital energy to power lives around the world. To meet Shell's target for net-zero emissions by 2050 and contribute to building a new energy future in the state, Shell is working with its stakeholders to keep energy flowing today and transform its facilities to deliver lower-carbon fuels and products, such as circular plastics, biofuels, and specialty chemicals. Shell does this with a strong commitment to protect the places where it operates.

Shell is deeply invested in Louisiana, where it employs close to 3,000 people, over 4,500 retirees live, and paid more than \$240 million in taxes in 2021. Last year, Shell also invested close to \$6.7 million in projects to help build a better Louisiana, from the environment to health and education to disaster relief. Shell also made a landmark investment in Louisiana State University to help establish the Institute for Energy Innovation to advance a reliable, affordable, and environmentally responsible energy system along with the skills and technologies needed to enable this future.

Shell's employees also contribute thousands of volunteer hours to community projects. Shell looks forward to nurturing our deep Louisiana roots in the decades ahead as they work together to create new jobs and invest in the low-carbon technologies that will be so important globally to the future of energy. Shell believes the successes seen in Alberta Canada can be replicated in St. Helena Parish, Louisiana.

The Louisiana Gulf Coast has a large network of refineries, chemicals plants, and other industrial emitters. More than 50 Million Tons Per Annum (MTPA) of CO₂ is emitted from the Louisiana Gulf Coast, with much of that centered around the lower Mississippi river between Baton Rouge and New Orleans². The Shell refining and chemicals assets at Geismar, Convent, and NORCO are also in this corridor. The objective of this application is to gain authorization for a wide-scale deployment of CCS by combining carbon capture technology to geologically favorable sites, where it is intended to deploy safe injection well technology that follow all Class VI Permitting rules and standards as set forth by the United States Environmental Protection Agency (USEPA).

The Shell Gulf Coast Project seeks to construct a CO₂ Storage Site in St. Helena Parish, Louisiana to decrease the carbon footprint from existing and future company assets, enable the suite of lower carbon projects, and help support the decarbonation of other emitters in the region. The proposed CO₂ storage site will include minimal surface facilities, injection wells, monitoring wells, access roads and an underground CO₂ injection reservoir. The CO₂ will be transported from the Mississippi River industry corridor area through an underground pipeline to multiple injection pad locations targeting the Frio, Wilcox, and Lower Tuscaloosa sandstone formations. This storage complex in St. Helena Parish represents a significant storage opportunity potentially over a 25-year project period.

The local geology in St. Helena is described later in this permit, and is favorable for CCS because it meets the following subsurface requirements:

² LSU Centre for Energy Studies 2021

- There are limited legacy wells in the leasehold area reducing associated CO₂ containment risk.
- Sink depths are favourable at 3,500-14,000 feet True Vertical Depth – Subsea (TVDSS) for supercritical CO₂ injection which increases site efficiency.
- The sink area has limited faulting and low structural dips (approximately 1-1.5 degrees), reducing associated CO₂ containment risk and keeping the plume localized to a small area.
- There are three potential stacked injection zones improving site capacity and efficiency.
- There is a thick (average ~370 feet), regionally correlative primary confining zone above the Frio Injection Zone.
- The injection zones are sandstone dominated with heterogeneity that is effective at providing substantial local trapping and containment of CO₂.
- The mineralogy of the storage complex and formation water is not reactive with the injected CO₂ stream.

The following chapters of this Class VI Permit Application will demonstrate the Shell technical team has performed a commercial, large-scale characterization of the proposed storage site using currently available published and private data and databases. Additional site-specific data will be collected during the drilling of two Class V Stratigraphic Test wells to support and validate the project.

1.2.1 Stratigraphic Test Wells

Shell is planning to drill two stratigraphic test wells, classified as Class V wells under the State of Louisiana, one for the Frio Formation and one for the Lower Tuscaloosa Formation. These wells will be drilled at the proposed project injection sites to generate site-specific information about geologic, hydrogeologic and biogeochemical conditions. Shell plans to convert these appraisal wells into Class VI injection wells and the wells have been designed accordingly. Using this approach, Shell expects to minimize the number of well penetrations in the storage complex.

To meet the Class VI required standards for construction, corrosion resistant alloy (CRA) casing has been selected across the injection intervals and multiple strings of carbon steel casing will be

used across all other zones. These appraisal wells will provide detailed geologic characterization of the proposed injection zones (porosity, permeability and injectivity etc.) and prove the efficiency of confining zone. Data acquisition will also support requirements of Class VI permit application including coring, logging, pressure, samples, rock strength and well testing.

1.2.2 CO₂ Stream

The St. Helena Parish site is expected to receive CO₂ from the Shell assets in the Mississippi River corridor via a high-pressure CO₂ trunk line, which will be distributed by a smaller in field network. Additional future sources are expected to come from the projects at the same sites supporting the growth of hydrogen, low carbon fuels, and low carbon chemicals and products. With additional capacity, Shell can commercially accept other CO₂ sources from third parties, allowing others in the area to reduce their carbon intensity and create lower carbon end products. All sources of CO₂ will have strict injection specifications and will be purified, dehydrated, and compressed before entering the pipeline for transportation to the injection wells.

1.2.3 Injection and Confining Zones

In order to assess the feasibility of CO₂ injection into and storage within the Oligocene to Upper Cretaceous strata of eastern Louisiana, (specifically St. Helena Parish), this project is designed to answer the following fundamental geological and geophysical questions pertaining to the efficacy of CO₂ storage in the study area: 1) are there porous horizons with the potential to store Shell's targeted CO₂ within a 25 year injection period; 2) are the trapping formations structurally competent enough to contain the injected CO₂ from migrating upward into the overlying aquifers; 3) are the physical and chemical properties of the possible porous horizons conducive for CO₂ injection and permanent storage; and 4) will the injection of CO₂ enhance continuing injectivity or reduce injectivity.

Shell's integrated study identified potentially three targeted Injection Zones; 1) Frio Formation, 2) Lower Tuscaloosa Formation, and 3) Wilcox Formation (to be assessed in more detail). Shell has reviewed seismic data, core databases, geophysical logs, and modeled the potential plume and critical pressure front at the end of injection (25-years) and post-closure observation (50-years).

All three targeted injection zones, as well as the regional seal, are described in their regional, local, and detailed analysis in **Section 2.0 – Site Characterization**.

1.2.4 Injection Wells and Capacity

On the issuance of a Class VI permit from the EPA or the State of Louisiana (once primacy is established), Shell will convert their Class V wells for the Frio and Lower Tuscaloosa Formations. Each injector will be completed on their own pad approximately 5 miles apart (see **Figure 1-1**).

[REDACTED]

[REDACTED] The Wilcox reservoir, between the deeper Lower Tuscaloosa and shallower Frio Formations will be appraised during the drilling and testing of the Frio and Lower Tuscaloosa Injection Wells. This data will be used to determine the capacity and viability of the formation in the project area. If the data supports, Shell will use this additional reservoir capacity as evaluated and return for Class VI data such as water sample, core and well testing. The evaluation of the Wilcox target will be made after the initial appraisal results have been assessed. [REDACTED]

[REDACTED]

[REDACTED] The Wilcox Formation is included as a proposed injection zone in this permit application as it is situated between the two primary target sinks and has been adequately studied for future storage. [REDACTED]

[REDACTED]

[REDACTED]

[REDACTED]

[REDACTED]

The Construction and Operations Plan developed by Shell to meet the requirements of 40 CFR 146.82 are presented in Section 5.0 of this narrative. The Injection Well Plugging Plan has been developed to meet the requirements of 40 CFR 146.92. An overview of the injection plugging plan is summarized in Section 9 of this project narrative report. The detailed report is submitted as “*E.2 – Injection Plugging Plan*” submitted in **Module E**.

1.2.5 Monitoring Program

Pursuant to 40 CFR 146.82(a)(15) and 146.90, Shell has developed a site-specific comprehensive Monitoring, Measurement and Verification program that will be implemented to verify containment of the injected CO₂ and non-endangerment to the Underground Source of Drinking Water (USDW). The monitoring program will cover pre-injection, injection, and post injection site care (PISC) and site closure phases. It will include monitoring wells in the injection zone, in the first permeable strata above the confining zone (ACZ), and indirect and direct monitoring of the plume and pressure front. The monitoring program will cover the St. Helena Parish site, and considers all CO₂ injected into the ground from both the Frio and Lower Tuscaloosa proposed injection wells, to ensure there are no threats to long-term security of the CO₂ storage site. In the unlikely event of unintended migration, Shell has developed an Emergency and Remedial Response plan, which has been submitted in detail in **Module E**.

1.2.6 Project CO₂ Details

CCS in Louisiana is key to decarbonizing Shell's existing assets and is the foundation for a new Clean Hydrogen business which underpins the creation of ultra-low carbon biofuels ³. Success at the St. Helena Parish site is initially enabled by the pure volumes at the Shell Geismar Plant in Ascension Parish and enables future blue hydrogen and biofuels projects at Convent to supply Shell biofuels projects. Additional Shell and third-party volumes can drive scale and infrastructure development that will enable other local businesses to decarbonize – further reducing Louisiana's CO₂ footprint.

The St. Helena Parish site is expected to receive initial CO₂ from the Shell Geismar Plant via a high-pressure CO₂ trunk line, which will be distributed by a smaller in field network.

Additional future sources are expected to come from the Shell Convent site, which supports the growth of blue hydrogen and other 'blue' products. Blue Hydrogen is the process where natural

³ [Shell confirms shuttered Convent facility will become an alternative fuels complex | Business | theadvocate.com](https://theadvocate.com/business/shell-confirms-shuttered-convent-facility-will-become-an-alternative-fuels-complex/)

gas-based hydrogen production is combined with CCS, *i.e.*, when substantial amounts of CO₂ from natural gas reforming are captured and permanently stored the clean hydrogen is categorized as ‘blue.’ If capacity allows, Shell may commercially accept other CO₂ sources from third parties, allowing others in the area to reduce their carbon footprint. All sources of CO₂ will have strict injection specifications and will be purified, dehydrated, and compressed before entering the pipeline for transportation to the injection wells.

2.0 SITE CHARACTERIZATION

The geologic suitability of a specific stratigraphic interval for the injection and confinement of carbon dioxide (CO₂) is determined primarily by the following criteria:

- Lateral extent, thickness, interconnected porosity, permeability, and geomechanical properties of the injection zone;
- Lateral extent, thickness, minimal porosity, impermeability, and geomechanical properties of the overlying confining zone;
- Hydrogeologic compatibility of the injected carbon dioxide with the rock formation material and in-situ brine solutions;
- Faulting or fracturing of the injection zone, overlying aquiclude, and confining zone; and
- Seismic risk.

These criteria can be evaluated based on the regional and local depositional and structural histories of the geologic section.

In the following sections, the depositional and structural framework of the sedimentary column (Figure 2-1) utilized for the sequestration of CO₂ at the site St. Helena Parish is outlined. Information has been obtained from the regional and local data interpretations and conclusions of the Area of Review (AoR) study. A type-log of the anticipated formations beneath the sequestration site is included as Figure 2-2. Geologic maps and cross sections illustrating the regional geology, hydrogeology, and the geologic structure of the local area are provided per 40 CFR 146.82(a)(3)(vi) standard.

2.1 REGIONAL GEOLOGY

Figure 2-3 is a series of cross-sections illustrating the evolutionary stages of the development of the northern region of the Gulf of Mexico and East Texas Basin. The first cross section is of the pre-rift phase of the Lower Triassic. Upper Triassic rifting and the deposition of the Eagle Mills (continental red beds) are seen in the second cross section. The third cross section shows continued

ripping in the Middle Jurassic coincident with the deposition of evaporites in restricted marine basins. Finally, cross section four covers the Upper Jurassic and Lower Cretaceous Divergent Margin. The earliest record of sedimentation in the Gulf of Mexico Basin occurred during the Early to Middle Jurassic period, between 200 and 160 million years ago. At this time, the early phases of continental rifting resulted in the deposition of non-marine red beds and deltaic sediments (shales, siltstones, sandstones, and conglomerates) composing the Eagle Mills Formation in a series of restricted, graben fault-block basins. These sediments were unconformably overlain by a thick sequence of Middle Jurassic anhydrite and salt beds, the Werner Anhydrite and Louann Salt (Jackson and Galloway, 1984; Ewing and Galloway, 2019).

The deposition of the Louann Salt beds was localized within major basins that were defined by the major structural elements in the Gulf Coast Basin. The clastic Norphlet Formation (sandstones and conglomerates) overlies the Louann Salt and is more than 1,000 feet thick in Mississippi thinning and fining to the west into a sandstone and siltstone across Louisiana and into Texas. Norphlet conglomerates were deposited in coalescing alluvial fans near Appalachian sources grading downdip into dune and interdune sandstone deposited on a broad desert plain (Mancini et al., 1985). Although the Norphlet Formation is non-fossiliferous, based on dating of the overlying and underlying sequences, the Norphlet Formation is late Middle Jurassic (Callovian) in age (Todd and Mitchum, 1977).

Shallow-water carbonate and clastic rocks of the Smackover, Buckner, and Haynesville Formations and the Cotton Valley Group were deposited over the Norphlet Formation from the Late Jurassic into the early Cretaceous. Jurassic, non-skeletal, carbonate sands and muds accumulated on a ramp-type shelf with reefal buildups developed on subtle topographic highs (Baria et al., 1982). A high terrigenous clastic influx in eastern Louisiana and Mississippi occurred during deposition of the Haynesville and diminished westward where the Haynesville Formation grades into the Gilmer Limestone in East Texas. The top of the Jurassic occurs within the Cotton Valley Group, with the Knowles Limestone dated as early Cretaceous (Berrassian) in age (Todd and Mitchum, 1977). The early to middle Cretaceous was a period of tectonic stability and low terrigenous sediment influx, permitting the development of extensive, shelf-edge reef complexes (Baria et al., 1982).

In the Mid to Late Cretaceous, tectonism resulted in uplift in western United States and northern Mexico resulted in a large influx of terrigenous sands and muds into the Gulf of Mexico Basin. Uplift mechanisms likely include movement of the North American plate over the Bermuda hotspot in mid-Cretaceous, the Laramide Orogeny, between 70-80 and 35-55 million years ago, and the Ouachita Uplift, all of which contributed to early erosion and subsequent deposition of sediments of the Washita-Fredericksburg and Tuscaloosa Formations (Cox, R.T. and Van Arsdale, R.B., 2002; Sneddon et al., 2015; Ewing and Galloway, 2019). This effectively shuts off the production of carbonates, except in the Florida and Yucatan regions. Note that since the Cretaceous period, the rate of terrigenous sediment influx has been greater than the rate of basin subsidence, resulting in a significant progradation of the continental shelf margin (Figure 2-4).

During the Cretaceous post-rift stage, structural highs and lows were formed (or in the case of the Sabine Uplift and Wiggins Arch were reactivated) resulting in regional angular unconformities in the northern onshore Gulf of Mexico Basin. The Sabine Uplift, Monroe Uplift, Wiggins Arch, and Jackson Dome all experienced some degree of igneous activity during the late Cretaceous (Ewing, 2009). Mesozoic igneous activity of the onshore Northern Gulf of Mexico Basin was examined and discussed in multiple studies and local reports (Kose, 2013; Byerly, 1991; Kidwell, 1951; Moody, 1949; Ewing, 2009; Nichols et al., 1968). The Monroe Uplift has the largest volume of magma and the greatest compositional diversity in the Northern Gulf of Mexico Basin with at least four major igneous rock groups have been defined thus far: 1) intermediate rocks; 2) alkaline rocks; 3) basalts; 4) lamprophyres (Ewing, 2009; Kidwell, 1951). It is not well understood why igneous activity occurred but there appears to be a relation between igneous activity and the movement of the uplift in the Monroe Uplift area (Ewing and Lopez 1991; Kidwell, 1951).

During the Cenozoic era, the geometry of the deposition in the Gulf of Mexico Basin was primarily controlled by the interaction of the following factors:

1. Changes in the location and rates of sediment input, resulting in major shifts in the location of areas of maximum sedimentation.
2. Changes in the relative position of sea level, resulting in the development of a series of large-scale depositional cycles throughout Cenozoic time.

3. Diapiric intrusion of salt and shale in response to sediment loading.
4. Flexures and growth faults due to sediment loading and gravitational instability.

During the first 35 million years of Cenozoic deposition, the Gulf Coast Region in general experienced four major eustatic events. These major high stands events are marked by the Midway Shale, Cane River Shale, Cook Mountain Shale, and Jackson-Vicksburg Shale.

Early Tertiary sediments are thickest in the Rio Grande Embayment of Texas, reflecting the role of the ancestral Rio Grande and Nueces Rivers as sediment sources to the Gulf of Mexico. By Oligocene time, deposition had increased to the northeast, suggesting that the ancestral Colorado, Brazos, Sabine, and Mississippi Rivers were increasing in importance (Figure 2-5). Miocene time is marked by an abrupt decrease in the amount of sediment supply entering the Rio Grande Embayment, with a coincident increase in the rate of sediment supply in southeast Texas, Louisiana, and Mississippi. Throughout the Pliocene and Pleistocene epochs, large depocenters of sedimentation were controlled by the Mississippi River and developed offshore of Louisiana and Texas.

Tertiary sediments accumulated to great thickness where the continental platform began to build toward the Gulf of Mexico, beyond the underlying Mesozoic shelf margin and onto transitional oceanic crust. Rapid loading of sand on water-saturated prodelta and continental slope muds resulted in contemporaneous growth faulting (Loucks et al., 1986). The effect of this syndepositional faulting was a significant expansion of the sedimentary section on the downthrown side of the faults. Sediment loading also led to salt diapirism, with its associated faulting and formation of large salt withdrawal basins (Galloway et al., 1982a).

Sediments of the Tertiary progradational wedges were deposited in continental, marginal marine, nearshore marine, shelf, and basinal environments and present a complex depositional system along the Gulf Coast. Overlying the Tertiary progradational wedges along the Gulf Coast are the Pleistocene and Holocene sediments of the Quaternary Period. Pleistocene sedimentation occurred during a period of complex glacial activity and corresponding sea level changes. As the glaciers made their final retreat, Holocene sediments were being deposited under the influence of an

irregular, but rising, sea level. Quaternary sedimentation along the Texas Gulf Coast occurred in fluvial, marginal marine, and marine environments.

2.1.1 Regional Maps and Cross Sections

The preceding overview section outlined the main tectonic and depositional events controlling the architecture of the Gulf of Mexico Basin. In this section, regional geology will be described in more detail through the use of regional maps and cross sections.

Figure 2-6 is a published regional map illustrating the structural features of the Northern Gulf Coast of Mexico modified from the published Decade of North American Geology (1991). The positive structural elements in the East Texas, Louisiana, and Mississippi region are the Sabine Uplift, Monroe Uplift, La Salle Arch, Jackson Dome, and the Central Mississippi Deformed Belt, and the Wiggins Uplift. The negative structural elements are the East Texas Basin, North Louisiana Salt Basin, and the Mississippi Salt Basin.

The regional geology section is based upon available published maps and cross sections, as well as published studies on the formation and deposition of the Gulf of Mexico. The data evaluated covers the Gulf Coast Region and the State of Louisiana. These regional maps are contained as “Figures” referenced within their respective description sections as follows. Figure 2-7 and Figure 2-8 are published North-South regional cross sections with a location index map from Bebout and Gutierrez (1983). The north-south cross sections M-M’ and N-N’ illustrates the increase in the southernly regional dip towards the Gulf of Mexico.

2.1.2 Regional Stratigraphy

The regional stratigraphy of the Gulf of Mexico Basin is well documented throughout Louisiana and is presented on Figure 2-1. The following sections describe the regional formations that may be penetrated in the St. Helena Parish sequestration site. These formations are described in ascending order beginning with the Upper Cretaceous-aged Tuscaloosa Group.

For the Shell St. Helena Parish site, the proposed zones for sequestration are as follows:

- Injection Zone 1 – Frio Formation

- Injection Zone 2 – Wilcox Formation
- Injection Zone 3 – Lower Tuscaloosa

Each of the targeted Injection Zones are overlain by regionally extensive Confining Shales and Sealing units that will impede the vertical migration of fluids out of the sequestration zone. This has been identified as the following:

- Confining Zone 1 – Frio, Anahuac, and Lower Miocene Shales

The Anahuac Formation is a regionally extensive confining zone that is present south of the sequestration project at shallow depths and extends to the Gulf of Mexico. It is not present to the north of the target site. Specific details on the characteristics of each formation are discussed in **Section 2.3 – Description of Confining and Injection Zones** of this document.

2.1.2.1 Tuscaloosa Group

The period of Tuscaloosa deposition is characterized by a full transgressive cycle event during the Late Cretaceous (Pair, 2017). The Tuscaloosa is subdivided into two formations, an Upper and a Lower. In southern Mississippi and central-eastern Louisiana area, the Lower Tuscaloosa Formation unconformably overlies the Washita-Fredericksburg group. The formation is bounded above uncomfortably by the Eutaw Formation in Alabama and Mississippi and conformably overlain by the Eagle Ford Shale in Louisiana (Woolf, 2012).

2.1.2.1.1 Lower Tuscaloosa

In southwest Mississippi and southeast Louisiana, the Lower Tuscaloosa Formation contains non-marine and marine facies (Berg and Cook, 1968; Chasteen, 1983; Hearne and Lock, 1985; Stancliffe and Adams, 1986; Shirley, 1987). The Lower Tuscaloosa may then be further subdivided into three sections, from oldest to youngest: the Massive Sand member; the Marine section; and the Stringer (also referred to as the shale and sand) section. The non-marine facies are the Lower “Massive” Tuscaloosa Sand, which is composed of a basal braided stream deposit and a meander belt point-bar complex transitioning downdip into deltaic deposits. Figure 2-9 from Ewing and Galloway (2019), demonstrates that the transition between these environments lies in the vicinity of the Mississippi-Louisiana border.

The Lower Tuscaloosa “Massive” Sand is composed of stacked massive sandstones with few well-defined shale breaks. Chert-conglomerate is commonly present at the base of the stacked channel sand (Chasteen, 1983). The Lower Tuscaloosa “Massive” Sand sediments are structureless, well-sorted, micaceous, locally fossiliferous (marine bivalves), calcareous, glauconitic, fine-grained, and quartz rich. All of these characteristics are indicative of a more marginal marine (more downdip equivalent) environment of deposition than the lower Tuscaloosa section in southwestern Mississippi and eastern Louisiana (Mancini et al., 1987). The stacking of channel sandstones with basal conglomerates is typical of a braided-stream environment. Regional isopach maps of the braided-stream unit show a sheet-like geometry with thick sand areas corresponding to persistent drainage patterns where major streams existed (Chasteen, 1983). Overlying the braided-stream deposits are meander belt point bar and associated facies deposits.

The overlying marine facies includes the “Marine” and “Stringer” sections. It is composed of sandstones interbedded with siltstones and shales that exhibit intense bioturbation. This intense bioturbation suggests deposition in shallow water, brackish to marine environment. In addition, cores and sample logs commonly record the presence of oysters as solitary and bedded forms in the shales, which would support a shallow-water marine origin for the unit (Chasteen, 1983). Sandstones in the marine interval of the Lower Tuscaloosa Formation are generally thin, exhibit a lenticular nature, and are commonly intensely bioturbated (Chasteen, 1983).

The “Stringer” section consists of alternating gray, fine to medium grained sandstones with associate gray and red, silty shales. In Southern Mississippi, these sandstones are found at depths of 10,000 to 12,000 feet. This is interpreted as estuarine facies capping the earlier sequences of fluvial deposits filling broad incised valleys associated with uplift at the mid-Cretaceous (Woolf, 2012; Ambrose et al., 2015). They are variable in thickness, discontinuous, and exhibit sinuous patterns on sand isopach maps (Devery, 1980).

2.1.2.1.2 *Tuscaloosa Marine Shale*

Continued transgression, caused by a major global rise in sea level during the early Late Cretaceous, inundated the marginal marine Tuscaloosa sequence, leading to the deposition of middle marine shales of the Middle (Tuscaloosa Marine Shale) and Upper Tuscaloosa (Vail et al.,

1977; Stancliffe and Adams, 1986). The Tuscaloosa Marine Shale (TMS) is composed almost entirely of a grey to black, fissile, and sometimes sandy marine shale which thickens down dip (John et al., 1997). The TMS represents the flood stage (end transgressive system) and is regionally extensive across Louisiana and into Mississippi (Figure 2-10).

The Tuscaloosa Marine Shales along the basin contain a diverse assemblage of macrofossils, including ammonites, gastropods, inoceramids, other bivalves, and a rich assemblage of planktonic foraminifera and calcareous nannofossils typical of Cretaceous open-shelf environments (Mancini et al., 1987). Microfauna analysis of samples from Liberty Field in Amite County, Mississippi (just north of St. Helena Parish), presents a vertical change from a fauna dominated by the agglutinated species *Ammobaculites* and *Trochammina* to one characterized by the calcareous species *Heterohelix* and *Lenticulina* (Stancliffe and Adams, 1986). This faunal succession suggests a transition from restricted marine to open marine neritic conditions for Middle and Upper Tuscaloosa shales (Stancliffe and Adams, 1986). Fluvial deposition was confined to extreme updip positions in the northern Gulf of Mexico Basin (Chasteen, 1983).

2.1.2.1.3 *Upper Tuscaloosa*

The Upper Tuscaloosa is separated by the Lower Tuscaloosa by a major unconformity, with the Lower Tuscaloosa wedging out updip and being overlapped by the Upper Tuscaloosa (McGlothlin, 1944). The Upper Tuscaloosa formation consists of glauconitic, fossiliferous, sandstone interbedded with shale units. The formation has characteristics of an open marine and marginal marine depositional environment and has an average thickness of approximately 375 feet. The Upper Tuscaloosa is a southward thinning wedge which complements the northward thinning middle Tuscaloosa marine shale wedge (Spooner, 1964). The Upper Tuscaloosa in Mississippi is limited on the northeast by its outcrop, but underlies the balance of the state, except where it truncates on the flank of the Sharkey platform. It also overlies the Jackson Dome in Mississippi and has been pierced by salt domes in the Mississippi Salt Basin.

2.1.2.2 *Eagle Ford Group*

The Eagle Ford is one of the most prolific and actively explored oil and gas shale plays in the USA. It is the source of many conventional plays and is also an exploited unconventional resource

throughout Texas. During the Late Cretaceous period, a large swath of central North America (including Texas, Louisiana, and Mississippi) was submerged below the Western Interior Seaway. The Eagle Ford was deposited during this global eustatic sea level rise in a marine shelf, transgressive environment. The organic rich shales of the Eagle Ford in Louisiana can be characterized as a fossiliferous, calcareous mudstone with authigenic minerals such as frambooidal pyrite, glauconite, and apatite (Donovan and Staerker, 2010; Dawson, 2000). To the north, in Mississippi, the Eagle Ford is part of the Lower Eutaw Formation grading into micaceous, calcareous, glauconitic, fine-grained sandstone near the updip marine margin (Mancini et al., 1987). The formation is truncated wedge of deep-water shale (where present) in front of the shelf margin. In these locations, the top of this group is an unconformity overlain by the Austin chalk, which was deposited in deeper water.

2.1.2.3 Austin Group

The Upper (late) Cretaceous aged Austin Group (also referred to as the Austin Chalk) is present throughout Texas, Louisiana, and Mississippi and was deposited during a global highstand event (Figure 2-11). In relation to the Early Cretaceous shelf edge (located south of the St. Helena parish site) paleowater depths deepened towards the basin, to the south-east. In Texas, the Austin Chalk deposited in shallow marine waters with paleodepths ranging from 30 to 300 feet. These paleowater water depths indicate that carbonates deposited below storm wave base on the inner-middle shelf environment and deeper (Pearson, 2012). The *Planolites*, *Thallasinoides*, and *Chondrites* trace fossils observed by Dawson and Raser (1990) also suggest an open marine environment of deposition with normal salinity. Folk (1959) classified the Austin Chalk as a biomicrite comprised of *coccolithophores* (Dawson et al., 1995).

Depositional environments across Louisiana include distributary channels (overlying the Eagle Ford Shale or Group), prodelta, transgressive marine settings, shallow marine bars, shoreface to barrier or beach complexes, and marsh or tidal flats and channels. Bioturbation, storm deposits, soft-sediment deformation, rip-up clasts, volcanic clasts, and glauconite are all present (Clark, 1995).

The Austin Chalk is divided into the Lower chalk, Middle marl, and Upper chalk and ranges in thickness from 150 to 800 feet. The Lower chalk is characterized as having thicker alternating chalks transitioning into thinly laminated organic rich marl. The marls contain pyrite and high Total Organic Carbon (TOC) (3.5%) suggesting deposition in a dysaerobic basin during a transgressive interval. The thicker chalk units are likely deposited during highstands in the Lower chalk. The Middle marl has alternating packages of clay and burrowed chalk. The older strata deposited during a regressive phase while the younger units deposited during a transgressive phase (Hovarka and Nance, 1994). Relative to the Lower chalk, the Middle marl has higher proportions of light-colored clays. The formation also contains cyclic layers of chalk and marl; however, they are less regular and apparent. The Upper Chalk was deposited during a highstand, and trace fossil assemblages indicate normal marine waters (Hovarka and Nance, 1994).

2.1.2.4 Taylor Group

The Late Cretaceous global rise in sea level reached its maximum extent soon after the end of Eutaw deposition. Much of the Gulf Coast (including most of Mississippi) was inundated and remained below sea level through the end of Cretaceous time.

The Campanian/Maastrichtian-aged Taylor Group is separated from the Austin Chalk by a regional disconformity at the base of the unit. Figure 2-12 is a paleogeographical map illustrating conditions during the deposition of the Taylor Group from Ewing and Galloway, 2019. The Lower Taylor Group is comprised of mud, calcareous claystone, and fossiliferous limestone indicating deposition in a deeper marine environment. Outcrops in Arkansas record glauconite, shells, and phosphorite which are characteristic of a condensed zone. Though the sea levels were relatively high, there were smaller fluctuations in sea level. The short episodes of sea level falls renewed sandy terrigenous sediment influx in the Upper Taylor in a shallow shelf and shoreface environment (Galloway, 2008).

In the area of northern Louisiana, sedimentation took place on the submerged Lower Cretaceous shelf during the Campanian. This deposition period was dominated multiple chalk series (Ozan, Annona, and Marlbrook Formations) that comprise the Taylor Group and are extensive throughout central and northern Louisiana. The Taylor Group then transitions into the Navarro Group with a

gradation of chalks to marls, which corresponds with the changes of sea level at time of deposition. However, the Gulf Coast was still inundated and remained below sea-level through the end of Cretaceous time.

2.1.2.5 *Navarro Groups*

The Uppermost Cretaceous-aged Navarro Group overlies the Taylor Group and is bound at the base by a maximum flooding surface, recording the end of a marine transgression and bound at the top by an erosional unconformity. As sea levels were falling, the Navarro Group records a forward stepping progradational and shoaling event dominated by siliciclastic material provided from the Olmos Delta and Nacatoch clastic system (Figure 2-12). Lag deposits on the bounding erosional surface consist of shell debris, fish, shark teeth, and mud clasts that indicate deposition in a nearshore to inner shelf paleoenvironment (Galloway, 2008). The Nacatoch delta and shore-zone system provided a clastic pulse to north-east Texas, south-west Arkansas and North-west Louisiana, while the larger Olmos delta prograded across the Rio Grande embayment from northern Mexico (Galloway, 2008).

The Navarro Group extends through East Texas, Louisiana, and Arkansas and contains interbedded layers of sandstone, mudstone, and marls. In northeast Texas, from oldest to youngest, the Navarro Group is comprised of the Neylandville Marl, Nacatah Sand, and Kemp Clay Formations. The Neylandville Formation is a gray marl with calcareous sands that has a varying thickness of 50 to 400 feet. The Nacatoch Formation consists of massive calcareous sandstones and mudstones, sourced from the East Texas Embayment, and can range in thickness from 100 to 200 feet in East Texas and 400 feet in Arkansas (Esker, 1968; Adkins, 1933). The Kemp Clay formation (Arkadelphia Marl equivalent in Louisiana) is characterized as greenish to gray silty calcareous mudstone that contains glauconite (Martin, 2014).

In Arkansas and Louisiana, the Navarro Group is split into the Saratoga Chalk (Arkansas), Nacatoch Sand, the Arkadelphia Marl, and Selma Chalk (Louisiana) Formations in ascending order. The Selma Chalk Formation is laterally extensive throughout central and north Louisiana and was deposited in a relatively shallow epicontinental sea and consists of chalk, marl, shale, and

minor beds of sandstones. The Late Cretaceous Sea remained relatively shallow throughout deposition of the Selma Formation, with sedimentation and subsidence in near equilibrium.

2.1.2.6 Midway Group

The Paleocene-aged Midway Group sediments were deposited during the first major Tertiary regressive cycle. The Midway shale is regional in extent, thickening from the East Texas Basin toward the Gulf of Mexico. The Midway Group is a thick calcareous to non-calcareous clay, locally containing minor amounts of sand. Conformably overlying marine Cretaceous sediments within the Midway Group is the Clayton Formation. The faunal succession across the Upper Cretaceous/Tertiary boundary shows a sharp break in both macro-fauna and micro-fauna types, making it possible to accurately determine the base of the Tertiary in the Gulf Coast Basin (Rainwater, 1964a). At the beginning of the Tertiary, an epicontinental sea still covered most of the Mississippi Embayment, with the Clayton Formation being deposited in an open marine environment. The unit is generally less than 50 feet thick and is composed of thin marls, marly chalk, or calcareous clays (Rainwater, 1964a).

As the epicontinental sea became partially restricted in the Mississippi Embayment, the Porters Creek clay was deposited on the Clayton marl. Fossil evidence, although scarce, indicates a lagoonal to restricted marine environment for the Porters Creek Formation (Rainwater, 1964b). The Porters Creek Formation is composed mainly of massively bedded montmorillonite clay. Open marine circulation was re-established in the Mississippi Embayment during the deposition of the shallow marine Matthews Landing Formation. The Matthews Landing Formation was deposited above the Porters Creek clay in a shallow marine environment and is composed primarily of fossiliferous, glauconitic shales with minor sandstone beds (Rainwater, 1964a).

A major regression marks the deposition of the late Paleocene Naheola Formation that overlies the Matthews Landing Formation. Uplift in the sediment source areas of the Rocky Mountains and Appalachian regions supplied an abundance of coarse-grained fluvial sediments for the first time in the Tertiary. Sedimentation rates along the Gulf Coast exceeded subsidence rates and produced the first major regressive cycle in the Tertiary. Alluvial environments dominated throughout most

of Naheola time. The Naheola Formation consists of alternating sand, silt, and shale, with lignite interbeds near the top of the unit (Rainwater, 1964a).

The upper contact with the overlying Wilcox Group is gradational. Wood and Guervara (1981) defined the top of the Midway as the base of the last Wilcox sand greater than 10 feet thick. The precise thickness of the Midway is difficult to measure because it often cannot be differentiated from the underlying upper Navarro Group (Upper Cretaceous) using electric logs but overlies the Selma Chalk. The Midway, upper Navarro Clay (also called Kemp Clay), and the Navarro Marl are generally grouped together during electric log correlations. These formations compose a low-permeability hydrologic unit in the regional area greater than 900 feet thick. The marine clays of the Midway Group grade upward into the fluvial and deltaic sediments of the Wilcox, which is composed of interbedded lenticular sand, mud, and lignite (Fogg and Kreitler, 1982).

The Midway-Navarro section serves as an aquiclude, isolating the shallower freshwater Eocene aquifers from the deeper saline flow systems. Exceptions to the confining ability of the Midway-Navarro include at fault zones and along flanks of salt domes where vertical avenues for flow may exist (Fogg and Kreitler, 1982). In a regional map published from Hosman, 1996 (Figure 2-13) the Midway continues to thicken to greater than 2,000 feet towards the Gulf Coast at depths exceeding 14,000 feet. Outcrops of the Midways exist from north-central Alabama up into Tennessee in the east.

2.1.2.7 Wilcox Group

The Paleocene-aged Wilcox Group is a thick clastic succession that flanks the margin of the Gulf Coast Basin. This geologic group contains fluvial and deltaic channel-fill sand bodies distributed complexly in a matrix of lower permeability inter-channel sands, silts, clays, and lignites. Most of the sands are distributed in a dendritic pattern, indicating a predominately fluvial depositional environment (Fogg et al., 1983).

The Wilcox Group is divided into the Lower, Middle, and Upper intervals. The semi-regional Yoakum Shale divides the Upper and Middle Wilcox, and the Big Shale Marker separates the Middle and Lower Wilcox. During Wilcox Group deposition, the Laramide Orogeny displaced the Paleocene shelf eastward from the relict Lower Cretaceous reef and formed Laramide uplands

which sourced the majority of sediment (Galloway et al., 2000; Galloway et al., 2011). The East Texas Basin ceased to be a marine basin during the Tertiary and Quaternary Periods, when major Eocene, Oligocene, Pliocene, and Pleistocene depocenters shifted toward the Gulf of Mexico.

The Lower Wilcox sediments were transported via two ancestral fluvial-dominated delta systems in the central Gulf; the Houston Delta and the Holly Springs Delta (Figure 2-14a) (Ewing and Galloway, 2019). This is a major Gulf Coast prograding delta system located primarily in the ancestral Mississippi trough that encompassed central Louisiana and southern Mississippi (Galloway, 1968). The Houston Delta, supplied by a bed-load fluvial system, was the largest and was sand dominated. East of the Houston Delta, shore-zone facies deposits separated the Houston Delta from the smaller Holly Springs Delta system. The Holly Springs Delta was the first Cenozoic Delta to be aligned with the axis of the later Central Mississippi fluvial-delta system. The very high rate of sediment influx ($150,000 \text{ km}^3/\text{Ma}$) rapidly prograded the delta and shore-zone deposits towards the shelf edge and offlapping onto the continental slope (Galloway et al., 2000; Galloway et al., 2011).

Two transgressive events bound the Middle Wilcox at the base and top. The early transgressive event deposited the Big Shale, and the later transgressive episode deposited the Yoakum Shale. During Middle Wilcox deposition (Late Paleocene-Early Eocene), the LaSalle wave-dominated delta and the fluvially-dominated Calvert delta supplied sufficient sediment to prograde the ancestral Gulf shelf (Galloway et al., 2000). Relative to the Lower Wilcox, the Middle Wilcox sedimentation rate was roughly half (Galloway et al., 2000; Galloway et al., 2011).

During Upper Wilcox deposition, a wave-dominated delta in the Mississippi axis prograded onto the central Gulf shelf. Reworking shifted the delta westward and deposited shelf and shore zone sands covering the central Gulf (Figure 2-14b). An increase in the carbonate content and glauconite content in upper Wilcox sediments suggests an increase in marine conditions compared to lower Wilcox. An examination of Wilcox hydrocarbon producing trends in Louisiana and Mississippi led Paulson (1972) to conclude that the Wilcox is a transgressive sequence.

Figure 2-15 provides a published regional isopach and configuration map of the Wilcox Group from Hosman, 1996 as presented in the USGS Report 1416. The composite thickness of the Wilcox

Group is about 3,000 feet in east-central Louisiana (Galloway, 1968) and thickens to the south and can reach a maximum thickness of 4,000 feet (Lowry, 1988). Thickness trends mimic the Mississippi Embayment in the northeast and thicken to the south and southwest at the front of the Holly Springs Delta System.

2.1.2.8 Claiborne Group

The Claiborne Group of the Gulf Coastal Plain is widely thought of as a classic example of strata produced by alternating marine-nonmarine depositional cycles (Hosman, 1996). There are multiple sand and shale units that have been identified across the region that were deposited during the Eocene. These are (in ascending order) the Cane River Formation, the Sparta Sand, the Cook Mountain Formation, and the Cockfield Formation.

Cane River Formation

The Cane River Formation represents the most extensive marine influx during Claiborne time. In the central part of the Mississippi Embayment (Arkansas, Louisiana, and Mississippi), the formation is composed of marine clays and shales. It is glauconitic and calcareous in part, as well as containing sandy clay, marl, and thin beds of fine sand. Well-developed sand bodies are found only around the margins of the Mississippi Embayment. Regionally, the sand percentage decreases markedly to the south and southwest, so that in southeastern Arkansas, southwestern Mississippi, and all of Louisiana, the Cane River Formation contains virtually no sand. Along the flanks of the Mississippi embayment and over the Wiggins arch area the formation is generally 200 to 350 feet thick (Payne, 1972). It ranges from a thickness of 200 feet to 600 feet and deepens in bands towards the Gulf of Mexico (Figure 2-16). The Cane River is absent of the regional Sabine Uplift structure in the northwestern part of Louisiana. In the northern Louisiana region, the Cane River Formation acts as an additional regional confining unit, isolating the upper Sparta Aquifer from the deeper saline formations.

Sparta Formation

The Sparta Formation is one of the Gulf Coastal Plain's most recognized geologic units. Overlying the Cane River Formation, the Sparta extends northward to the central part of the Mississippi

Embayment deposited in a deltaic to shallow marine environment. The Sparta sand is composed of mostly very fine to medium unconsolidated quartz that is ferruginous in places to form limonitic orthoquartzite ledges. It is primarily beach and fluviatile sand with subordinate beds of sandy clay and clay. The Sparta ranges in thickness from less than 100 feet in outcrop (east and west) to more than 1,000 feet near the axis in the southern part of the Mississippi Embayment (Hosman, 1996, Figure 2-17). The Memphis sand is the equivalent formation in the northern part of Arkansas and southern Tennessee. Outcrops of the Sparta sands are in north central Louisiana along the edge of the Sabine Uplift. Note: that the Sparta is not deposited across this structural high.

Cook Mountain Formation

The Cook Mountain Formation is predominantly a marine deposit that is present throughout the Gulf Coastal Plain. It is generally less than 200 feet thick in the Mississippi Embayment but thickens in Southern Louisiana and Texas to more than 900 feet (Figure 2-18). Along the central and eastern Gulf Coastal Plain, the Cook Mountain Formation is composed of two lithologic units (Hosman, 1996). The lower unit is glauconitic, calcareous, fossiliferous, sandy marl or limestone. The upper unit is sandy carbonaceous clay or shale which is locally glauconitic. The Cook Mountain Formation thickens downdip as the clay facies gradually becomes the predominant lithologic type.

Cockfield Formation

Lithologically similar to the Wilcox Group, the Cockfield Formation is present throughout most of the Gulf Coastal Plain, but less expansive in the interior than the other units in the Claiborne Group (Figure 2-19). Its Texas equivalent is the Yegua Formation. It is composed of discontinuous and lenticular beds of lignitic to carbonaceous, fine to medium quartz sand, silt, and clay (Hosman, 1996). The Cockfield is generally sandier in the lower part. It is non-marine in origin and is the youngest continental deposit of the Eocene Series in the Gulf Coastal Plain. The Cockfield is thickest in the west-central part of Mississippi, with thicknesses ranging from 10 to 550 feet as it thins east and southeast as is shown by Hosman, 1996.

2.1.2.9 Jackson Group

The Eocene-aged Jackson Group was deposited during a regional transgressive episode which flooded the Gulf and retracted the ancestral Fayette delta landward. This landward shift of the Fayette delta reduced extra-basinal sediment supply and spread muddy shelf deposits extending from the Central Gulf to the Mississippi Embayment (Galloway et al., 2000). The Jackson Group extends from Texas to western Alabama in the Gulf Coast. The northern and southern terrigenous facies of the lower Jackson Group was formed as a destructional shelf facies by reworking of the upper surface of the Claiborne delta systems (Dockery, 1977). In Louisiana, this was comprised of the deposits from the Mississippi Embayment.

With the transgressive and regressive shoreline movement and decrease in terrigenous classic supply, the Jackson Group mudstones and claystones alternate with carbonate deposits in an offshore-nearshore environment. The Jackson Sea was the last maximum extent of sea level across the Mississippi Embayment and resulted in much of the Jackson Group deposition in a marine a nearshore origin (Sun, 1950).

The Moodys Branch Formation is the basal part of the Jackson Group and consists of fossiliferous, glauconitic sands, calcareous clays, and some limestones (Dockery, 1977). Multiple Eocene-aged fossils specific to these deposition cycles are found within the Moodys Branch. Overlying these units is the Yazoo Clay Formation. The Yazoo Clay is primarily argillaceous, with thin sand lenses, that are not regionally extensive. The clays have been described as fossiliferous and highly calcareous.

2.1.2.10 Vicksburg Group

The Vicksburg Formation lies within the Tertiary depositional wedge of the Texas Gulf Coastal Plain. Alluvial sands were funneled through broad valleys and grade seaward into deltaic sands and shales and then into prodelta silts and clays. These sediments were deposited during periods of marine transgression, separated by thicker sections deposited during period of regression in the early Oligocene. The shoreline advanced and retreated in response to both changes in the rates of subsidence and sediment supply. Rapid down dip thickening occurs along the syndepositional

Vicksburg Flexure fault zone, where there may be as much as a ten-fold increase in formation thickness.

The contact between the Eocene-age Jackson Group and the Oligocene-aged Vicksburg group is almost indistinguishable in parts of the Gulf Coast. The lower part of the Vicksburg is marine and the lithology changes between the two groups are based upon paleontological breaks, which are not seen on logs. Therefore, the Jackson-Vicksburg Group is combined as a larger “megagroup” for discussion. The Jackson-Vicksburg is mapped across the Gulf Coast region (Figure 2-20) showing that the unit outcrops almost parallel with the current Gulf of Mexico coastline as shown by Hosman, 1996.

2.1.2.11 Frio Formation

The Middle Oligocene Frio Formation is a thick sequence of mainly regressive sediments that were deposited rapidly in alluvial, lagoonal, marginal marine and deep marine environments, forming a major progradational wedge along the Gulf. Frio thickness and depth increases southwards, with localized variations occurring around salt diapirs and major faults. Non-marine sands were deposited in constantly shifting deltas and are interbedded with marine shales that were deposited during periods of local transgression.

On a regional scale, the Frio Formation and Catahoula Formation (updip equivalent) can be divided into a number of distinct depositional systems that are related spatially and in time. Four major progradational delta complexes, designated the Central Mississippi, Houston, Norias, and Norma delta systems, identified by Galloway et al., (1982b), were centered in the central and western portions of the Gulf of Mexico (Figure 2-21). Three fluvial systems, the ancestral Mississippi, Chita/Corrigan, and the Gueydan supplied sediment to the delta complexes. These four dispersion axes supplied thick shore-zone sands on the underlying muddy Vicksburg shelf (Galloway et al., 2000). In areas between major delta systems, shoreface and shallow marine environments deposited broad sandstone units interbedded with marine silts/shales during transgressive periods.

Deposition of the progradational Frio wedge was initiated by a major global fall in sea level, with subsequent Frio sediments being deposited under the influence of a slowly rising sea (Galloway et al., 1982b). Shoreline conditions remained fairly constant during Frio deposition. This, coupled

with aggregational processes, developed a thick, narrow, homogenous sand section (Galloway et al., 1982b). Strike-parallel growth faults accentuated the coast-parallel geometry of the Greta/Carancahua barrier island/strandplain system. A similar but smaller barrier strandplain system (Buna) developed by longshore currents off the eastern flank of the Houston delta system in east Texas/ southwest Louisiana (Galloway et al., 1982b).

In southeast Texas and southwest Louisiana, a transgressive, deep-water shale and sandstone unit referred to as the “Hackberry” occurs in the middle part of the Frio Formation (Bornhauser, 1960; Paine, 1968). In some places, the Frio is regionally overlain by the Anahuac Formation, an onlapping, transgressive marine shale that occurs in the subsurface of Texas, portions of southern Louisiana, and southwestern Mississippi (Galloway et al., 1982).

Within Louisiana, the Frio Formation transitions into fine-grained, mix-load dominated fluvial sediments updip, north of Beauregard Parish, ultimately pinching out in central Louisiana. To the south (offshore Gulf of Mexico) the downdip limit of the Frio is defined by large-scale fault-related juxtaposition against thick, fine-grained formations in the overlying Neogene (Swanson et al., 2013). East of the paleo-Mississippi delta, the eastern Gulf of Mexico was the site of minimal clastic influx during the Oligocene Frio time, and Frio siliciclastics grade both easterly and southerly into the time equivalent carbonates of the Heterostegina or Amphistegina shelf (Krutak and Beron, 1993; Galloway et al., 2000). Local structural highs are the result of salt diapirism and associated faulting, in combination with the regional structural fabric of major faults dipping dominantly southwards, parallel with the Gulf coastline.

To the west, a regional uplift in Mexico and explosive volcanism in southwestern United States sourced siliciclastics, volcaniclastics, and volcanic ash into the west and central Gulf of Mexico (Galloway et al., 2000). In the early Oligocene, when sea level was rising, the Frio sedimentation rate was at its highest (55,000 km³/Ma). In the late Oligocene, sedimentation rates declined as a result of the sea level increase and transgressive Anahuac Shale deposition (Galloway et al., 2011).

Updip from the Oligocene Frio Formation, the time-equivalent Catahoula Formation accumulated on the progradational continental platform inherited from Yegua, Jackson, and Vicksburg deposition (Galloway et al., 1982b). Sandstone composition in the Catahoula Formation reflects

the nature of transport of volcanic debris and distance from the volcanic source. East Texas/West Louisiana samples have heavy mineral assemblages containing ultra-stable, polycyclic, metamorphic, and igneous minerals such as rounded zircon, sphene, tourmaline, staurolite, kyanite, apatite, rutile, sillimanite, and garnet (Ledger et al. 1984). South Texas samples contain abundant hornblende, zircon, apatite, and biotite (Ledger et al., 1984). The Trans-Pecos volcanic area is the probable source for the volcaniclastic material found in the Catahoula Formation (Ledger et al., 1984). In southeastern-central Louisianan, the Catahoula Formation is characterized by gray and greenish-gray silty clays, and unconsolidated to indurated, fine- to coarse-grained alluvial sands. Farther basinward, a few limestone and marl beds are present (Rainwater, 1964b).

2.1.2.12 Anahuac Formation

As sea level continued to rise during the late Oligocene, the underlying Frio progradational platform flooded. Wave reworking of sediment along the encroaching shoreline produced thick, time transgressive blanket sands at the top of the Frio Formation and base of the Anahuac Formation (Marg-Frio) section (Galloway et al., 2000; Galloway et al., 2011). The transgressive Anahuac marine shale deposited conformably on top of the blanket sands throughout the Texas and Louisiana coastal region. The Anahuac shale has regional extent, thickening from its inshore margin to nearly 2,000 feet offshore in the Gulf of Mexico (Swanson et al., 2013). The Anahuac shale was deposited in an inner-shelf, shallow marine, proximal deltaic, distal deltaic, and slope environments (Swanson et al., 2013). In western and central parts of Louisiana, the formation mostly comprises shales with lesser sandstones. Limestones and calcareous clastics dominate in eastern Louisiana and the eastern Gulf of Mexico, where clastic influx was minimal (Swanson et al., 2013).

2.1.2.13 Miocene-aged Formations

The Miocene strata of the Gulf Coastal Plain contain more transgressive-regressive cycles than any other epoch. Rainwater (1964) has interpreted the Middle Miocene as a major delta-forming interval comparable to the present-day Mississippi Delta system. The Miocene sediments of the Fleming Group of Louisiana are equivalent to the Oakville and Lagarto Formations of Texas, and to the Catahoula, Hattiesburg, and Pascagoula Formations of Mississippi. Deposition of the

Fleming Group occurred in relatively shallow water across a broad, submerged, shelf platform constructed during Frio and Anahuac deposition. Three major depositional regimes characterize the Fleming Group. Figure 2-22 (Ewing and Galloway, 2019) presents the distribution of the lower Miocene depositional systems across the Gulf Coastal Plain.

Along the northeastern boundary of Texas, the Newton Fluvial system (also includes the Red/Rockdale River) supplied sediment to the Calcasieu delta system of Southeast Texas and Southwest Louisiana. Sands of the Newton fluvial system are fine to medium-grained, with thick, vertically, and laterally amalgamated sand lithosome geometries typical of meander belt fluvial systems (Galloway, 1989). Depositional patterns within the Oakville Formation (lower Fleming) of Southeast Texas show facies assemblages typical of a delta-fringing strand plain system (Galloway, 1989). The Calcasieu delta system is best developed in Southeast Texas in the Lagarto Formation of the upper Fleming. The Mississippi Delta system is supplied sediment from the Mississippi delta and is comprised of undifferentiated sands that comprise the Fleming Group. These delta systems consist of stacked delta-front, coastal-barrier, and interbedded delta destructional shoreline sandstones that compose the main body of the delta system, with interbedded prodelta mudstones and progradational sandy sequences deposited along the distal margin of the delta (Galloway, 1989).

The Middle Miocene represents much of the entire Miocene interval, with only the site of deposition changing in response to various transgressions and regressions. The result is a complex of interbedded shallow neritic clays; restricted marine clays, silts, and sands; and deltaic deposits of sands, silts, and clays. If a composite were made of the thickest Miocene intervals around the Gulf Basin, more than 40,000 feet of accumulated sediment would be obtained, of which about 20,000 feet were deposited in southern Louisiana (Rainwater, 1964).

Per Hosman, 1996, the complexity and heterogeneity of the myriad of facies making up Miocene strata preclude development of continuous horizons and have frustrated attempts at regional differentiation. Figure 2-23 shows that the Miocene Formation exists north of the St. Helena Parish location and extends to depths below 8,000 feet along the southeastern portion of Louisiana. Operators in the southern portion of Louisiana have historically used terminology for the sands based upon their depth interval location at their sites (*i.e.*, sand packages at 6,400 feet are termed

“6,400-Foot Sand”). Therefore, the Fleming Formation has sub-divisions of members based on the geographical locations within the Gulf of Mexico.

The Fleming Group is also differentiated into members that vary across central Louisiana to Mississippi. In central Louisiana to the Texas border, the Miocene Formation is present as a shallow aquifer-aquitard system, subdivided in ascending order:

- Lena Member – Confining Unit
- Carnahan Bayou Member – Aquifer
- Dough Hills Member – Confining Unit
- Williamson Member – Aquifer
- Castor Creek Member – Confining Unit
- Blounts Creek - Aquifer

However, in Mississippi, the Fleming Group, is subdivided in ascending order:

- Catahoula Formation
- Hattiesburg Formation
- Pascagoula Formation

Terrigenous clastics of the Miocene section were derived from the Eocene and Cretaceous terrane of the Mississippi Embayment as well as from the Appalachian terrane (Rainwater, 1964b). The Catahoula Formation is characterized by gray and greenish-gray silty clays and unconsolidated to indurated, fine- to coarse-grained alluvial sands. Farther basinward, a few limestone and marl beds are present (Rainwater, 1964b). The formation at outcrop is approximately 300 feet thick and thickens into the subsurface to approximately 1,000 feet thick near the Louisiana-Mississippi border. Most of the Miocene sediments of southern Mississippi are referred to as the Hattiesburg and Pascagoula formations. The marine shoreline was located south of the present day Mississippi shoreline during most of the Miocene, although at least two major marine transgressions are recorded in the late Miocene section (Rainwater, 1964b).

2.1.2.14 Pliocene-aged Formations

Pliocene aged formations in Louisiana, although separated into upper and lower units, are mostly undifferentiated and unnamed. Much of the Pliocene and younger sediments were deposited offshore of the present coastline. Nearer to shore, sediments were deposited under predominantly fluvial-deltaic conditions and exist as a complex of channel sands, splays, and overbank flood plain marsh deposits. Further south along the coast in southern Plaquemines Parish, the Pliocene section is approximately 6,000 feet thick (Everett et al., 1986). See Figure 2-24 for regional extent and thickness of the Pliocene Formation.

At the project site, the Pliocene-aged Formation is comprised of the Citronelle and terrace deposits Formations (Figure 2-25) and disconformably overlies the Miocene-aged Fleming Group. The Citronelle Formation was deposited on broad coalescing flood plains that occupied a wide belt between the Mississippi River and the Atlantic coast. Heavy mineral spectra of the unit indicate an Appalachian metamorphic belt source area.

The Citronelle Formation ranges in thickness from a thin veneer to a maximum of 160 feet (Brown et al., 1944). The most common feature of the Citronelle Formation is the strongly oxidized brick-red sands that form ridge crests at the surface (Brown et al., 1944). Road cuts through the Citronelle Formation exhibit large-scale fluvial cross-beds in the coarse sands and gravels. Citronelle sediments are interpreted to be erosional remnants of distributary channel deposits (Brown et al., 1944).

2.1.2.15 Pleistocene and Holocene Formations

Pleistocene sediments were deposited during a period of fluctuating sea level and represent a fluvial sequence of post-glacial erosion and deposition. The formations were deposited in both fluvial and deltaic environments, and they thicken in a southeastward dip direction as well as southwest along strike toward the southwest. Pleistocene sediments thicken along the Texas Louisiana border and in a dip direction where there was significant deposition along growth faults during Pleistocene sea level lowstands (Aronow and Wesselman, 1971). Thickest portions of the formation are along and towards the Gulf of Mexico. These sediments are relatively shallow

(approximately 2,000 feet deep) and up to 5,000 feet thick. Pleistocene sediments grade conformably into the overlying Holocene depositional units.

With the retreat of the Pleistocene glaciers, sea level began a final irregular rise to its present-day level. Holocene sediments were deposited following the final retreat of glacial ice. The slow rise of the Holocene sea level marked the beginning of the recent geologic processes that have created the present-day Texas and Louisiana coastal zone. During recent times, sediment compaction, slow basin subsidence, and minor glacial fluctuations have resulted in insignificant, relative sea level changes. The coastal zone in Louisiana has evolved to its present condition through the continuing processes of erosion, deposition, compaction, and subsidence periods. The Holocene sediments in central Louisiana unconformably overlie the Miocene-aged Fleming Formation, representing a long period of time of non-deposition and erosion. The Holocene formations in the area are deposited in terrace and coastal deposits, loess, and Mississippi River Valley alluvium. The river valley meander belts are primarily composed of point bar sandstones, with interbedded finer-grained overbank deposits and alluvium deposits. At the project site, Holocene deposits unconformably overlie the Pliocene-aged deposits, and is represented as a thin layer of Alluvium at the surface,

2.1.3 Regional Structural Geology

The interaction between sediment accumulation and gravity has played a major part in contemporaneous and post-depositional deformation of Tertiary strata. However, the continental margins and deep ocean basin regions of the Gulf of Mexico, are relatively stable areas (Foote et al., 1984). During the Late Triassic to Early Jurassic, large volumes of eroded material were deposited on areas of regional subsidence. The sediments of the Gulf Coast generally possess a homoclinal dip (southward) toward the Gulf of Mexico (Murray, 1957). The Central Gulf Coast can be divided into regions or provinces in which the regional dip has been modified. Positive regions in the area include the Sabine and Monroe uplifts, the Wiggins, San Marcos, and La Salle arches, and Jackson Dome (Figure 2-6). Structurally negative regions in the area include the North Louisiana Basin, the Houston Embayment, the East Texas Embayment (including the Tyler Basin), and various salt basins. The LaSalle Arch (northwest of site) and Wiggins Uplift (southeast of site) are two regional uplifts that created a broad low relief syncline/embayment that was present at

least through Oligocene time.

The LaSalle Arch divides the Mississippi and Louisiana Salt Basins. It is rooted within a basement high, a relict Paleozoic continental crustal block (Lawless & Hart, 1990). It is supported by basement paleo-highs with the eastern limb of the arch formed by regional tilting to the east and the western limb formed from differential subsidence to the southwest. (Lawless & Hart, 1990). The southern most extent of this feature is approximately 80 miles northwest of the St. Helena Parish site. The western limb developed syndepositionally due to differential subsidence and the eastern limb developed due the relative regional tilting to the east after deposition of the Claiborne Sparta Formation (Lawless & Hart, 1990). The central and southern regions of the arch have been hydrocarbon productive, primarily from Wilcox sands.

The St. Helena Parish site is geologically located northwest of the Wiggins Arch. The Wiggins Arch is a major east-west basement uplift that formed during Mesozoic Age. The area is structurally stable and relatively unfaulted with a regional dip towards the south-southwest. The Late Cretaceous clastic section and major Tertiary progradational wedges were less affected by growth faulting than the equivalent downdip expanded sedimentary sections located offshore beyond the Cretaceous shelf edge. The structural style of the lower coastal section of Louisiana is characterized by salt diapirism with its associated faulting and salt withdrawal basins (Galloway et al., 1982). The impact of diapirism on sedimentation is varied. If an area becomes a positive feature during a depositional period, the sedimentary section will be thinner above the diapiric structure. Conversely, the area from which the salt (or shale) has withdrawn will accumulate a greater thickness of sediment. Examples of such conditions are the rim-synclines adjacent to diapirs and, on a larger scale, salt-withdrawal sub-basins. However, this mechanism does not have an impact on the local structural geology of the injection site.

In Louisiana, there are bands of growth faults in addition to the salt domes. These fault zones include the Mamou, Tepetate-Baton Rouge, Lake Arthur, and Grand Chenier Fault zones. The closest fault zone to the project area is the Baton Rouge Fault system, which is a major regional tectonic feature that marks the Cretaceous shelf margin. This fault system strikes east west and trends along the north edge of Lake Pontchartrain, Louisiana, eastward through the Chandeleur Sound into the Gulf of Mexico (Figure 2-26).

2.1.4 Regional Groundwater Flow in the Injection Zones

Regional groundwater flow is fairly well documented in aquifers from the Holocene to mid-Miocene, but reliable data for deeper aquifers have not generally been available to date. Many of the studies for flow rates in deep saline aquifers come from the search for nuclear waste disposal sites. These studies show sluggish circulation to nearly static conditions in the deep subsurface (Clark, 1987). Studies in other areas, such as for the Mt. Simon Formation by Nealon (1982) and Clifford (1973), and the Frio Formation on the Texas Gulf Coast by Kreitler et al. (1988), have been used to demonstrate regional flow rates in the subsurface. Additional studies of Class I injection along the Gulf Coast have also provided insight movement in the subsurface.

A southern (downdip) direction of regional flow established for geologic formations in the Gulf Coast area is consistent with the theory of deep basin flows and the physical mechanisms (topographic relief near outcrops and deep basin compaction) identified as contributing to natural formation drift (Bethke et al, 1988; Clark, 1988; Kreitler, 1986). General flow of groundwater, as indicated by Kreitler et al. (1988), has been locally modified by the production of oil and gas. The bulk of the historical hydrocarbon production in St. Helena Parish is largely from the Lower Tuscaloosa reservoir where there are commercial hydrocarbon accumulations. Lateral facies changes, which can result in localized sand pinch-outs, are known to occur in the direction recharge areas (updip), therefore, background hydraulic gradients in the targeted injection zones may be highly restricted.

There are conservative estimates of background horizontal hydraulic gradients for Miocene-aged sediments which can be made from previous studies and applied to the injection formations for the St. Helena Parish site. Data published by Clifford (1973 and 1975), Slaughter (1981), and Bently (1983) provide estimated natural hydraulic gradients from three aquifers that are approximately 3,000 feet deep. The natural horizontal hydraulic gradient in these Miocene-aged aquifers ranged from 0.021 feet/yr. to 1.58 feet/yr., averaging 0.70 feet/yr. For deeper formations, such as the underlying Frio aquifers in the Texas Gulf Coast, within the depth range of approximately 6,000 feet below ground, the natural hydraulic horizontal gradient is estimated to be much smaller and, as indicated by Kreitler et al. (1988). Clark (1988) found similar sluggish-slow circulation in the

Frio Formation in the Houston area, with groundwater velocities expected to be inches to a few feet in scale.

Original formation pressure gradient data for Class I wells completed in the Frio Formation in the east Houston area substantiates the lack of a large hydraulic gradient within these deeper sandstones in the regional Gulf of Mexico. Original formation pressure gradients for the Frio Formation from the Sasol Plant Well No. 1 (WDW147), from the Lyondell Chemical Company, Plant Well 1 (WDW148) located approximately 33,000 feet northeast of WDW147, and from the Equistar Plant Well 1 (WDW036), located approximately 49,500 feet north-northwest of WDW147, are nearly identical (+0.001 psi/feet). Therefore, based on this information, estimates for the natural background reservoir velocity in Frio Injection Zone in the regional Gulf Coast are placed at inches to feet per year and in a downdip direction.

The actual value for the natural hydraulic horizontal gradients in the Injection Zone units of the St. Helena site are expected to be less than 1.0 feet/yr. Where local salt dome features are present, flow due to dissolution of salt domes is expected to be on the order of a few centimeters per year, or substantially less than 1.0 feet/yr., at distances greater than one mile from the source of dissolution according to Miller (1989). Therefore, the estimate of 1.0 feet/yr. in the easterly (downdip) direction for the natural hydraulic gradient near the proposed sequestration site is a conservative estimate for all injection zones.

2.2 LOCAL GEOLOGY OF THE SHELL ST. HELENA PARISH SITE



(Figure 2-27). The following sections detail the geology on a locally affected scale, specific to the area for the Shell sequestration project.

2.2.1 Data Sets Used for Site Evaluation

Multiple sets of data were used to evaluate and characterize the geology for the project sequestration site. Various forms of input data were available (publicly, commercially, and internal to Shell) for generating the integrated subsurface description of the Shell St. Helena Parish site.

2.2.1.1 *Offset Well Logs*

Over 2,000 wells were examined within a larger regional area including the Shell St. Helena Parish site and surrounding parishes. The larger selection of data was used to build a large structural model to incorporate details of the project at local, semi-local, parish, and regional scales. These wells used for analysis were drilled between 1928 and 2020 and have logs of varying quality and format. Many of the wells in the study area have publicly available raster image logs, while fewer contain commercially available digital data. Out of the 2,000 wells examined, 653 wells contained a digital spontaneous potential (SP) or gamma ray (GR) curve and 131 wells had digital density or delta-t (DEN or DT) curves. Of those with digital data, a subset was suitable for petrophysical evaluation and was subsequently used in the construction of the static models. Wells with digital SP logs are the primary well set used for geological structural interpretation. These wells were also used to provide information on the lateral extent and continuity of the confining and injection zones. Well logs for the project come from Louisiana Department of Natural Resources' (LDNR) Strategic Online Natural Resources Information System (SONRIS) and publicly available commercial log libraries that contain Gulf Coast data.

Published data for the formations of interest are cited in Section 2.1.2 and are listed alphabetically in Section 14.0. These include the American Association of Petroleum Geologists, Gulf Coast Association of Geological Societies, United States Geological Survey, and state agencies.

2.2.1.2 *Seismic Data*

Seismic data was used in order to confirm general structural attitudes in the area and evaluate potential faulting in the area. There are forty-six proprietary licensed two-dimensional (2D) seismic lines over a regional area of interest. Of those forty-six 2D seismic lines, only twenty-six have sufficient quality for meaningful interpretation. No three-dimensional (3D) seismic data is

available in the area. All of the 2D seismic lines available for licensing are currently owned and licensed by commercial vendors and are held business confidential. The available 2D seismic data that crosses the project area is of sufficient quality to be utilized in a seismic interpretation (Figure 2-28).

Time-depth conversion was based on updated checkshot from well to seismic match at the [REDACTED] using a consistent datum at a Frio reflector. Seismic resolution is approximately 40 feet at the Frio formation and 50 feet at the Lower Tuscaloosa, assuming a dominant frequency of 20 Hz and velocity varying from 3,000 to 4,000 m/s. The seismic data was used for fault identification and to condition the structural surfaces between well control.

Seismic data was interpreted from the twenty-six 2D seismic lines and assisted in the construction of top of structure depth maps. As the seismic quality is better in the northern portion of the study area, the northern portion has better control. The uncertainty at deeper reservoirs, Wilcox and Lower Tuscaloosa, is larger than at the shallow Frio reservoir, due to minor seismic alignment issues. All of the 2D seismic data are aligned at the Frio reservoir to correct datum issues.

Two-dimensional (2D) lines were interpreted with the intent to further understand the structural framework, mainly:

- Calibration of structural control and structural depth trends
- How far the faults cut up towards the surface
- The lateral extent and throw of major faults
- The time-depth relationship to locate and map the key reservoirs and seals
- Calibration as to which units are juxtaposed across the faults for understanding reservoir plumbing and potential risks to containment

2.2.1.3 Stratigraphic Test Well

Shell plans to drill two Class V Stratigraphic Test Wells in the 4th quarter of 2022 and the 1st quarter of 2023 to appraise the storage complex. These appraisal wells have been designed to meet

Class VI injection construction and testing standards. These wells will be drilled and tested in accordance with the “*Pre-Operational Testing and Logging Plan*” submitted in **Module D**. The data collected will include a vast suite of logs, whole and rotary core, and formation testing to provide site-specific details that will pertain to the Shell St. Helena Parish site. Data will be collected at future dates and used to reduce uncertainties and support assumptions made in the initial permit application.

2.2.2 Local Stratigraphy

The injection and confinement system present beneath the St. Helena Parish site is composed of sediments that range in age from Late Cretaceous to Holocene (Figure 2-1). The local stratigraphy is established on a type log (Figure 2-2) and used as a basis for correlating with the offset well data. Using this type log, the following local stratigraphic formations were evaluated for potential viability for a sequestration complex:

- Tuscaloosa Group
- Eagle Ford Formation (Eutaw Equivalent in Mississippi)
- Austin Chalk (Selma Chalk Equivalent in Mississippi)
- Midway Shale
- Wilcox Formation
- Claiborne Group
- Frio Formation
- Anahuac Formation
- Miocene Formation
- Holocene Formation

At the St. Helena Parish location, there are three proposed injection zones: Frio, Wilcox, and Lower Tuscaloosa Formations. These injection zones are confined by the overlying Frio Confining Zone. This zone is comprised of the Upper Oligocene Anahuac Formation, which records a significant transgression across the Oligocene Gulf Coast and the shales of the Lower Miocene Formation. There has been no production or injection into the Frio Formation in the area

surrounding the sequestration site. Note: Regional publications may have equivalents of formations in the near area and are identified above with the nomenclature.

In the Shell project area, these three primary reservoir injection intervals are identified as the “storage complex” zone. Each zone has an overlying containment interval, but the storage complex, as a whole, is capped by a Miocene/Oligocene aged “Primary” Confining Zone.

The following discussion defines and briefly describes the formations of interest that underlie the surface in the project area, beginning with the Miocene/Oligocene aged combination for the Frio Confining Zone and ending with the Lower Tuscaloosa Injection Zone, the deepest targeted injection zone. Gross isopach maps have been developed for the local area for each of the proposed regulatory zones. All maps referenced in this discussion are contained in Appendix A – Local Geologic Maps (see Table 2-1).

Shales of the Lower Miocene and the Oligocene Anahuac Formation (including Heterostegina Lime) collectively are called the Frio Confining Zone (above the Frio Formation), and this is considered the “Primary” Confining Zone for the St. Helena Parish site. The Anahuac lithologies in eastern Louisiana contain abundant carbonate that grades to the west into clastic shales (Swanson, S. and Karlsen, A. 2009). The Frio Confining Zone thickens from approximately 200 feet to 550 feet from northeast to southwest across the site area (Figure A.1). The Frio Confining Zone is characterized by abundant high resistivity high density streaks and lithologies, which are calcareous shales with occasional carbonate beds and/or calcite cemented sandstones, and minor discontinuous silty sands, interpreted from the wireline logs.

The Middle Oligocene Frio Formation is a thick sequence of deltaic, coastal, and marine deposits across the project area. Sediment was predominantly sourced from the paleo-Mississippi delta system and the axis of deposition shifted toward the west through the end of the Oligocene (Figure 2-21). East of the paleo-Mississippi delta in Louisiana, the Frio is characterized by minimal clastic influx, with siliciclastics grading both easterly and southerly into the time equivalent carbonates of the Heterostegina or Amphistegina shelves (Krutak, P.R. and Beron, P., 1993; Galloway et. al., 2000). Ultimately, the Frio is capped by the Upper Oligocene Anahuac Formation, which records a significant transgression across the Oligocene Gulf Coast. As with the Frio Formation, the

Anahuac lithologies in eastern Louisiana contain abundant carbonates that grade to the west into clastic shales (Swanson, S. and Karlsen, A. 2009).

The updip extent of the Oligocene sedimentary wedge occurs approximately 100 miles north of the project area in Mississippi, where the Miocene is observed to directly overlay the Eocene Jackson group in outcrop (Swanson, S. and Karlsen, A., 2009). The Frio gross thickness increases slightly downdip from approximately 1,300 feet in the northeast to 1,400 feet in the southwest (Figure A.2).

The Paleocene-aged Wilcox Group is a thick clastic succession that flanks the margin of the Gulf Coast Basin. This geologic group contains fluvial and deltaic channel-fill sand bodies distributed in a matrix of lower permeability inter-channel sands, silts, clays, and lignites. Most of the sands are distributed in a dendritic pattern, indicating a predominately fluvial depositional environment (Fogg et al., 1983).

The Wilcox Group is divided into the Lower, Middle, and Upper intervals. The semi-regional Yoakum Shale divides the Upper and Middle Wilcox, and the Big Shale Marker, which separates the Middle and Lower Wilcox. During Wilcox Group deposition, the Laramide Orogeny displaced the Paleocene shelf eastward from the relict Lower Cretaceous reef and formed Laramide uplands which sourced the majority of sediment (Galloway et al., 2000; Galloway et al., 2011). The East Texas Basin ceased to be a marine basin during the Tertiary and Quaternary Periods when major Eocene, Oligocene, Pliocene, and Pleistocene depocenters shifted toward the Gulf of Mexico. The Wilcox gross thickness is approximately 4,000 feet across the Shell St. Helena Parish site (Figure A.3)

The Late Cretaceous Lower Tuscaloosa formation at St. Helena Parish site unconformably overlies the Early to Middle Cretaceous deposits of the dominantly carbonate Washita and Fredericksburg groups (Mancini E. A. et al., 1987) (Woolf, 2012). Known as the ‘mid-Cenomanian unconformity’ or the ‘mid-Cretaceous sequence boundary,’ this unconformity likely reflects a concurrent tectonic uplift and sea level fall that resulted in significant downcutting and incision into Washita/Fredericksburg group during the mid-Cenomanian time. At the regional scale, the Tuscaloosa formation deposits are sourced by the paleo-Ouachita and Appalachian Mountains to

the north and northeast. The Tuscaloosa Formation above the basal unconformity is divided into Lower, Middle and Upper Tuscaloosa in Mississippi and Alabama. The Lower Tuscaloosa is then divided into three units, called ‘Massive, Stringer, and Pilot sands’ in Mississippi and Alabama. However, the ‘Stringer sand’ of the Lower Tuscaloosa and the Upper Tuscaloosa both thin to the south and west and are not present in the project area in Louisiana. The Lower Tuscaloosa and Tuscaloosa Marine Shale are conformably overlain by the Eagle Ford Shale in the local area (Woolf, 2012).

The Lower Tuscaloosa ‘Massive’ sand in the Shell project area is interpreted as compound, incised valley fill deposits comprised of aggrading to backstepping fluvial (braided and meandering river) and estuarine facies resulting from sea level rise following mid-Cenomanian incision. Major existing structural features influenced the subsequent fluid flow and sediment deposition, including the western and eastern Wiggins arches and the Cretaceous shelf edge in the regional proximal to the Shell prospect site (Stephens, 2009), (Woolf, 2012).

The early fluvial deposits grade downdip (southwest) of the Shell St. Helena Parish site into associated unconfined, valley-mouth deltaic deposits which are later reworked during continued marine transgression. This section is highly expanded south of the Shell project site in association with large growth faults near the paleo-Cretaceous shelf edge. As marine transgression continued, the massive sand is overlain by low overall net to gross ‘backstepping’ deposits of nearshore marine and marine bar complexes, which are finally overlain by the fully marine capping sediments of the Tuscaloosa Marine shale and the Eagle Ford. The gross thickness (True Vertical Thickness (TVT)) of the Lower Tuscaloosa Injection Zone at the local site ranges from approximately 200 feet in the central injection area to greater than 400 feet south downdip to the southwest as the section expands near the paleo-shelf (Figure A.4). The thick Eagle Ford/Tuscaloosa Marine Shale section (approximately 1,200 feet TVT) can be correlated across the St. Helena Parish site between the base of the Austin Chalk and the top of the Lower Tuscaloosa Injection Zone. A maximum flooding surface mapped inside this interval, entitled the ‘High Resistivity Zone’ (Rouse et al., 2018). The top of the ‘High Resistivity Zone’ within the Tuscaloosa Marine Shale records the maximum seal level rise and drowning of the incised valleys (Woolf, 2012) (Ambrose, 2015) (Shell internal research). The gross thickness of the ‘High Resistivity

Zone' ranges from 75 feet to 125 feet in the Shell St. Helena Parish project area. This 'High Resistivity Zone' serves as the Confining Zone for the Lower Tuscaloosa Injection Zone.

The top of the 'High Resistivity Zone' within the Tuscaloosa Marine shale records the maximum seal level rise and drowning of the incised valleys (Woolf, 2012) (Ambrose, 2015) (Shell internal research). This marine shale serves as the local confining zone for the Lower Tuscaloosa reservoir.

2.2.3 Local Structure and Faulting

The Shell St. Helena Parish site is located in a structurally quiescent area updip of the paleo-Cretaceous shelf margin (Figure 2-29). The Cretaceous shelf margin exhibited control on structures and depositional architecture through much of the Cenozoic, with relatively low dips and structural complexity north of the shelf margin and increasing complexity and structural dips to south. The Shell St. Helena Parish site exhibits low dips (1-1.5 degrees) and minimal faulting only clearly observed in the deepest stratigraphic level of the Lower Tuscaloosa.). Downdip of the project site and the paleo-Cretaceous shelf margin, sediment loading from large paleo-delta systems caused into-the-basin growth faulting and local structuration associated with salt withdrawal (Salvador, 1991; Galloway et al., 2000). Top of Structure maps have been developed for the local area for each of the proposed regulatory zones. All maps and cross sections referenced in this discussion are contained in Appendix A – Local Geologic Maps (see Table 2-1).

As presented by the structure and isopach maps prepared for the Shell St. Helena Parish site [40 CFR 146.82(a)(3)(ii)], there is no evidence of faults or subsurface structures in the delineated AoR (Figures A.5, A.6, A.7, A.8). Low throw, minor fault surfaces were interpretable from available 2D seismic and supported by available field-scale maps of the Lower Tuscaloosa in the public domain (Yuma Energy, 2014) outside the AoR (Figure A.8). These faults were included in the greater site evaluation and computational modeling (as discussed in **Module B**). The fault(s) interpretation has a high degree of uncertainty with respect to continuity and amount of throw at the Lower Tuscaloosa level. The vertical resolution of the 2D seismic data is approximately 50 feet at the Lower Tuscaloosa level and the fault offset is near 50 feet, therefore making the faults difficult to interpret. The faults are likely expressed as a series of en echelon fault segments as opposed to singular continuous fault planes (Yuma Energy, 2014).

Faults exhibit down to the SW offset (normal faults into the paleo-basin) and have approximately 50-70 feet of throw that decreases up section. Based on evaluation of shale content, fault offset, the fault-related shale-gauge ratio, and associated fault transmissibility the faults are not considered to be a dynamic barrier to flow or pressure dissipation, and at low risk to containment (discussed in Section 2.5 below and in **Module B**). The Confining and Injection Zones within the AoR for the St. Helena Parish site are all laterally continuous and free of transecting, transmissive faults or fractures (to be confirmed with collection and evaluation of site-specific appraisal data) as presented in two cross sections (Figure A.9 – along strike (W-E) and Figure A.10 along dip (N-S)). A thorough literature search, interpretation of the available site-specific seismic data, creation of structure and isopach maps using available well data, and dynamic evaluation (discussed in **Module B**) indicates that potential faulting in the larger project area would not compartmentalize the proposed Injection Zones (Frio, Wilcox, and Lower Tuscaloosa) or permit vertical movement of fluids into a USDW or freshwater aquifer.

2.3 DESCRIPTION OF THE CONFINING AND INJECTION ZONES

This section contains the information on the confining and injection zones for the St. Helena Parish sequestration site per the 40 CFR 146.82(a)(3)(iii) standard. Details pertaining to the formation characteristics, lateral and vertical extent, and mineralogy are identified for each zone of interest. Demonstration of security for injection includes a geologic containment demonstration and the absence of vertically transmissive faults that could form breaches of the containment system.

A confining zone is defined as “a geologic formation, group of formations, or part of a formation stratigraphically overlying the injection zone(s) that acts as barrier to fluid movement.” For the Shell St. Helena Parish site, the “Primary” confining zone is designated as the Frio Confining Zone (comprised of the Heterostegina Limestone and Anahuac, as well as the correlative shale in the Lower Miocene), located between -4,125 feet and -4,538 feet TVDSS (depths based upon the type log presented in Figure 2-2). Furthermore, alternating saline sands and shale layers in the Miocene-aged formation overlying the Frio Confining Zone will act as additional containment intervals and barriers to vertical flow, providing an added measure of fluid confinement. Geophysical well logs will be generated during the testing of the appraisal wells to provide site specific depths of the Frio Confining Zone.

An injection zone is defined as “the geologic formation, group of formations, or part of a formation that is of sufficient areal extent, thickness, porosity, and permeability to receive carbon dioxide through a well or wells associated with a geologic sequestration project.” Injection targets have been usually identified as formations below a depth of 3,000 feet to ensure CO₂ stays in the supercritical phase. Three sequestration reservoirs have been identified (depths are based upon the type log presented in Figure 2-2 and will be updated with site specific data acquired during the testing of the appraisal wells). All depths are presented TVDSS.

1. Frio Formation: - 4,538 feet to - 6,116 feet;
2. Wilcox Formation: -7,443 feet to -11,583 feet; and
3. Lower Tuscaloosa Formation: -14,039 feet to -14,255 feet

All targeted geologic intervals have the necessary characteristics to be effective sequestration reservoirs and are located more than 2,000 feet below the lowermost aquifer that meets the criteria for being a USDW (less than 10,000 mg/l total dissolved solids content) at the Shell St. Helena Parish site.

2.3.1 Confining Zones

Demonstration of security for injection includes a geologic containment demonstration and evidence of the absence of vertically transmissive faults that could form breaches of the containment system. In accordance with the EPA 40 CFR §148.21(b) the confining zone is a laterally extensive layer that restricts the vertical flow of injectate due to sufficiently low porosity and permeability.

At the Shell St. Helena Parish site, the identified the Primary Confining Zone is the Frio Confining Zone. This confining zone is at a depth of approximately -4,500 feet TVDSS and is approximately 450 feet thick TVT across the AoR (Figure A.1 in Appendix A).

The deeper Wilcox and Lower Tuscaloosa injection reservoirs are overlain by thick, regionally extensive shales that will act as internal secondary seals for containment and restrict vertical migration out of an authorized permitted zone. As such, understanding shale characteristics in the gulf coast is required.

As there is currently no site-specific data for the proposed confining zone, shale porosities via published literature were reviewed as part of the seal efficiency assessment. These published shale porosities were used to estimate permeabilities and entry pressures (via understanding textural components such as pore throat size) in the proposed confining zone. Although log evaluation of the shales may indicate high total porosity (as defined on the “*Area of Review and Corrective Action Plan*” submitted in **Module B**), a review of published literature was used to evaluate effective porosities as an indicator of the clay bound volume.

Effective shale porosities developed for Gulf Coast shales are presented in Porter and Newsom (1987) and shown on Table 2-2. These minimum effective shale porosities decrease as a function of depth due to lithification and no local overpressures are assumed. The "effective" shale porosity,

which discounts the bound water within the clay structure as well as water contained in dead-end pores, represents an appropriate choice of a porosity value for such a calculation.

Using the Porter (1987) relationship for the minimum effective porosity in a shale versus depth, the maximum porosity in the shales is expected to range between 11% for shales above the Frio Injection Zone and 9% for shales below 7,000 feet. Effective porosities are expected to be less than 11 percent below the Lower Tuscaloosa Injection Zone.

Site specific core data will be collected from the drilling of two appraisal wells for the site. Core analysis will be used to determine mineral composition and petrophysical characteristics of the sealing formations, as well as geomechanical properties such as ductility.

2.3.1.1 Primary Confining Zone – Frio Confining Zone

Shales of the Lower Miocene and the Oligocene Anahuac Formation (including Heterostegina Lime), collectively called the Frio Confining Zone, are considered the Primary Confining Zone for the St. Helena Parish site. The Anahuac lithologies in eastern Louisiana contain abundant carbonate that grades to the west into clastic shales (Swanson, S. and Karlsen, A. 2009). There is no available core, x-ray diffraction (XRD) or image information for the Frio Confining Zone in publicly available data relevant to the St. Helena Parish site. From available log evaluation, the Frio Confining Zone is characterized by abundant high resistivity, high density streaks that exhibit fast sonic transit times (indicating low porosity/permeability). Lithologies interpreted from the wireline logs are calcareous shales with occasional carbonate beds and/or calcite cemented sandstones and minor silty or sandy sand stringers.

Additional site-specific data will be collected during the drilling of two appraisal wells. Core data and analysis, along with a comprehensive suite of logging and formation testing has been developed to collect data focused on the Confining Zone. This data will be updated into the site characterization and modeling to reduce uncertainties based upon lack of site-specific data. The wells will be constructed, tested, and logged in accordance with Class VI standards set forth by the USEPA, for potential future conversion. Detailed information on the data acquisition is contained in the “*Pre-operational Testing and Logging Plan*” contained in **Module D**.

2.3.2 Injection Zones

A carbon dioxide sequestration injection zone is defined as “the geologic formation, group of formations, or part of a formation that is of sufficient areal extent, thickness, porosity, and permeability to receive carbon dioxide through a well or wells associated with a Geologic Sequestration project.” Sandstones of the Frio, Wilcox, and Lower Tuscaloosa Formations contain the necessary characteristics to be effective injection zones at the Shell St. Helena Parish site. The Shell injection zones have been designated as follows:

- Injection Zone 1 – Frio Formation
- Injection Zone 2 – Wilcox Formation
- Injection Zone 3 – Lower Tuscaloosa Formation

All characteristics for the proposed injection zones are discussed in the following sections. Please note, that the porosity type is highly dependent on the mineral composition of the rock and defines how much pore volume is accessible to reservoir fluids, *i.e.*, ratio of total and effective porosities. Primary intergranular porosity results from preservation of pore space after deposition and lithification of sediments. Microporosity, which is associated with clays, is present in the matrix and greatly affects the volume of effective porosity accessible to reservoir fluids. As the Frio and Wilcox formations are void of production, little interest, and therefore little site-specific data, is currently available

2.3.2.1 *Injection Zone 1 – Frio Formation*

The Oligocene-aged Frio Formation consists of an interbedded sandstone and shale sequence that rests conformably on the Vicksburg Shale. The uppermost portion of the strata is comprised of a limestone, calcareous sandstone of the Anahuac Formation (Howe, 1962), most specifically the Heterostegina Limestone which has been identified as a component of the Primary Confining Zone. There is little to no core data publicly available from the Frio formation in St. Helena Parish. Therefore, details are provided from surrounding parishes in east Louisiana.

The depositional environmental of the Frio Formation in the project area is deltaic and comprised of marginal marine sandstones and shales (progradational wedge, westward marching) overlain by the transgressive Anahuac shale; coeval with off-axis carbonate shelf (Amphistegina).

Total mineralogy and clay mineralogy available from the CoreLabs RAPID™ database (Gulf of Mexico Regional Oligocene study) indicate the Frio injection zone is dominated by quartz with progressively minor components of feldspar, clay, and calcite (Appendix B, Table B.1). The clay component is primarily kaolinite, illite, chlorite and mixed illite/smectite (Appendix B, Table B.2). (This dataset was purchased from the CoreLabs RAPID™ database and is, therefore, quantitative confidential business information (CBI) which is included in **Appendix B**).

Porosity and horizontal permeability for the Frio Injection Zone in the Shell St. Helena Parish site is estimated using a publicly available core data collated from SONRIS and the Louisiana Geological Survey for the Frio reservoir within 50 miles of the Baton Rouge area near the Shell St. Helena Parish site. Porosity ranges from 16% to 30% and the horizontal permeability ranges from 0.06 mD to 2,000 mD from available core data.

Expected Zone Capacity



This is based upon the current understanding of porosity, permeability, thickness, and lateral extent and will be updated after collection and calibration to site specific data. Specific modeling parameters related to the relative permeability, saturation curves, and compressibility of the formation and injectate characteristics are contained in the “*Area of Review and Corrective Action Report [40 CFR 146.84(b)]*” submitted with this permit application in **Module B**.

2.3.2.2 *Injection Zone 2 – Wilcox Formation*

In lieu of site-specific core data and due to limited published data for the St. Helena Parish site, additional details on the proposed Wilcox Injection Zone is supplied from petrophysical analysis from logs in the project area. The Wilcox in southwestern Mississippi consists of interbedded shallow marine, brackish, and alluvial sand and shale (Rainwater, 1962).

Mineralogy and Petrology

A Wilcox regional study ternary diagram published by the BEG shows Lower and Upper Wilcox XRD results from different locations along the Gulf Coast (Figure 2-30). The results show these sands within the feldspathic litharenites classification. Pore types are largely primary intergranular, with microporosity from secondary dissolution of lithic fragments. Quartz overgrowth is identified but limited. Mechanical compaction and quartz cementation were the most important porosity-reducing diagenetic events identified by Dutton and Loucks, 2014. Please note that this applies to both the Upper Wilcox and Lower Wilcox sub-divisions.

The Upper Wilcox is composed of abundant amounts of quartz, mica, and carbonaceous material as described by Glawe and Bell, 2014. Additionally, traces of glauconite and pyrite have been identified as minerals with the uppermost Wilcox. Lowery (1988) described the varying facies associated with the Upper Wilcox as containing extensive burrows, shell debris and bioturbated sandstones along the stable shelf margin. Much of the facies are missing internal physical structures, such as cross-beds. Glawe and Bell (2014) also described thin carbonate rich beds in a core sample that were either calcareous fossils, limestone concretions, or calcite cements. Land and Fisher (1987) determined that carbonate cement was the dominant cement in the shallower onshore Wilcox sands.

Porosity and horizontal permeability for the Wilcox Injection Zone in the Shell St. Helena Parish site is estimated from log evaluation and porosity to permeability transforms using publicly available core data. This core data was collated from SONRIS and the Louisiana Geological Survey for the Wilcox Formation within 50 miles of Baton Rouge. Porosity ranges from 10% to 26% and the horizontal permeability ranges from 0.02 mD to 500 mD from available core data.

Expected Zone Capacity

The Wilcox reservoir, located between the deeper Lower Tuscaloosa and shallower Frio Formations, will be appraised during the drilling and testing of the Frio and Lower Tuscaloosa appraisal wells. If the early appraisal analysis confirms feasibility of the Wilcox Injection Zone, then additional required data for Class VI wells, such as water sample, core and well testing, will be collected at a future date. [REDACTED]

[REDACTED] The Wilcox Formation is included as a proposed injection zone in this permit application as it is situated between the two primary target sinks and will be adequately studied for future storage.

The injection rates and storage capacity are estimated based upon the current understanding of porosity, permeability, thickness, and lateral extent and will be updated after collection and calibration to site specific appraisal data. Specific modeling parameters related to the relative permeability, saturation curves, and compressibility of the formation and injectate characteristics are contained in the *“Area of Review and Corrective Action Report [40 CFR 146.84(b)]”* submitted with this permit application in **Module B**.

2.3.2.3 *Injection Zone 3 - Lower Tuscaloosa Formation*

The Lower Tuscaloosa Formation is separated from the base of the Wilcox (Injection Zone 2) by over 2,400 feet of impermeable layers of the Midway Shale, the Austin Chalk (Selma Formation in Mississippi), and the Eagle Ford Formation (Eutaw Formation in Mississippi). This thick sequence of impermeable formations provides additional containment barriers for the Lower Tuscaloosa Sand Injection Interval.

Regional core analysis data of the Midway Shale was procured from the Mississippi DuPont Delisle MDEQ Class I Permit Application – Well No. 5. An x-ray diffraction (XRD) analysis indicated that the core samples consisted of mainly of clay and quartz. The dominant mineralogy was illite/smectite with calcite and quartz. Minor components of plagioclase and potassium feldspars were also present. The predominant lithology of the Midway Shale is a dark gray to black, fissile, carbonaceous, and pyritic shale. The core samples occasionally included thin fine laminae of fine to very fine, moderately sorted micaceous and carbonaceous sands. Overall, the 1,200 feet of cored Midway Shale at the Delisle Site was described as uniform throughout, with swelling illite dominated clays. The formation has little to no sands, which bolster the low to impermeable characteristics that are expected to be representative of the St. Helena Parish site.

Mineralogy and Petrology

The lithology of the Lower Tuscaloosa Injection Zone is a consolidated siliciclastic reservoir, which consists of cross-bedded conglomerates, sandstones, and muddy sandstones. XRD data for eighteen samples in St. Helena Parish were available from the CoreLabs RAPID™ database (Lower Tuscaloosa Formation study). The analysis indicated that the total mineralogy of the formation is predominately quartz, with lesser clay, and minor amounts of dolomite and calcite (Appendix B, Table B.3). The clay mineralogy was comprised of chlorite, kaolinite, and illite (Appendix B, Table B.4).

The Lower Tuscaloosa sands are the subject of a CO₂ flood in Cranfield Field, located in Adams County, Mississippi (just north of the St. Helena Parish site). The Lower Tuscaloosa has been extensively studied at Cranfield as part of the Department of Energy's carbon sequestration efforts in conjunction with the CO₂ flood. This work has been performed by the Bureau of Economic Geology, located at the University of Texas at Austin, under the auspices of SECARB, the Southeast Regional Carbon Sequestration Partnership. The Lower Tuscaloosa Formation is composed of fining-upward fluvial cycles consisting of basal cherty conglomerates overlain by coarse-grained light gray sandstones (Kordi et al, 2010). Within the sandstone beds, chlorite is a major cement type that helped preserve initial porosity and permeability by preventing secondary mineralization in the pores (Kordi et al., 2010). Secondary porosity results from rock fragment dissolution (Kordi et al., 2010). In low permeability zones, destruction of the reservoir quality includes compaction, carbonate and quartz cements, and the formation of other authigenic minerals (Kordi et al., 2010). The sandstone beds are separated by laminated mudstones and siltstones (Hosseini et al. 2012).

Porosity and horizontal permeability for the Lower Tuscaloosa in the Shell St. Helena Parish site is estimated using commercially available core data from the CoreLabs RAPID™ database (Lower Tuscaloosa Formation study). Porosity ranges from 8% to 26% and the horizontal permeability ranges from 0.05 mD to 500 mD from available core data. This is aligned with transmissibility and permeability of Lower Tuscaloosa sands estimated at several injection well sites north of the Shell St. Helena Parish site in Mississippi. Permeability data for the Lower Tuscaloosa sands are available from core, well tests, and modeling studies (Lu et al., 2013; Hosseini et al., 2012; among

many others) at the Cranfield test site. Core permeabilities from Field Well 29-12 exceed 100 millidarcies, as do permeabilities from the 31F-2 DAS test well. Some core permeabilities range up to 1,000 millidarcies (Lu et al., 2013).

Expected Zone Capacity



This is based upon the current understanding of porosity, permeability, thickness, and lateral extent and will be updated after collection and calibration to site specific data. Specific modeling parameters related to the relative permeability, saturation curves, and compressibility of the formation and injectate characteristics are contained in the *“Area of Review and Corrective Action Report [40 CFR 146.84(b)]”* submitted with this permit application in **Module B**.

2.4 GEOMECHANICS AND PETROPHYSICS

This section details the mechanical rock properties and in situ fluid pressures per the 40 CFR 146.82(a)(3)(iv) standard and includes information on ductility, stress, pore pressures, and fracture gradients of the sequestration complex. Mechanical rock properties describe the behavior of the framework rock matrix and pore space under applied stresses. Mechanical rock properties are described by Elastic properties (Young, Shear, and Bulk Modulus as well as Poisson’s ratio) and inelastic properties (ductility, creep, clay swelling).

Changes in in-situ stresses and strains, ground surface deformation, and potential risks, such as new caprock fracture initiation and propagation or preexisting fault opening, and slippage are crucial geomechanical aspects of large-scale and long-term CO₂ storage (Rutqvist, 2002). It is important to assess all the geomechanical risks before commencing the operations of CO₂ injection. Although all the processes involved are not always fully understood, integration of all available data, such as ground surveys, geological conditions, micro-seismicity, and ground level deformation, has led to many insights into the rock mechanical response to CO₂ injection (Pan et al, 2016).

Site specific data will be collected during the drilling and testing of two appraisal wells. Geomechanical data across the Injection Zone and the Confining Zone will be collected, along with laboratory analyses of recovered core samples. The appraisal wells will be drilled in accordance with the construction and testing standards for Class VI wells set forth by the USEPA, for potential conversion at a future date. Details on the data acquisition are contained in the “*Pre-operational Testing and Logging Plan*” contained in **Module D**.

2.4.1 Ductility

Ductility refers to the capacity of a rock to deform to large strains without macroscopic fracturing. Ductile deformation is typically characterized by diffuse deformation (*i.e.*, lacking a discrete fault plane) and is accompanied on a stress-strain plot by a steady state sliding.

Yield point, compared to the sharp stress drop observed during brittle failure. In other words, when a material behaves in a ductile manner, it exhibits a linear stress vs. strain relationship past the elastic limit.

The ductility of a shale top seal is a function of compaction state. Uncompacted, low-density shales are extremely ductile and can thus accommodate large amounts of strain without undergoing brittle failure and loss of top seal integrity. Inversely, highly compacted, dense shales are extremely brittle and may undergo brittle failure and loss of top seal integrity with very small amounts of strain. Figure 2-31 shows the relationship between ductility and density observed for 68 shales by Hoshino et al (1972).

Other parameters are expected to influence ductility, such as confining pressure and time. The mechanical behavior of rock formations is not constant but changes with various conditions, such as progressive burial as the top seal is converted from a mud to a more competent material, thus developing higher strength. Compaction decreases ductility while confining pressure increases ductility. Compaction is typically related to depth. Figure 2-32 from Hoshino et al (1972) shows density and ductility vs. brittleness against depth. Ductile samples are displayed as gray circles and brittle samples are displayed as black circles. Ductile shales did not fracture whereas brittle shales did fracture during the experiment. According to the figure, a low-density shale at a depth

of 500 m is more ductile than a highly compacted shale at a depth of 5,000 m. Finally, ductility varies not only with depth of burial but also with time.

Holt et al (2020) emphasize how important it is to characterize to what extent shales may fail in a brittle or ductile manner, in both cases causing possible hole instabilities during drilling, and in the case of ductile shales, enabling permanent sealing barriers. Triaxial tests, creep tests, and other tests tailored to follow the failure envelope under simulated borehole conditions were performed on two soft shales. The more ductile shale was proved to form barriers both in the laboratory and in the field. By comparing their behavior, the authors noticed that the ductile shale exhibits normally compacted behavior while the more brittle shale is over-compacted. This points to the stress history and possibly the grain cementation as keys in determining the failure mode. Porosity, clay content, ultrasonic velocities, unconfined compressive strength, and friction angle may be used as other indicators of brittle or ductile failure behavior.

Contrary to borehole collapse during drilling, shale ductility has however proved to be useful. Successful natural shale barriers have been reported, where the annulus between casing and formation has closed after drilling, forming an efficient seal (Williams et al, 2009; Kristiansen et al, 2018). This is of large importance for plug and abandonment of oil wells but may also be considered as an alternative to cement in new wells, provided that the barrier has sufficient thickness and is formed fast enough. Obviously, the well needs to be completed in a stable condition prior to the formation of the barrier.

On another note, ductile formations have a higher propensity to creep than brittle ones under the same loading conditions. Creep is the tendency of solid material to deform permanently under a certain load that depends on time and temperature. Typically, creep is divided into three distinct stages which are primary creep (transient elastic deformation with decreasing strain rate), secondary creep (plastic deformation with constant strain rate), and tertiary creep (plastic deformation with accelerating strain rate), as summarized in Figure 2-33 from Brendsøl (2017) (see also Fjaer et al., 2008; Hosford, 2005). Unless stresses are reduced, tertiary creep eventually leads to brittle failure.

The following factors have the potential to increase or enhance creep (Kristiansen et al, 2018):

- High clay content, especially smectite,
- High shear stresses,
- Thermal deformation from heating,
- Shale/brine interaction effects.

Indeed, according to Chang & Zoback (2009), the amount of creep strain in shales is significantly larger than that in sands with less clay, which corroborates previous observations that creep strain increases with clay content. Microscopic inspections show that creep in shales appears to generate a packing of clay minerals and a progressive collapse of pore spaces. The authors observed a porosity loss and an increase of dynamic moduli in shales during creep.

Strain in uncompacted sediments is typically accommodated by creep behavior which itself may be enhanced by high clay content that induces self-sealing properties (Meckel and Trevino, 2014; Zoback, 2010; Ostermeier, 2001; Hart et al., 1995). This has major implications on the suitability of confining zones because ductile deformation of mudstone seals potential leakage pathways to the surface. These include natural pathways such as faults and man-made pathways such as well boreholes (Clark, 1987).

Loizzo et al (2017) discuss how key parameters, such as the in-situ stress and creep properties, can be measured or estimated from geophysical logs, geological and geomechanical information, and active well tests. Any sedimentary formation with a clay matrix predominantly composed of smectite is a good candidate for natural barrier. Signs of sloughing shales during drilling are an excellent indicator of this phenomenon, but a series of geophysical investigations, provided by logging while drilling or wireline logging, are recommended at the initial characterization stage. Density, neutron porosity, and possibly spectral gamma ray can clarify the mineralogical composition; these logs are routinely acquired as part of a triple combo, together with sonic wave velocities. They will be included in the formation evaluation program for the Injection Wells at the St. Helena Parish site. The processing of the logs to identify facies, extract petrophysical and mineralogical properties, and estimate the strength of the rock will also be performed.

Defining the maximum operating pressure of the natural barrier requires the knowledge of mechanical properties and far-field stresses. The characterization of rock mechanical properties (elastic properties, anisotropy, and non-linearity) has been well documented for measurements, protocols, and practices. Young's modulus and Poisson's ratio can be estimated from the compressional and shear wave velocities and density values obtained from the offset sonic logs, using standard rock physics equations.

Finally, cement evaluation logs are very effective in identifying creeping shales. In fact, they precisely measure the ultimate effect of creep, *i.e.*, the annulus bridging by a natural barrier. One log immediately after cementing and another one approximately a week later can help distinguish between cement and creeping shale.

2.4.1.1 Ductility in Gulf Coast Examples

The ductility of clay/shales both in the Injection Zone and in the Confining Zone, is a function of compaction state. Uncompacted, low-density shales are extremely ductile and can thus accommodate large amounts of strain without undergoing brittle failure and loss of integrity. However, highly compacted, dense, deep shales may be extremely brittle and undergo brittle failure and loss of integrity with very small amounts of strain. Figure 2-31 shows the relationship between ductility and density for 68 shales from the literature. All samples were deformed in compression.

Gulf Coast shales are known to exhibit viscoelastic deformational behavior that causes natural fractures to close rapidly under the action of in situ compressive stresses (Aumman, 1966; Neuzil, 1986; Bowden and Curran, 1984; Collins, 1986). Evidence of this includes rapid borehole closure often encountered while drilling and running casing in oil and gas wells along the Gulf Coast (Johnston and Knape, 1986; Clark et al., 1987). Furthermore, old abandoned (legacy) boreholes have been observed to heal across shale sections to the extent that reentering them requires drilling a new borehole (Clark et al., 1987).

This property of viscoelastic deformation behavior will cause any fractures and/or faults to close very rapidly in response to the in-situ compressive stresses, like squeezing into the fault plane from both sides. This well-known ductile (or plastic) behavior of the geologically young Gulf Coast

shales is amply demonstrated by the presence of shale diapir structures and the natural closure of uncased boreholes with time (Johnston and Greene, 1979; Gray et al., 1980; Davis, 1986; Clark et al., 1987; Warner and Syed, 1986; and Warner, 1988). Jones and Haimson (1986) have found that due to the very plastic nature of Gulf Coast shales, faults will seal across shale-to-shale contacts, allowing no vertical fluid movement along the fault plane.

In 1991, DuPont Borehole Closure Test Well was conducted as an integral part of an EPA No-Migration Petition demonstration for DuPont Sabine River Works (now INVISTA Orange) to test the natural healing of boreholes through clay/shale sections due to clay swelling and creep and to quantify natural borehole closure (Clark et al., 2005). A test well was drilled to provide additional information on the sealing effectiveness of Miocene formations, especially the clay/shales, in a simulated abandoned borehole located on the flanks of Orange Dome (salt dome) near Orange, Texas. In the testing, a worst-case strategy was evaluated, where the mechanism of swelling and plastic creep of the clay/shales was simulated by allowing the clay/shale to heal over a week's duration and then injecting fluids into the lower test sand while monitoring pressure in the next sand vertically in the section (upper monitor sand), similar to a vertical interference test. The upper gauge in the shallow monitor sand showed no change during the testing, indicating that there was no “out of zone” movement across the 90-foot thick, healed clay/shale bed. The lack of out of zone movement was confirmed via the Schlumberger Water Flow Log® that showed no migration of fluids vertically along the walls of the borehole in the healed clay/shale section.

2.4.1.2 Site Specific Ductility of the Confining Zone

To date, there are no site-specific brittleness or ductility/creep measurements area available for the confining shales and the Heterostegina Limestone specific to the AoR. All assumptions have been made using the available sonic logs, the drilling reports, and as discussed in the literature above. Ductility is assessed by measuring sample strains under applied stresses at representative reservoir conditions (*e.g.*, injection or depletion). Elastic moduli are often used as an indicator of rock creep compliance and strength, which can be related to mineral rock composition (Sone and Zoback, 2013). Site specific data will be acquired and tested on cores collected during the drilling of the injection wells (see **Module D** for the “*Pre-Operational Testing and Logging Plan*”).

2.4.2 Stresses and Rock Mechanics

In-situ stress and strain are basic concepts in the geomechanics discipline. A stress is defined as a force over an area. If a force is perpendicular to a planar surface, the resulting stress is called a normal stress. If a force is applied parallel to a planar surface, it is called a shear stress. A normal stress is called either a tensile stress if the stress is pulling the material apart or a compressive stress if the stress is compressing the material. In geomechanics, compressive stresses are conventionally shown as positive. Strain is the deformation of the rock material in response to a change in the corresponding effective stress. A normal strain is defined as the change in length (caused by the change in normal effective stress) divided by its original length. A shear strain is the ratio of the change in length to its original length perpendicular to the principal stress axes of the element due to shear stress. A volume (or volumetric) strain is the ratio of the change in volume to its original volume, also called a bulk strain, when all-around change in effective confining stress is applied. These stress and strain concepts are illustrated in Figure 2-34 (Han, 2021).

The Gulf Coast Basin is generally considered as a passive margin with an extensional (normal faulting) stress regime. In a normal faulting stress regime, the vertical stress is the greatest stress (maximum principal stress) and is typically referred to as the rock overburden. Regional literature from Eaton, 1969, indicates that the overburden stress gradient for normally compacted Gulf Coast Sediments ranges from about 0.85 psi/ft near the surface to about 1.00 psi/ft at depths of about 20,000 feet. Sedimentary rocks along the central portion of the Gulf Coastal Plain experience predominantly normal faulting, with a maximum horizontal stress oriented sub-parallel to the coastline (Lund Snee and Zoback, 2020) and a minimum horizontal stress (*i.e.*, the least principal stress) oriented orthogonal to the coastline.

Published data has been used to set the orientation of the principal horizontal stresses (Meckel et al., 2017; Nicholson, 2012; Zoback and Zoback, 1980) using regional fault-strike statistics (Figure 2-35). Geomechanical assumptions for the rock properties estimated at the St. Helena Parish site are contained in Table 2-3. The geomechanical properties of the primary Confining Zone will be further measured during the drilling and completion of the project's injection and monitor wells.

Vertical Stress: S_v

The overburden stress, S_v , for normal-faulting stress regimes is assumed to have an average gradient of 1.0 psi/ft (Nicholson, 2012). This is equivalent to the lithostatic pressure exerted by rock with an average density of 2.3 g/cm³ (Hovorka, 2018). Meckel, 2017, assumed a value of 1.00 psi/ft for the Lower Miocene in the Texas Gulf of Mexico.

For the St. Helena Parish site, the S_v is calculated by integrating the composite density log obtained from the available offset well logs. The S_v gradient varies between 0.86 psi/ft and 1.05 psi/ft.

Minimum Horizontal Stress (S_{hmin}):

Minimum horizontal stress values are estimated using Eaton's method (Eaton 1969) and analogue Biot coefficients. The Biot coefficient is the ratio of the volume of fluid change, divided by the change in bulk volume (assumption that port pressure remains constant).

The range of estimated S_{hmin} resulted in values in the range of 0.60 to 0.75 psi/ft.

$$Sh_{min} = (\nu / (1 - \nu)) * (\sigma_v - \alpha P_p) + \alpha P_p$$

Where:

S_{hmin} is the minimum horizontal stress,

ν is the Poisson's ratio,

σ_v is the vertical stress,

α is the Biot coefficient, assumed to be 1

P_p is the pore pressure.

Maximum Horizontal Stress (S_{hmax}): Maximum horizontal stress values were estimated by averaging the gradients of the vertical and minimum horizontal stresses at each depth. The S_{hmax} values are in the range of 0.75 to 0.85 psi/ft

Young's Modulus (E):

Inelastic property that describes the relation of tensile stress to tensile strain. The ability of a material to deform.

$$E = \frac{\sigma}{\epsilon}$$

Where:

E = Young's Modulus (pressure units)

σ = Uniaxial stress – or force per unit surface (pressure units)

ϵ = Strain, or proportional deformation (dimensionless)

The Young's modulus is calculated from density, P-wave and S-wave velocities using standard Rock Physics equations. Young's modulus impacts the calculation of the fracture gradient. Young's Modulus range is calculated at 7 – 12 GPa.

Poisson's Ratio (ν):

A constant that is used to determine the stress and deflection property of a material. It is a measure of the deformation of a material perpendicular to the load direction. Poisson's Ratio is also calculated from density, P-wave and S-wave velocities using standard Rock Physics equations.

$$\nu = \frac{d \epsilon_{trans}}{d \epsilon_{axial}}$$

Where:

ν = Poisson Ratio (dimensionless)

ϵ_{trans} = transverse strain

ϵ_{axial} = axial strain

Poisson's Ratio is used to calculate Sh_{min} using Eaton's method (1969). It should be noted that the Poisson's Ratio of most materials will fall within a range between 0.0 and 0.5. Lower Poisson's Ratio values indicate less deformation of the material when exposed to strain, and higher values indicate greater deformation when exposed to strain. A higher Poisson's Ratio would also indicate that the subject material would be harder to fracture. Poisson values for the site are between 0.2 and 0.3.

2.4.3 Pore Pressures of the Injection Zone

In general, the Gulf Coast subsurface can be separated into three hydrologic zones. The shallowest zone, fresh to moderately saline geologic section, corresponds to fresh waters (less than 10,000 mg/l total dissolved solids) and has a typically formation pressure gradient of 0.433 psi/ft of depth (*i.e.*, a freshwater gradient). Within the shallow interval, groundwater is directed away from the areas where the Fleming Group crops out eastward towards the Gulf of Mexico (Kreitler and Richter, 1986).

Underneath the fresh to moderately saline geologic section is what Kreitler and Richter (1986) call the “Brine Hydrostatic Section”. The transition is a mixing zone where meteoric waters mix with formation waters and this exchange prevents the buildup of pressures. Formation water salinity values range from 10,000 parts per million to 50,000 parts per million total dissolved solids (Kreitler and Richter, 1986). In the lower parts of the brine hydrostatic section, formation water salinity values range from 50,000 parts per million to 150,000 parts per million, with the bottom marked by a zone of weakly overpressured sediments (Kreitler and Richter, 1986) that transition to higher formation pressures. Kreitler and Richter (1986) propose a gradient value of 0.465 psi/ft (approximately equivalent to 9.0 pounds per gallon mud weight) to define the initial transition to overpressured sediments.

The third hydrologic zone is referred to as the overpressured zone. Overpressuring results when low permeability mudstones retard or restrict expulsion of waters from compacting mudstones (*i.e.*, mudstones are buried quicker than they can expel water). In this case, porosity of the sediments is reduced as water is expelled and a disequilibrium between increasing overburden due to sedimentation and the reduction in pore volume occurs (Zhang and Roegiers, 2010). The

remaining water in the pores must support part of or all of the overburden, causing the pore pressures of the trapped fluids to increase. This also allows for higher-than-expected porosities (Zhang and Roegiers, 2010). Regional overpressuring indicates a lack of communication with the shallower normally pressured brine hydrostatic section (Kreitler (1986), Zhang and Roegiers, (2011)).

From a practical standpoint, the top of overpressure represents a maximum depth for sequestration of carbon dioxide. For one, the system compression would need to overcome the elevated pore pressures in the overpressured intervals, requiring higher energy demands for operations. Secondly, as indicated above, the presence of overpressure indicates a compartmentalized system that does not allow pressure bleed-off. This is akin to storage in a tank that does not allow for pressures to escape the overpressured system. Lastly, in the overpressured zone the rate of pore pressure gradient increases faster than the fracture gradient, which reduces the allowable operating envelope as the pore pressure approaches the fracture pressure of the formations.

For the St. Helena Project, the targeted injection zones are all located in the second identified zone: the “Brine Hydrostatic Section.” As such, pore pressure data have been determined from not only available pressure data but can be evaluated from drilling mud weights across geologic intervals.

Note: Site-specific in-situ formation pressure will be collected during the drilling of the appraisal and injection wells at a future date. Details on testing and data acquisition are contained in the *“Pre-operational Testing and Logging Plan”* submitted in **Module D**.

2.4.3.1 Available Data Sets

Pore pressure data was located within St. Helena Parish, in the form of three wells containing limited Repeat Formation Testers (RFT) data and five wells with data in the form of mud logs. Figure 2-36 is a series of location maps identifying the location of the proposed injection wells for the sequestration project and the locations of the existing wells with data. Table 2-4 summarizes the available mud weight data.

Repeat Formation Testers

Formation fluid pressures may be obtained downhole through the use of wireline devices known as Repeat Formation Testers (RFT). Initially designed to primarily sample formation fluids, the RFT has also been applied to recorded downhole pressures, provide evaluations of downhole formation conditions (e.g., permeability and formation pressures). As the use of the tool evolved, it became more commonly used to assess reservoir pressure, recording both the pressures of the fluids within the well, and the pore pressures of the formations encountered and pressure transient due to fluid withdrawal for sampling.

Available RFT data was identified from three wells, the R.M. Carter No. 1 (LA SN: 190227), Cavenham Forest Industries SWD No. 4 (LA SN: 210847), and the Leach No. 1 (LA SN: 185101). The location of these three wells can be found in Figure 2-36 introduced above. From these three wells, five relevant data points within the Lower Tuscaloosa were identified and evaluated. All five points are at hydrostatic pressure. This data set did not allow for a correlation between DT and VES.

Mud Log Data

Mud Log Data was located for five wells in northern St. Helena Parish. Mud logs with data on mud weights and background gas levels while drilling, were located for the D. E. Wales No. 1 (LA SN: 215166), Weyerhaeuser No. 43-1 (LA SN: 252280), C.J. Cole No. 1 (LA SN: 181663), Mina Travis No. 1 (LA SN: 227762), and the Weyerhaeuser SWD No. 2 (LA SN: 238089) wells. The location of these wells is shown in Figure 2-36.

Information available on a mud log may allow for the estimation of an expected minimum pore pressure through the evaluation of locations on the mud log where increases in gas readings (both background and total gas) occur, as well as changes in mud weight as the well is drilled. The table of the records of the five mud logs are contained on Figure 2-36 and Table 2-4.

For the five wells studied, no increase in total gas was observed until the penetration of the Lower Tuscaloosa. Figure 2-37 is an example of one of the mud logs wherein a sudden spike in the total gas was observed as the well drilled into the Tuscaloosa Marine Shale. The mud weight at the time

was a 10.2 pound per gallon (ppg), corresponding to the minimum pore pressure. Additional mud weight analysis from three fields surrounding the St. Helena Parish site can be observed in the Figure 2-38. Beaver Dam and Baywood are located downdip of the project site, and Greensburg is located updip. Conclusions from this work indicated only slight overpressures were observed during drilling. All wells finished drilling with mud weights less than 11.1 ppg. The highest mud weights obtained were at total depth (TD). Most of the wells were drilled with a mud weight of 9.5 ppg or lower until reaching the Lower Tuscaloosa. Only one field, the Greensburg, saw an increase in mud weight prior to reaching the Lower Tuscaloosa.

2.4.3.2 Pore Pressure Determination Methodology

For estimating the pore pressure to be encountered at the St. Helena Parish site, a five-point prediction method was employed. This was done by subdividing the data into a table (Table 2-5). The five-point prediction method uses five different pore pressure scenarios, from absolute low to absolute high, with the idea that there will be little to no risk of encountering pore pressure variables outside of the prediction range.

This gradient is derived by first calculating the mud column gradient from wellbore mud (Table CC) from available data in the AoR. An example of a calculation, using a 9.0-lb/gal as mud weight is shown below:

$$0.052 \times 9.0 \text{ lb/gal} = 0.468 \text{ psi/ft} \quad (\text{mud column gradient, modified from Barker, 1981})$$

0.052 is a conversion factor and has units of gal/ft-in²

The results are plotted as a function of depth for the geologic formations on graphs on Figure 2-38 from all three field in the St. Helena Parish site used in the analysis.

2.4.4 Calculated Fracture Gradient

Sonic and Density logs located within the area of interest were checked against caliper logs to ensure data quality. The map in Figure 2-39 shows the location of the wells with available Sonic and Density Logs. The table on the figure lists the names of the eight wells with Sonic data with additional information. Figure 2-40 is a well section showing all eight of the wells with log

coverage presented in digital format that were used for analysis. Of the eight wells identified, the Easterly Number 1 (SN: 180858) well has the best formation coverage. However, none of the wells have shallow formation coverage. Both Sonic and Density data were quality checked using the equivalent Caliper and Gamma Ray logs.

Rock properties were calculated from the available dataset. Specifically, Poisson's Ratio, Young's Modulus, Cohesion and Friction angle. Multiple realizations were calculated, including base, low and high cases. These curves were then used to calculate both the expected Fracture Gradient and Bore Hole Stability for the proposed Injection Wells. Due to the scarcity of data, a composite log was generated to cover all intervals. Figure 2-41 is a display of the Rock Property Model for the Injection Wells. With the calculated rock property model, the Sh_{min} , Fracture Gradient, and Bore Hole Stability were then calculated.

For the shallow section (< 2,500 feet), these properties were generated from the Hauberg JH et al, well (SN: 169854). The Sh_{min} was calculated using Eaton's equation using mixed mode analysis derived from Hauser (2021) and Bore Hole Stability using STABOR (a Shell proprietary elasto-plastic finite-element model), a standardized borehole stability analysis tool within Shell (Hansen et al., 2013). The computational core of STABOR is based on the DIANA finite-element software. The required inputs for STABOR include rock properties, earth stresses/formation pore pressure, and borehole geometry. Optimum mud weight can be estimated based on the inputs and tolerable plastic strain to ensure stable borehole during drilling.

Sh_{min} is estimated by Eaton's Method (Eaton, 1969) using Poisson's ratio. Eaton's Method has been historically used by the EPA and State Regulatory agencies to define maximum injection pressures for Class I injection wells that have historically operated throughout the Gulf Coast Region. However, in Shell, we use Mixed Mode Analysis for Fracture Gradient. As evidenced by Figure 6 in Hauser (2021) (Figure 2-42), all available data points indicated that Fracture Gradient have a wide range of values between Sh_{min} and Tensile Initiation Point. Hence Mixed Mode Analysis, taking into account tensile strength of the rock, is chosen as appropriate for this analysis.

In order to further assess a range of possibilities based on the stress regime, two sets of Fracture Gradient were generated both using the base case pore pressure, one using a more isotropic stress

($0.8 \text{ Sh}_{\min} + 0.2 \text{ OBG}$) and the other a less isotropic stress ($0.5 \text{ Sh}_{\min} + 0.5 \text{ OBG}$). Figure 2-43 shows a plot of both cases, with the less and more isotropic stresses considered. Both cases can be classified as a normal faulting stress regime with the overburden stress as the maximum principal stress consistent with the stress state observed in the region.

In accordance with 40 CFR 146.88(a), Shell will operate the St. Helena Parish site at operating pressures of less than 90 percent of the calculated fracture pressure. The maximum safe operating pressures for each formation are presented in Table 2-5 and graphical form in Figure 2-44. Note that the presence of overpressure in the Lower Tuscaloosa strata is not considered in the analysis and may limit the depth of available sequestration sandstones in the area.

Site-specific testing for formation pressures in the subsurface will be undertaken during construction of project wells. Mini-frac tests on wireline or step rate tests performed after well construction, along with the results of other logs and core tests, will be used to verify that information provided in the permit application related to the fracture pressure of the injection and confining zones is correct. If the calculated fracture pressures of the injection and/or confining zones differ from the assumptions on which injection rates and pressures in this Class VI permit are based, permit conditions will be revised accordingly. Additionally, if there is/are any uncertainty or inconsistencies in calculated fracture pressures within the injection or confining zones, the maximum injection pressure limit may need to be reevaluated based on these data and may be revised to less than 90 percent of the fracture pressure of the injection zone.

2.5 SEISMICITY

An earthquake is a sudden shaking of the ground caused by the passage of seismic waves through the Earth after two blocks of rock material suddenly slip past one another beneath the Earth's surface. The plane where they slip is called the fault. The location below the Earth's surface where the earthquake starts is called the hypocenter, and the location directly above it at the surface of the Earth is called the epicenter. Seismic waves are elastic and travel at the speed of sound. These waves may be felt by humans and can produce significant damage far away from the epicenter.

The size of an earthquake can be expressed by either intensity or magnitude. Magnitude is based on an instrumental recording that is related to energy released by an earthquake, while intensity describes the felt effects of an earthquake:

Intensity - Number describing the severity of an earthquake evaluated from the effects observed at the Earth's surface on humans, structures, and natural features. Several scales exist, but the Rossi-Forel scale (before 1931) and the Modified Mercalli scale (after 1931) are the most commonly used in the United States. Intensity observations are employed to construct isoseismal maps wherein areas of equal shaking effects are contoured.

Magnitude - Instrumental measurement of the energy released by an earthquake recorded by seismometers or seismographs. The seismometers record the degree of ground shaking at a distance from the event and all stations should read similar values from the same seismic event. In other words, the magnitude of the earthquake does not change with distance and a single value describes the earthquake. Dr. Charles F. Richter introduced the Richter Scale, which measured the scale of earthquake magnitudes. Following the Richter Scale, there have been several magnitude scale modifications based on the type of seismic wave, epicenter distance, and other factors (Leeds, 1989).

Instrumental seismology is equally as important as historic records. Instrumentation (such as seismographs) allows determination of seismic events much smaller than those which can be felt at the Earth's surface. Thus, a catalog of seismic events may contain a wide range of events that are instrumentally recorded but not felt by humans. Also, since seismic waves attenuate with distance and because all regions cannot be adequately covered by seismographs, many small events are felt, but not always detected. Sensitive seismographs, which greatly magnify these ground motions, can detect strong earthquakes from sources anywhere in the world. The time, locations, and magnitude of an earthquake can be determined from the data recorded by seismograph stations.

The Richter magnitude scale was developed in 1935 by Charles F. Richter of the California Institute of Technology as a mathematical device to compare the size of earthquakes. The magnitude of an earthquake is determined from the logarithm of the amplitude of waves recorded

by seismographs. Adjustments are included for the variation in the distance between the various seismographs and the epicenter of the earthquakes. On the Richter Scale, magnitude is expressed in whole numbers and decimal fractions. For example, a magnitude 5.3 might be computed for a moderate earthquake, and a strong earthquake might be rated as magnitude 6.3. Because of the logarithmic basis of the scale, each whole number increase in magnitude represents a tenfold increase in measured amplitude; as an estimate of energy, each whole number step in the magnitude scale corresponds to the release of about 31 times more energy than the amount associated with the preceding whole number value.

At first, the Richter Scale could be applied only to the records from instruments of identical manufacture. Now, instruments are carefully calibrated with respect to each other. Thus, magnitude can be computed from the record of any calibrated seismograph.

Earthquakes with magnitude of about 2.0 or less are usually referred to as micro-earthquakes; they are not commonly felt by people and are generally recorded only on local seismographs. Events with magnitudes of about 4.5 or greater - there are several thousand such shocks annually - are strong enough to be recorded by sensitive seismographs all over the world. Great earthquakes, such as the 1964 Good Friday earthquake in Alaska, have magnitudes of 8.0 or higher. On average, one earthquake of such size occurs somewhere in the world each year.

The Richter Scale has no upper limit. Recently, another scale called the moment magnitude scale has been devised for more precise study of great earthquakes. The Richter Scale is not used to express damage. An earthquake in a densely populated area which results in many deaths and considerable damage may have the same magnitude as a shock in a remote area that does nothing more than frighten the wildlife. Large-magnitude earthquakes that occur beneath the oceans may not even be felt by humans.

The effect of an earthquake on the Earth's surface is called the intensity. The intensity scale consists of a series of certain key responses such as people awakening, movement of furniture, damage to chimneys, and finally - total destruction. Although numerous *intensity scales* have been developed over the last several hundred years to evaluate the effects of earthquakes, the one currently used in the United States is the Modified Mercalli (MM) Intensity Scale. It was developed in 1931 by the

American seismologists Harry Wood and Frank Neumann. This scale, composed of 12 increasing levels of intensity that range from imperceptible shaking to catastrophic destruction, is designated by Roman numerals. It does not have a mathematical basis; instead, it is an arbitrary ranking based on observed effects.

The Modified Mercalli Intensity (Figure 2-45) value assigned to a specific site after an earthquake has a more meaningful measure of severity to the nonscientist than the magnitude because intensity refers to the effects experienced at that place. After the occurrence of widely felt earthquakes, the Geological Survey mails questionnaires to postmasters in the disturbed area requesting the information so that intensity values can be assigned. The results of this postal canvass and information furnished by other sources are used to assign an intensity within the felt area. The maximum observed intensity generally occurs near the epicenter.

The *lower* numbers of the intensity scale generally deal with the manner in which the earthquake is felt by people. The *higher* numbers of the scale are based on observed structural damage. Structural engineers usually contribute information for assigning intensity values of VIII or above.

2.5.1 Regional Seismic Activity

Seismically, the Gulf Coastal Plain is one of the least active regions of North America (Figure 2-46) as detailed by seismic hazard. This area of Louisiana and adjacent states has a very low rating for seismicity as determined via the United States Geological Survey (USGS). Natural seismicity in the Gulf Coastal Plain is attributed primarily to flexure of sediments along hinge-lines that parallel the coast. This flexure is due to compression and down warping of the immature Gulf of Mexico basin sediments in response to extreme sediment loading. Structural features such as salt domes and growth faults, although capable of storing and releasing some seismic energy, are weak and ineffective in generating even modest ground motion.

Salt domes are the result of plastic flowage of salt that pierces or ruptures adjacent sedimentary layers or causes doming in the overlying sedimentary layers. These sediments have low density, poor cementation, and low shear strength, which results in a low shear modulus. It is doubtful that a salt dome could develop earthquakes with a magnitude greater than 3.0 on the Richter Scale. Small earthquakes may be felt locally but are unlikely to propagate damaging ground motions. As

indicated in Section 2.2.3 the sequestration site is not located near any salt diapirs as the facility is located well south of the Mississippi Salt Dome Basin. No salt domes exist within St. Helena Parish.

The regional fault systems in southernmost Louisiana are syndepositional growth faults, originally formed during periods of accelerated basin subsidence and sedimentary deposition. In general, mechanisms invoked to explain the formation of growth faults have included overloading in areas of rapid sedimentation, differential compaction of deposited sediments, abnormally high fluid pressures, and gravity sliding. An extensional stress province is associated with growth faulting from northeastern Mexico to Louisiana. The maximum horizontal stress is subparallel to the coastline, following the strikes of the growth faults (Lund Snee and Zoback, 2016).

The seismic activity in this part of the coastal plain is among the lowest in the United States and has been assigned the lowest coefficients. It should be also noted that none of the earthquakes that have occurred in Louisiana has been attributed to any specific fault, however, this may be due to the paucity of seismograph stations located in the state (Stevenson and McCulloh, 2001).

The largest regional earthquake occurrence in Louisiana is the 1983 event at Lake Charles, which originated at a depth of 14+ km and had a Mercalli magnitude of approximately IV (light shaking and dishes rattling). This depth is located well below the proposed injection depths beneath the proposed sequestration site. Even more distant seismic regions (*e.g.*, New Madrid Zone in Southeastern Missouri) have not developed events great enough to cause damage at a sequestration site.

2.5.2 Seismic Risk of the Project Site

A preliminary seismic risk evaluation is conducted for the project area. The sequestration area is within the Shell St. Helena Parish, in an area with no faulting or salt dome movement. Overall seismic risk is rated **very low** based on:

- Low frequency of natural earthquake events near the sequestration area;
- Low intensity of natural earthquakes felt in the sequestration area, with maximum ground motion on the surface being less than or equal to a Modified Mercalli Intensity (MMI) range of IV;
- Low population density in the area limiting exposures and impacts;
- Lack of injection-induced seismicity in Class I or Class II wells operating in the area;
- Lack of current large-scale oil and gas production in the area; and
- No known faults in the AoR and only minor faults in the extended Area of Interest (AoI), primarily interpretable in the Lower Tuscaloosa strata

Typical geologic structures characterizing this province are gently southernly dipping and thickening sedimentary strata. These strata are show minimal disruption by minor normal fault systems primarily interpretable in the deepest interval of interest (Lower Tuscaloosa) outside the AoR within the St. Helena Parish (Figures A.8 and A.9 in Appendix A) The nearest major fault feature/system is located much further south in Livingston Parish (Figure 2-47).

The sequestration site in St. Helena Parish, Louisiana is found in area IV of the Modified Mercalli Intensity Scale (MMI) (Figure 2-46). Structural features such as salt domes and growth faults, although capable of storing and releasing some seismic energy, are weak and ineffective in generating even modest ground motion. None of these features are located near the sequestration site.

Evaluations have been performed to determine the possible effects of natural events on (1) the integrity of well construction materials; and (2) the integrity of both the Injection and Confining Zones beneath the St. Helena Parish sequestration site. A review of “The National Earthquake Information Center” (NEIC) (<http://earthquake.usgs.gov/contactus/golden/neic.php>) indicates that the St. Helena Parish area has a low potential for seismic activity. In 1989, David J. Leeds, a certified geophysicist and engineering geologist, conducted a regional evaluation on seismicity. Leeds (1989) identified seismogenic sources, modeled a “design earthquake,” and discussed the effects of the “design” earthquake on potential Injection and Confining Zones. The natural

seismicity by the Leads' study indicates that seismicity is not expected to be significant issue at the project site.

A NEIC database search within a 100-kilometer (approximately 62 miles) radius of the proposed injection sites (blue circle on Figure 2-48) was conducted in November 2022. A tabulation of the results is contained in Table 2-7 and are presented in Figure 2-48. The search shows that since 1900, three earthquakes with magnitudes greater than 2.5 were recorded within 100 kilometers (approximately 62 miles) of the project site. Only one of these events have occurred near St. Helena Parish (Figure 2-49) and are highlighted in yellow on Table 2-7.

The closest recorded earthquake occurred in 2010 which was recorded as a 3.0 magnitude earthquake, at a relatively shallow depth of 0.4 km. It was located at the western border of the St. Helena Parish, approximately 10.9 miles west of Greensburg, St. Helena Parish, Louisiana (Figure 2-49). Note that many of the recorded earthquakes are located outside of Louisiana, supporting the low regional hazard assessment provided by the USGS.

At the project site, the likelihood of an earthquake caused by natural forces or fluid injection is considered remote. Injection into the formations will be at relatively low pressures and will take place into deep, high-porosity formations that are extensive over a broad area that is not subject to natural earthquakes. Therefore, the probability of an earthquake of sufficient intensity to damage the injection system, injection well, or the confining layer is very low.

2.5.3 Induced Seismicity Analysis at the Project Site

Real world examples for this sequestration project are available from Class I injection well sites located along the Texas-Louisiana-Mississippi Gulf Coast, roughly extending from Corpus Christi in South Texas to Pascagoula, Mississippi. These sites include both hazardous and nonhazardous fluid effluent disposal wells that typically operate in the +/- 300 to 500 gallons per minute injection range, with maximum injection approaching 1,000 gallons per minute. Many of these sites have been operating since the 1970's and a few as far back as the 1950's. There is no known evidence of injection-induced seismicity or suspected injection-induced seismicity at or near any of these Class I injection facilities, many of which are near high-population areas.

Assessment of the potential for induced seismicity at these locations follows the methodology outlined below, using the very conservative "zero-cohesion Mohr-Coulomb failure criterion" recommended by the USGS (Wesson and Nicholson, 1987). These analyses indicate very low potential for induced seismicity caused by pressures resulting from injection activities. Examples are available, such as long-term Class I injection operations at sites like Chemours Delisle, Denka Pontchartrain, INV-Orange, Lyondell Channelview, Rubicon Geismar, etc., among others, which are all regulated by the EPA.

Additionally, the sequestration project will be injecting into the Frio, Wilcox, and Lower Tuscaloosa Formations, which are located many thousands of feet above the crystalline basement complex. Injection into strata near or at the basement, with activation of pre-existing faults, has been identified as contributing to induced seismicity in those parts of the country where deep injection occurs.

Despite the long history of Class I and Class II disposal along the Texas-Louisiana Gulf Coast, there is no regional-scale or operational trends associated with induced seismicity in or near the sequestration project or in similar hydro-mechanical areas such as those documented in Skoumal et al. (2018, 2021) and Weingarten et al., (2015).

Finally, as mentioned in Section 2.5.1 typical regional geologic structures, characteristics of the Gulf Coast, include gently coastward dipping and thickening sedimentary strata of Tertiary to Cretaceous age that are disrupted by radial faults originating from salt or shale piercement domes, syndepositional growth and regional fault systems, and post-depositional faults. However, in the AoR of the proposed site, there are no known faults or salt structures that would impact the integrity of the injection zone or have the potential for fault reactivation due to injection operations. Minor faults outside the AoR have been evaluated for fault stability under the pressures increases predicted during injection of the volumes of CO₂ possible for the site and the risk of reactivation is estimated to be very low.

2.5.4 Seismic Risk Models for the Project Site

The purpose of an earthquake model is used to evaluate any potential effects of natural earthquakes on subsurface geological structures associated with the sequestration project. In general, a source

mechanism is required when designing a “model” earthquake. In these cases, it is usual to have a “known” active fault system with a measured strain or stress field. In more active regions of the earth, faults with strain (movement across the fault without a rupture) develop at a rate of up to 5 centimeters per year, or more (Leeds, 1989). As a meter or more of strain develops, stress accumulates and eventually the system releases this stored strain energy in the form of elastic waves (*e.g.*, an earthquake). Although the Texas/Louisiana Gulf Coast contains several geological features capable of storing and releasing stored energy, all are weak or ineffective in terms of generating even modest ground motion (Leeds and Associates, 1989).

Growth faults have also developed along the Texas/Louisiana Gulf Coast which may be responsible for seismic activity. Considering the Gulf Coast as a whole, a level of $M_b=4.2$ is considered an upper level for this kind of source in this area (Leeds and Associates, 1989). The several low magnitude events within about 50 miles of the coastline are probably attributable to this mechanism.

The possibility that growth faults may be triggered by faults in the basement is suggested by Stevenson and Agnew (1985) in their discussion of the Lake Charles Earthquake. Details of the event were developed from recordings of Department of Energy supported microseismic networks deployed for monitoring geothermal experiments (withdrawal and injection) in southern Louisiana. The interpreted depths of 14+ km for these events are deeper than have previously been reported and well beneath anticipated injection depths for the sequestration project. Additionally, none of the events were attributable to the geothermal extraction/reinjection operations (Stevenson (pers comm.), in Leeds and Associates, 1989).

However, in the area of St. Helena Parish and neighboring parishes, there are no known faults in the AoR, minor faults in the larger study area, and the risk level is estimated to be very low. The closest known major regional tectonic feature is the Baton Rouge Fault system, which is located more than 20 miles south of St. Helena Parish. However, the movement associated with this fault system is that of gradual creep as opposed to the rapid breaking of brittle rock associate with earthquakes. No earthquakes have been documented associated with the Baton Rouge Fault System (Stevenson and McCulloh, 2001).

2.5.4.1 Design Earthquake Model

For the evaluation of the potential impact of seismicity on a Class VI Sequestration facility in the St. Helena Parish, a modeled seismic event with a body-wave magnitude Mb of 4.2 ± 0.2 (as presented above for growth faults in the region) can be used as a conservative working model for the design earthquake. It is presumed that the nearest seismic source area would be along one of the coast parallel growth faults (Leeds and Associates, 1989). Another assumption is that the maximum ground motion at the surface generated by the design earthquake would be within the Modified Mercalli Intensity range of $MMI=V$, which equates to a horizontal surface acceleration of $0.05g$ (Leeds and Associates, 1989). The empirical correlation between intensity and acceleration has a wide spread of data, with recordings varying from horizontal accelerations of $0.025g$ to $0.150g$ for an $MMI=V$ event. This is the same value used for an “Operating Basis Earthquake” (OBE) for certain Gulf Coast nuclear power plant electric generating stations. For example, the Nuclear Regulatory Commission’s estimate for the risk each year of an earthquake intense enough to cause core damage to the reactor at River Bend (north of Baton Rouge) was 1 in 40,000 according to an NRC study published in August 2010 (Hiland, 2010).

The Operational Basis Earthquake (OBE) is defined by US Federal Regulations 10 CFR 100, Appendix A, as follows:

‘The Operating Basis Earthquake is that earthquake which, considering the regional and local geology and seismology and specific characteristics of local subsurface material, could reasonably be expected to affect the plant site during the operating life of the plant; it is that earthquake which produces the vibratory ground motion for which those features of the nuclear power plant necessary for continued operation without undue risk to the health and safety of the public are designed to remain functional.’

The design earthquake in this study is based on the empirical data of normal shallow focus (<20 km) earthquakes on soft sites (Leeds and Associates, 1989). It is also assumed that in the Gulf coastal seismic environment, the release of energy from less competent materials than usual would result in longer surface rise times; therefore, the ground motion would be biased to longer periods

(lower frequencies) than usual, and result in low accelerations, large displacements, and long durations.

Over the years, studies of the effect of depth on seismic ground motion have all noted a clear attenuation. Observations in deep mines and boreholes have confirmed this phenomenon. Data strongly indicates dampening of amplitude with depth to an average of one-half, or less, of the ground motion. The motion may become as low as one-fifth while for small motions, where the materials remain completely elastic, the diminution of amplitude may be as small as one-tenth (Leeds and Associates, 1989).

The effect of ground motion on saturated granular soils is buildup in pore water pressure. If the water table is located near the surface (within about 15 to 20 feet), if the sands are reasonably well sorted and clean (free of clay), and if accelerations exceed about 0.25g, a type of soil failure known as liquefaction can occur (Leeds and Associates, 1989). Liquefaction causes a loss of shear strength of the soil and may result in ejection of sand and water to the surface (sand boils), and collapse of the foundations of structures supported by the soil. In extreme cases, multistory buildings have rolled over (Niigata, Japan Earthquake in 1964) and buried tanks have “floated” to the surface (Leeds and Associates, 1989). There is indeed settlement and densification of the soil following liquefaction. The sequestration project area does not meet the conditions expected to trigger liquefaction since the predicted acceleration levels (0.05g) would only be about one-fifth of that required (Leeds and Associates, 1989).

With depth increasing, there is less ground motion. While pore pressures could increase, the soils framework is not required to support the lithostatic sediment column. Additionally, within the short duration of shaking, there is insufficient time or room for the fluids to go to. Thus, it remains incompressible. Leeds and Associates (1989) conclude that possible interactions between sedimentary horizons due to casing penetration and cement are minimal since there are only minor differential movements as the seismic waves pass through the matrix. They conclude that there might be only several centimeters of displacement over the wavelength of the seismic waves and that the normal elasticity of well casing and tubing is sufficient to accommodate the strain (Leeds and Associates, 1989). It is only in extreme cases, such as in 1952 in Kern County, California, where surface accelerations can reach 0.50g and there are many miles of surface rupture, that

existing wells may be affected. During the 1952 event, approximately 2% of the wells in the area had some surface damage due to settlement of surficial soils (Leeds and Associates, 1989). This event caused some subsurface damage including collapsed tubing near the surface due to the sharp rise in casing pressure accompanied the shock. However, all wells returned to normal status within 2 or 3 weeks of the event (Leeds and Associates, 1989).

After reviewing data from the largest historic events of the province and modeling a “design earthquake,” the hypothetical modeling results show an event with little damage to engineered structures or facilities. Ground motion due to seismic activity is attenuated with depth. Thus, no damage to the well systems would be anticipated.

In the Gulf Coast region and St. Helena Parish area, only small earthquakes have occurred in the area, such as the 2010 earthquake with a magnitude earthquake of 3.0 that occurred west of the St. Helena Parish area. Larger earthquakes of $MMI=V$ (equivalent to a 4.0-4.9 magnitude earthquake, according to Leeds, this is still classified as small) have occurred in the Gulf Coast region and did not cause damage to nearby facilities and structures. The few historical seismic events in the Gulf Coast area indicate that there is little chance of an event occurring in the vicinity of Shell St. Helena Parish Site.

2.5.4.2 Induced Seismicity Model

Shell employs conservative assumptions to the causative mechanisms of induced seismicity and the geomechanical conditions within the St. Helena Parish area of interest to conservatively constrain parameters. The potential for induced seismicity at the proposed injection site can be evaluated using the very conservative “zero-cohesion Mohr-Coulomb failure criterion,” recommended by the U.S. Geological Survey (Wesson and Nicholson, 1987). This method is based on the following equation:

$$P_{crit} = \frac{S_v(3\alpha - 1)}{2} \quad (1)$$

where:

P_{crit} = the critical injection zone fluid pressure required to initiate slippage along faults

and fractures

S_v = the total overburden stress (which represents the maximum principal stress in the Gulf Coast region)

α = the ratio of the minimum principal stress (horizontal in the Gulf Coast region) to the maximum principal stress (overburden stress)

Inherent in Equation (1) are a number of conservative assumptions, guaranteed to produce a worst-case lower bound to the critical fluid pressure for inducing seismicity. These are:

- 1) It neglects the cohesive strength of the sediments
- 2) It assumes that a fault or fracture is oriented at the worst possible angle
- 3) It assumes a worst-case value of 0.6 for the coefficient of friction of the rock (see Figure 4 of Wesson and Nicholson, 1987)

For present purposes, Equation (1) can be expressed in a more convenient form by introducing the so-called matrix stress ratio (K_i) (Matthews and Kelly, 1967; Eaton, 1969), which is defined as the ratio of the minimum to the maximum "effective" principal stresses. Effective principal stress is equal to actual principal stress minus fluid pore pressure (p_o). Thus:

$$K_i = \frac{\alpha S_v - p_o}{S_v - p_o} \quad (2)$$

Substituting Equation (2) into Equation (1) yields:

$$\Delta P_{crit} = \left(\frac{3K_i - 1}{2} \right) (S_v - p_o) \quad (3)$$

where ΔP_{crit} is the critical injection zone pressure build-up required to induce seismicity, with:

$$P_{crit} = p_o + \Delta P_{crit} \quad (4)$$

Equation (3) will be used to evaluate induced seismicity at the St. Helena sequestration site.

Initial plots at the injection depths were evaluated for a pressure gradient across each of the injection zones. The analysis determined an initial pore pressure (p_o) of 0.47 and 0.48, square inch (psi) per foot of depth for the Frio and Wilcox Formations. The Lower Tuscaloosa gradient may range from 0.53 psi/ft (low-end) to 0.57 psi/ft (high-end), which is based upon the variable spread of the available data. Eaton (1969) provides a plot of the effective overburden stress (S_v) as a function of depth for locations along the Gulf Coast. This plot indicates S_v values exceed 0.90 psi/ft for the Injection Zone reservoirs. Matthews and Kelly (1967) provide a plot of the matrix stress ratio (K_i) for tectonically relaxed reservoir sediments along the Louisiana and Texas Gulf Coast.

The project injection wells will be completed across three Injection Zones: 1) Frio, 2) Wilcox, and 3) Lower Tuscaloosa formations at depths ranging from 4,500 feet to 14,500 feet (approximate). The conservatively calculated critical pressure increase required to induce seismicity on a pre-existing fault for each Injection Zone formation for the St. Helena sequestration site are contained in Table 2-8. This value is significantly higher than any of expected and modeled pressures at the injection site. Since there are no known faults or fractures within the AoR and only minor faults interpreted in the deepest strata in the larger study area for this project, there is low probability of induced seismicity at this sequestration project.

2.6 HYDROGEOLOGY

The primary regulatory focus of the USEPA injection well program is protection of human health and the environment, including protection of potential underground sources of drinking water (USDWs). A USDW, as defined in 40 CFR 144.3, means an aquifer or its portion:

- (a)
 - (1) Which supplies any public water system; or
 - (2) Which contains a sufficient quantity of ground water to supply a public water system; and
 - (i) Currently supplies drinking water for human consumption; or

- (ii) Contains fewer than 10,000 mg/l total dissolved solids; and
- (b) Which is not an exempted aquifer.

The following sections detail the regional and local hydrogeology and hydrostratigraphy [40 CFR 146.82(a)(3)(vi), 146.82(a)(5)].

2.6.1 Regional Hydrogeology

In August of 2019, the Council on Watershed Management agreed to use eight watershed regions within Louisiana and was designated the Louisiana Watershed Initiative. Watersheds are geographic areas that have drainage patterns to specific waterbodies. The watersheds for Louisiana are presented in Figure 2-50, with a focus on Region 7, which contains St. Helena Parish. The associated river basins are also presented. It is noted that the Region 7 Watershed contains the Mississippi, Pontchartrain, and Pearl rivers.

The predominant aquifers of Louisiana by location, presented in Figure 2-51, occur within Paleocene and younger formations, and contain usable quality water (<3,000 milligrams per liter (mg/L) TDS). These aquifer systems regionally crop out in bands parallel to the Mississippi Embayment and dip and thicken towards the southeast.

There are four major regional aquifer systems of importance in Louisiana (Figure 2-52):

- Sparta Aquifer
- Mississippi River Alluvial Aquifer
- Chicot Aquifer System
- Southern Hills Aquifer System

Figure 2-53 contains a hydrostratigraphic column for the State of Louisiana. This column denotes the aquifer units for the regions of the state, and the southeastern portion has been highlighted (red box outline) as this provides the regional context applicable to the study.

Groundwater moves through aquifer systems from areas of high hydraulic head to areas of lower hydraulic head. Regional uses from industry and the public water systems have some impacts on

diverting the direction of flow. Published potentiometric maps for the regional aquifers are provided and discussed in the sections below.

2.6.1.1 *Sparta Aquifer System*

The Sparta Aquifer extends from northeast Texas to central Mississippi and is comprised of Eocene-aged deposits. It is a major source of freshwater in the north-central part of Louisiana and Arkansas and mimics the ancestral Mississippi Embayment (Figure 2-54). The Sparta aquifer is recharged through direct infiltration of rainfall, the movement of water through overlying terrace and alluvial deposits, and leakage from the Cockfield and Carrizo-Wilcox aquifers (ASSET Aquifer Summaries 2012 [prepared by Louisiana Department of Environmental Quality] – Sparta Aquifer). The base of the unit is medium to fine grained sand that grades upwards into clay. The Sparta sand ranges in thickness from 500 to 900 feet in the areas it contains freshwater (Rollo, 1960). The Sparta sand thins over structural highs in the region, notably the LaSalle Arch and Monroe Uplift (see section 2.1).

Although the Sparta sand is predominantly of continental origin in the delta area, brief local invasions of the sea repeatedly covered low-lying areas of the land mass (Payne, 1968). Occasional inclusions of fossils and glauconite are representative of the change in source material. The multiple sand layers and lenses in the geologic unit may be connected locally (Brantly et al., 2002).

The Sparta is confined by the lower permeable strata of the Cook Mountain Formation (overlying) and the underlying Cane River Formation (see section 2.1).

The Sparta Aquifer provides usable groundwater for fifteen parishes in north-central Louisiana, primarily for public supply and industrial purposes (McGee and Brantly, 2015). This does not include the St. Helena Parish, where the sequestration site is located. Within the St. Helena Parish, the Sparta aquifer system is at much deeper depths than the USDW, and the formation fluid is highly saline (> 10,000 ppm TDS; based on log analysis and drilling records in the area). For the Sparta aquifer, hydraulic conductivity generally ranges from 10 to 200 feet per day (feet/d) with an average of about 70 feet/d over the extent of the Mississippi Embayment (Hosman and others, 1968). The regional flow direction for the Sparta Aquifer is eastward, towards the axis of the

Mississippi Embayment. Within Louisiana, the regional flow is towards the city of Monroe in Ouachita Parish (Figure 2-55).

2.6.1.2 Mississippi River Valley Alluvial Aquifer (MRVA)

This system is comprised of Pleistocene and Holocene-aged sediments. The Pleistocene deposits are of two general types; an approximately coastwise, gulfward thickening wedge of deltaic sediments and the relatively thin, veneer-like deposits which form the stream terraces and alluvial valley fill (Rollo, 1960). The system contains gravel to coarse-grained sand at the base and fines upwards into clays. In some localized areas, the surface is covered with impermeable clays.

It is a major source of freshwater in the north-northeastern part of Louisiana and into the Mississippi. Recharge to the Mississippi River alluvial aquifer is primarily from precipitation and, to a lesser degree, by leakage from underlying sediments such as the Cockfield aquifer (Prakken, et al., 2014). The MRVA discharge and recharge is also controlled by surface water features that may cross the strata, such as rivers and lakes. This aquifer system can be separated into two hydrogeologic units, an upper confining unit of silt, clay, and fine sand that impedes the downward movement of water into a lower coarse sand and gravel aquifer unit (Martin and Whiteman, 1985). The aquifer ranges in depth from 60 to 260 feet in the areas it contains freshwater.

The MRVA is used as a primary aquifer in twenty-seven parishes in central Louisiana, and runs north to south, mimicking the Mississippi River (Figure 2-52). The MRVA is hydraulically connected to the Mississippi River and flows from high to low hydraulic head. For the MRVA aquifer, hydraulic conductivity generally varies between 10 to 530 feet per day (feet/d). In 2015, withdrawals from the MRVA aquifer totaled 384.60 Mgal/d (Collier and Sargent, 2015) with the majority of the usage for rice irrigation and industry. A potentiometric map published from the USGS in 2016 is presented in Figure 2-56. Within the sequestration site of St. Helena Parish, the MRVA aquifer system is not present.

2.6.1.3 Chicot Aquifer System

The Chicot Aquifer System is the main regional aquifer system that provides the usable groundwater for southwestern Louisiana. These Pleistocene-aged sands are predominately

comprised of unconsolidated to loosely consolidated gravels and coarse graded sands. These gravel, sand, silt, and clay assemblages fine upwards and dip and thicken towards the Gulf of Mexico, thin to the west (towards Texas), and thicken to the east (towards Mississippi) (Nyman 1984).

In southwestern Louisiana and southeastern Texas, the aquifer is subdivided into three sub-units that are separated by confining layers (Sargent, 2011). The principal sand units within the aquifer are the “200-foot” sand, “500-foot” sand, and “700-foot” sand. In the northeastern portion of the Calcasieu Parish, these sands merge and the unit contain undifferentiated sands that are conducted hydraulically. Freshwater in the lower subsections of the Chicot deteriorates in quality with depth (LDEQ, 2003).

In Cameron Parish, the upper sand section contains freshwater underlain by saltwater (Nyman, 1984), except along the southeastern coast where no freshwater is present (Smoot, 1988). A freshwater to saline interface is driven northwards from the coast by water production for public supply, rice irrigation, and aquaculture (Sargent, 2011). Towards northwestern portions of Acadia Parish, there is saltwater present near the base of the lower sand at depths ranging from 700 to 800 feet below ground (Nyman, 1989).

Recharge to the Chicot Aquifer System in Louisiana occurs where the Chicot outcrops in southern Rapides and Vernon Parishes, and in northern Allen, Beauregard, and Evangeline Parishes. There is also minimal recharge to the system via vertical leakage from the shallow overlying alluvial deposits (Stuart et al, 1994).

A map of the potentiometric surface for the Chicot aquifer (Figure 2-57) shows the direction of groundwater flow. Lovelace et al. (2004) indicated that the flow direction is towards major pumping areas such as Lake Charles in Calcasieu Parish and the northern part of Acadia Parish and south Evangeline Parish, where there is heavy pumping for industrial and irrigation uses.

The Chicot Aquifer System yields the highest amount of groundwater for the state of Louisiana and is the primary source of water for Acadia, Calcasieu, Cameron, and Jefferson Davis Parishes. As the aquifer nears the coast, the lower units become saline due to saltwater encroachment and only the upper portions of the aquifer are used as a source of groundwater. Approximately 849.90

Mgal/d are produced from the entire aquifer based on data from the USGS Fact sheet for Calcasieu Parish. The largest withdrawal is associated with rice irrigation and aquaculture (such as the industry of crawfish harvesting) which are seasonal. The Chicot Aquifer system also provides the largest supply for public water supply at 95.60 Mgal/day (Sargent, 2011), for the region and supports large cities such as Lake Charles.

The Chicot Aquifer is not present in the St. Helena Parish, however the Chicot Equivalent Aquifer system (e.g., Upland Terrace Aquifer) is present. The Chicot Equivalent is also comprised of subdivided sand units within the shallow subsurface. The sand units provide freshwater to parishes north of the Baton Rouge fault, and geologically similar those of the Chicot System of southwestern Louisiana.

2.6.1.4 *Southern Hills Aquifer System (SHAS)*

The SHAS is the main regional aquifer system of interest for the Shell St. Helena Parish site and is a designated Sole Source Aquifer by the USEPA. Regionally, this system extends from the Gulf of Mexico in southeastern Louisiana and into southwestern Mississippi. The system is largely composed of three main aquifers referred to as the Chicot Equivalent Aquifer, the Evangeline Equivalent Aquifer, and the Jasper Equivalent Aquifer (White, 2017). Each of these aquifers contains alternating layers of clays and sands, that dip and thicken south, towards the Gulf of Mexico.

The SHAS is the primary source of freshwater water for Pointe Coupee, West and East Feliciana, St. Helena, Tangipahoa, Washington, St. Tammany, Livingston, and West and East Baton Rouge Parishes. As the aquifer nears the coast, the system becomes saline due to saltwater encroachment, and the boundary of freshwater to saltwater coincides with the Baton Rouge Fault Zone (White, 2017). North of the fault is freshwater, and south of the fault is saltwater. There is some leakage updip (north), through the Baton Rouge fault. Large groundwater withdrawals in the Baton Rouge area have induced the northward encroachment of saltwater across the Baton Rouge Fault into freshwater in some locations (Griffith, 2003).

Recharge to the system is from southwestern Mississippi and Louisiana Parishes that border the Mississippi border (Pointe Coupee, West and East Feliciana, St. Helena, Tangipahoa, and

Washington Parishes). Approximately 293 Mgal/d are produced from the aquifer for the 10-parish area (White, 2017). A potentiometric map from the USGS (1980) is provided for the combined aquifers within the Pleistocene-aged formations in southern Louisiana (Figure 2-58). Main groundwater withdrawal areas from the SHAS are Baton Rouge and New Orleans.

The Pleistocene-aged SHAS sands are predominately comprised of unconsolidated to loosely consolidated gravels and coarse graded sands (Martin and Whiteman, 1985). These gravel, sand, silt, and clay assemblages fine upwards, and dip and thicken towards the Gulf of Mexico, thin to the west (towards Texas), and thicken to the east (towards Mississippi) (Aronow and Wesselman, 1971).

2.6.2 Local Hydrogeology

The Shell sequestration site is located within St. Helena Parish in southeastern Louisiana, which is within the SHAS (Figure 2-59). As mentioned, the SHAS has been designated as a sole-source aquifer for the region. The SHAS is comprised of three main aquifer sub-systems (White, 2017). These are in ascending order:

- Chicot Equivalent Aquifer System
- Evangeline Equivalent Aquifer System
- Jasper Equivalent Aquifer System

Additionally, these sub-systems have multiple alternating sand aquifers and shale confining units. These subsets are shown in Figure 2-60. Hydrostratigraphic units of local importance for the St. Helena Parish site include in ascending order:

- Upland Terrace aquifer (400-Foot & 600-Foot sands)
- 800-Foot
- 1,000-Foot
- 1,200-Foot
- 1,500-Foot
- 1,700-Foot
- 2,000-Foot
- 2,400-Foot
- 2,800-Foot

For the St. Helena Parish, these aquifers contained groundwater ranging from freshwater (<1,000 mg/l) down to the USDW standard of 10,000 mg/l in isolated sands that dip to the south which are

separated by alternating clay layers. Figures 2-61 and 2-62 are published cross sections illustrating the distribution of the aquifers located above the base of the USDW. The cross-sections illustrate how the individual sands are discontinuous and not laterally extensive (along strike and dip), suggesting no regional hydrological communication among the sands.

The Chicot Equivalent Aquifer System in St. Helena Parish comprises the Upland Terrace aquifer (and the shallowest) which contains the local 400-foot and 600-foot systems, with the following characteristics (White, 2016):

- A broad, discontinuous, near-surface aquifer
- Present throughout parish
- Extends westward into East Feliciana Parish, eastward into Tangipahoa Parish, and northward into Mississippi
- Crops out along ridges and alongside stream valleys within the parish
- Generally, dips south to southwest at a rate of 10–30 feet per mile.
- Near the southern parish line, the Upland terrace aquifer correlates with the “400-foot” and “600-foot” sands of the Baton Rouge area.
- Sediments range in grain size from clay through silt and sand to gravel and can be over 300 feet thick. The aquifer is composed primarily of medium- to coarse-grained sand. Regionally, the proximity of the Upland terrace aquifer to the surface allows the aquifer to be recharged by infiltration of rainfall and to transmit some of this water to recharge deeper aquifers underlying the parish.
- Based on 2009 data, the general groundwater flow direction was southward, with localized flow direction towards the Amite River and the Tickfaw River (See Figure 2-63).

The Evangeline Equivalent Aquifer System in St. Helena Parish is comprised of the 800-foot, 1,000-Foot, 1,200-Foot, 1,500-Foot, and 1,700-Foot aquifers (White, 2017), with the following characteristics:

- Aquifers are generally fine- to coarse-grained sand, with layers of clay usually separating the individual sands. Note that some sands merge with overlying and underlying sands.
- Aquifers contain freshwater (Chloride concentration ≤ 250 mg/L)
- Groundwater flow direction is generally southwest towards Baton Rouge (See Figure 2-64)

The Jasper Equivalent Aquifer System in St. Helena Parish is comprised of the 2,000-foot, 2,400-foot, and 2,800-foot aquifers (White, 2017), with the following characteristics:

- Aquifers are generally fine- to coarse-grained sand, with layers of clay usually separating the individual sands. Note that some sands merge with overlying and underlying sands.
- Aquifers generally contain freshwater (Chloride concentration ≤ 250 mg/L)
- In 2006, the general groundwater flow direction in the “2,800-foot” sand in St. Helena Parish was to southwest from St. Helena Parish towards Baton Rouge water withdrawal center (See Figure 2-65).

Within St. Helena Parish, there are no aquifers that are used as sources of groundwater below the Jasper Equivalent System.

2.6.3 Determination of the Base of the Lowermost USDW

In order to determine the base of the Lowermost USDW, available USDW values were exported from the SONRIS database within a radius of at least 10 miles from the proposed injection wells. The exported values were then interpolated within the Petrel software across the area of interest. To spot cross-check and validate the exported USDW values from the SONRIS database, the following two approaches were used, which are based on the use of data from open-hole geophysical well logs:

- Determination of USDW values was spot checked from shallow logs across the area of interest using the Louisiana Department of Natural Resources’ Injection and Mining Division approach (identified below) on determining the base of the USDW using an electric log. The spot-checked values were used to verify the SONRIS reported values.

- The resistivity/spontaneous potential methodologies which are described in detail in Appendix 2-C. The “Spontaneous Potential Method” derives the formation fluid resistivity from the resistivity of the mud filtrate, and the magnitude of the deflection of the spontaneous potential response (SP) of the formation (the electrical potential produced by the interaction of the formation water, the drilling fluid, and the shale content of the formations). The “Resistivity Method” determines formation fluid resistivity from the resistivity of the formation (R_t) and the formation resistivity factor (F), which is related to formation porosity and a cementation factor (Schlumberger, 1987).

Using the resistivity method, it was calculated that sands with a formation resistivity of greater than 2.0 ohm-m would be considered USDWs. This site-specific calculation is in agreement with LDNR guidance http://www.dnr.louisiana.gov/assets/OC/im_div/uic_workshop/2_USDW.pdf, which indicates that the USDW should fall between:

- Ground surface to 1,000 feet: 3 ohms or greater is considered USDW
- 1,000 feet to 2,000 feet: 2 ½ ohms or greater is considered USDW
- 2,000 feet and deeper: 2 ohms or greater is considered USDW

Adopting a conservative approach, the base of the lowermost USDW across the evaluated logs was placed at the base of the deepest sand with a deep resistivity at 2 ohms. The cross check of the data showed good alignment.

2.6.4 Base of the Lowermost USDW

The lowermost USDW is defined by the sudden decrease of resistivity at the base of the last sand with an isolating shale below. For the St. Helena Parish injection site, the base of the lowermost USDW is located at a depth ranging from 2,700 feet to 2,800 feet below ground (corresponds to sands within the Jasper Equivalent Aquifer System) as shown in the USDW map (Figure 2-66). The base of the USDW deepens southwards towards the Gulf of Mexico.

Within a 5 miles radius of the proposed injection well locations, the separation of the base USDW to the top of the Frio Confining zone is around 2,000 feet. Multiple permeable aquifers and aquitards ('containment shales') are present between the lowermost USDW and the top of Frio Confining Zone. These additional sequences are comprised of Miocene-aged saline sands (buffer zones) that would allow for additional pressure and fluid bleed-off prior to reaching any USDW if a loss of containment event would occur. Collectively, these buffer saline intervals above the Frio Confining Zone, have at least 2 additional laterally extensive shale confining units. These are fine-grained Miocene deposits comprised of dominant shale with occasional sand/silt and referred to as the Miocene Shale 1 (MS1) and Miocene Shale 2 (MS2), which are approximately 100 feet to 150 feet thick. These two shaly units have been correlated across the Shell St. Helena Parish site.

2.6.5 Water Well Data Sets

Water well data was gathered from the SONRIS database (<https://www.sonris.com>). A water well search was performed through SONRIS in November 2022. Water well locations within 6 miles (purple boundary) of the two proposed injection well locations are shown on Figure 2-67 (blue dots). A total of 647 wells were identified and their information (e.g., well number identifier well depth, well status, use and aquifer description) are keyed to Table 2-9. Note that well depths ranged from 12 feet to 2,155 feet below ground level, with the majority of wells (84 percent) having a depth of less than 200 feet (Figure 2-68).

Out of the 647 wells, 575 wells are currently active. The remaining 72 wells are plugged and abandoned; one well is status unknown. The well usage is displayed in Figure 2-69 showing the breakdown by usage and current well status (Active vs Plugged).

Additionally, Figure 2-67 illustrates the surface water bodies within the local area. The Amite River runs north-south from Mississippi through St. Helena Parish (to the west of the project site). It is approximately 117 miles long, is the boundary between St. Helena, East Feliciana, and Baton Rouge Parishes. It continues south through Baton Rouge and Livingston Parish and empties into Lake Maurepas. There are also multiple branches and creeks, which are seasonally intermittent.

There are no quarries, springs, or subsurface mines within the local area (within the 5 miles radius from injection well pads).

Note: there are no Class I injection well operations within St. Helena Parish.

2.6.6 Local Water Usage

In St. Helena Parish, with population of approximately 10,227 people (per 2020 census), the main source of drinking water comes from the Upland Terrace Aquifer/Chicot Equivalent Aquifer System. Currently, there are fourteen public water systems in the parish that depend on groundwater as a source of freshwater (White and Prakken, 2016). Within 6-miles of the injection wells, there are 15 public supply wells that are used for the surrounding communities. Surface water resources are limited to the Amite Subbasin, the Tickfaw Subbasin, and the Tangipahoa Subbasin. Less than 0.01 million gallons per a day is supplied by surface water (White and Prakken, 2016).

The USGS in cooperation with the Louisiana Department of Transportation and Development (LaDOTD), produced a “Water Resources of St. Helena Parish” fact sheet with data up until 2010 (White and Prakken, 2016). The dominant water usage is supplied by groundwater (99 percent). The 2010 statistics showed that 1.05 Mgal/d were withdrawn from groundwater supply from the Upland Terrace and Jasper Equivalent Aquifer systems. Total for these aquifers were: (1) Upland Terrace provided 0.70 Mgal/d (~ 66%) and (2), Jasper Equivalent Aquifer System provided 0.35 Mgal/d (~ 33 %) for the Parish. (Table 2-10). Data for the table reflects the conditions of St. Helena Parish in 2010 and is provided by the Water Resources of St. Helena Parish Fact Sheet.

In November 2022, a water well search was tabulated and keyed to Table 2-9 and has a total of 648 water wells (active and plugged). Out of the 648 water wells, 575 of these wells are active, with over 500 wells used for domestic water supply. Thirty-two are used for public and public commercial supply. The remaining active forty-three water wells are used for industrial or irrigation purposes, including as oil/gas rig supply wells.

Out of the 575 active wells, the majority, 510 (88.7 percent) are completed within the shallow Upland Terrace Aquifer (included are aquifer names ‘shallow sands’, ‘400-ft sand’, ‘600-ft sand’

mentioned in SONRIS database) (Figure 2-70). Note that only nine of the active wells are completed within the deeper Jasper Equivalent Aquifer systems (2,000-Foot, 2,400-Foot, and 2,800-Foot Sands). Additional observations that can be made about these nine wells are:

- 5 have a well use classification of public supply;
- 3 have a well use classification of industrial; and
- 1 have a well use classification of domestic.

2.6.7 Injection Depth Waiver

The Shell St. Helena Parish site’s proposed injection zones are deeper than the base of lowermost USDW (which ranges from 2,800 to 2,900 feet TVD) as shown in Figure 2-66. An injection depth waiver is not required or requested for this project.

2.7 GEOCHEMISTRY

The proposed data collection program (submitted in “**Module D – Pre-Operational Testing**”) has been designed and implemented to determine the mineralogy of the Injection, Containment and Confining Zones, as well as characterize the interstitial fluids in each one of these zones.

Below the base of the lowermost USDW and throughout the entire interval of interest, all rock formations contain saline brines. Open hole log analysis techniques, such as wireline spontaneous potential and resistivity logging measurements and interpretation, can be used to define the vertical distribution of salt concentrations. For more accuracy, fluid samples will be collected in-situ and brought to the surface to be analyzed in the lab (as outlined in **Module D**). These different sources of data will be integrated and compared to existing data available in the region through literature papers and agency databases.

In this section, regional studies and commercially available data information from the CoreLab RAPID™ database have been used as proxies for site specific data.

2.7.1 Formation Brine Properties

Formation fluid samples will be collected from the appraisal wells from the targeted injection zones. In lieu of site-specific data at this initial stage, analogues and formation information have been reviewed for the Area of Interest and the targeted formations; Frio, Wilcox, and Lower Tuscaloosa. Regional subsurface data is supported from literature to make evaluations for expected properties of the native formation fluid.

2.7.1.1 Temperature

The formation temperature gradient can be estimated from temperature measurements previously performed in different wellbores drilled at various depths in the area of the proposed injection sites. However, both the borehole radius and the fluid invasion (mud filtrate) influence the temperature measured in the borehole while it is expected that this influence attenuates over time (Poulsen et al., 2012). Therefore, the borehole temperature is affected by the time duration from the end of circulation and the time the logging tool takes to reach the drilled bottom of the well. As such, temperature measurements are likely to be cooler than actual temperatures, as the mud column has not had sufficient time to reach temperature equilibrium.

In Figure 2-71, the bottomhole temperatures recorded in 96 offset wells are from published data collected by Drumm and Nunn (2012). Due to insufficient data (none of the wells had multiple logging passes at same interval) a Horner temperature correction was not applied. Instead, a modified version of Kehle (1971) was used to correct for effects of the drilling mud. The data are fitted by a linear trend which indicates an average temperature gradient of 1.6 °F/100 feet, using a surface temperature of 66 °F.

The subsurface temperature for each injection interval can then be estimated from the temperature gradient and the mean annual surface temperature. Using the available bottomhole temperature (provided from log headers) data was then calibrated for a geothermal gradient (Figure 2-72). Note: that all the bottomhole temperature (orange dots) are expected to be lower than actual formation temperature due to the drilling mud cooling effect.

The projected reference temperature for each injection zone (using the above gradient) at formation mid-point is:

- 1) 161 °F for Injection Zone No. 1 – Frio Formation (at a depth of 5,950 feet)
- 2) 217 °F for Injection Zone No. 2 – Wilcox Formation (at a depth of 9,450 feet)
- 3) 297 °F for Injection Zone No. 3 – Lower Tuscaloosa Formation (at a depth 14,440 feet)

2.7.1.2 *Salinity*

Different methods exist to determine the salinity of the formation water, but the most accurate one is through the analysis of fluid samples collected in-situ. In lieu of site-specific data, a vertical profile of formation fluid salinity properties can be estimated using open hole offset well analysis.

To estimate formation water salinity, one must first estimate formation water resistivity (R_w), which can be calculated by using the Archie equation (Schlumberger, 1988). The underlying assumption in the Archie equation is that the zone or permeable bed in which water resistivity is to be determined is 100% water saturated and must not contain any clay or shale (e.g., clean sand). It is further assumed that the bed is sufficiently thick so that the deep investigation resistivity open hole geophysical logging tool is not affected by shoulder beds or is affected by mud filtrate invasion.

The general form of the water saturation equation is:

$$S_{wn}^n = \frac{R_w}{(\phi^m \times R_t)}$$

where:

S_w = water saturation of the uninvaded formation

n = saturation exponent, which varies from 1.8 to 4.0

R_w = formation water resistivity at formation temperature

Φ = porosity

m = cementation exponent, which varies from 1.7 to 3.0

R_t = true resistivity of the formation, corrected for invasion, borehole, thin bed, and other environmental effects

In the case of a fully saturated formation, the resistivity (R_t in ohm-meters) is a function of 1) resistivity of the formation water, 2) amount and type of fluid present, and 3) the pore structure geometry. The rock matrix generally has zero conductivity (*i.e.*, has infinitely high resistivity) and therefore is not generally a factor in the resistivity log response. Induction geophysical logging determines resistivity or R_t by inducing electrical current into the formation and measuring conductivity (reciprocal of resistivity). The induction logging device investigates deeply into a formation and is focused to minimize the influences of borehole effects, surrounding formations, and invaded zone (Schlumberger, 1987).

Therefore, the induction log is considered to measure the true resistivity of the formation (Schlumberger, 1987). The conductivity measured on the induction log is the most accurate resistivity measurement for resistivities under 2 ohm-meters.

Electrical conduction in sedimentary rocks almost always results from the transport of ions in the pore-filled formation water and is affected by the amount and type of fluid present and pore structure geometry (Schlumberger, 1988). In general, high-porosity sediments with open, well-connected pores have lower resistivity and low-porosity sediments with sinuous and constricted pore systems have higher resistivity.

Once R_w has been calculated for each injection zone, the R_w is converted to NaCl concentration (salinity), using the formation temperature (Figure 2-73). The salinity in the proposed injection intervals is summarized in Table 2-11.

2.7.1.3 Viscosity

Viscosity is a measure of a fluid's resistance to flow. For the purpose of constructing the initial CO₂ sequestration model (without yet having the site-specific Pressure Volume and Temperature (PVT) data available), formation brine viscosity at subsurface conditions is estimated using the

correlation of Kestin et al (1981), which was derived following experimental measurements of dynamic and kinematic viscosity of NaCl solutions over a wide range of pressure, temperature, and salinity conditions.

The formation brine viscosity in the proposed injection intervals can be summarized as:

- 1) 0.54 cP for Injection Zone No. 1 – Frio Formation (at a depth of 5,950 feet)
- 2) 0.36 cP for Injection Zone No. 2 – Wilcox Formation (at a depth of 9,450 feet)
- 3) 0.28 cP for Injection Zone No. 3 – Lower Tuscaloosa Formation (at a depth of 14,440 feet)

As expected, viscosity decreases with depth since the formation gets hotter. However, this tendency to decrease may be impacted in intervals exhibiting higher salinities. In these zones, the formation water gets thicker and more viscous, having an inverse effect. These initial viscosity values are based upon no site-specific data and assumptions made for the site-specific salinity and temperature. The viscosity of the formation fluids for the injectors will be evaluated at time of analysis. The site-specific data on the formation fluid will be used to refine the static and dynamic simulation model, as well as to refine the geochemical modeling.

2.7.2 Compatibility of the CO₂ with Subsurface Fluids and Minerals

Interactions between carbon dioxide and the formation brine and matrix materials in the subsurface can be categorized as those that occur during the period of injection or immediately following injection, and those that occur over the long term of carbon dioxide storage. While interactions occurring during injection and in the early phase of carbon dioxide sequestration can be directly studied and evaluated, the longer-term interactions over tens to hundreds of years can only be evaluated through modeling and other forms of prediction. In general, geologic materials are not overly reactive, or very slowly reactive, with acids such as carbonic acid. Carbonic acid (H₂CO₃) is a weak acid that dissociates into a proton (H⁺ cation) and a bicarbonate ion (HCO₃⁻ anion).

Because the permeability of the confining and containment zones (shales) is expected to be several orders of magnitude lower than the permeability of the injection zones (sands), in a practical sense,

the carbon dioxide sequestered in the Injection Zones has a much higher potential to contact and react with the rocks and fluids in these intervals. Additionally, because of the low permeability of the aquiclude shales, only reactions near or at the shale/sand interface are likely to occur. Injection operations elevate pressure within the injection interval both during injection and for a period of time afterwards (during pressure recovery). This elevated pressure provides the driving force for vertical permeation of injected fluids and formation brines into the overlying aquitards. Buoyance of the sequestered carbon dioxide also provides an additive driving force. Permeation is the greatest immediately adjacent to the wellbore where the pressure buildup is large and involves primarily the injected fluids. Further from the injection well the vertical permeation drops off significantly and may only affect either the original formation brine or the injected fluids, depending on the location of the carbon dioxide plume.

Occasionally, fluids may move into the base of the overlying aquitard from the injection interval below and compress some of the native brines immediately above it. This compression raises the pressure within the lower portion of the aquitard and expands the pores immediately above the interface. Aquitard materials, such as clay/shales, are known to exhibit significant pore expansion (Neuzil, 1986). The combined effects of native brine compression and aquitard pore expansion provides the necessary space to store the entering fluids. This process does not occur uniformly throughout the thickness of the aquitard. It is rather confined to a narrow region very close to the lower aquitard boundary. Throughout the remainder of the aquitard, there is virtually no indication that any changes have taken place. This narrow region near the base of the aquitard is referred to as the “compression boundary layer.” It contains new fluids that have entered since the beginning of the injection, as well as original formation brines that have been pushed upward into the expanded pores and compressed by the entering fluids. The vast majority of the fluids within this layer are typically the original formation brines.

With continued injection, the compression boundary layer increases in thickness and may eventually encompass the entire aquitard thickness. Native fluids originally present at the top of the aquitard may then begin seeping out into the next overlying permeable layer. The time for this to occur is proportional to the square of the aquitard thickness and inversely proportional to the “hydraulic diffusivity” of the aquitard material (Bredehoeft and Pinder, 1970). Because the

hydraulic diffusivity of many aquitard materials (such as shales) is very low (Neuzil, 1986; Neuman and Witherspoon, 1969a and 1969b; and Hantush, 1964), the time is in the order of decades (Chen and Herrera, 1982) which is comparable to the operational lifetime of many underground sequestration facilities. Thus, compressive storage effects in the aquitard layers are important when modeling injection-induced permeation into an aquitard during injection and shortly after operation of the waste facility. When injection is discontinued, some of the waste may seep back into the injection interval from the aquitard. This reverse permeation phenomenon always occurs when the pressure in the injection interval decreases.

The vertical permeation distance reaches an absolute maximum either during injection (typically at the end of the injection period) or after an infinite time has passed since injection operations have stopped. The time necessary to attain the maximum distance depends on the compressive storage properties of the aquitard. For aquitards with high compressive storage capabilities, the maximum permeation distance occurs at the end of the injection period. For aquitards with low storage capabilities, the maximum will occur at an infinite time.

Long after injection operations have stopped, the driving force for vertical permeation usually dissipates, along with the compressive storage of fluids in the aquitard. The pressure-driven rate of fluid movement into the overlying aquitard decreases to zero, leaving only the residual buoyance force. Before the carbonic acid from the sequestered carbon dioxide can react with the clay/shales of the aquitard, it must first migrate from the injection interval strata into the base of the overlying aquitard. During the movement within the injection interval, the acid can be partially or totally neutralized by the carbonates, clays, and other silicates (e. g., feldspars) in the formation. This neutralization halts any further dissolution of carbonate minerals, so that the fraction of dissolved carbonates (relative to pre-injection carbonate mineral amount) is extremely small.

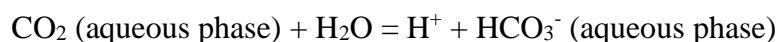
The modeling of strong acids injected into Class I wells presented by DuPont indicates that:

- During injection, injected acids react with at most 2 inches per year of the shale in the overlying arresting aquiclude layer. This rate drops to less than 0.1 inch per year if the waste is injected at least five feet below the base of the arresting shale.

- After injection ceases, injected acids react with at most an additional two feet of the overlying arresting aquiclude layer for all eternity.
- In the unlikely event that the overlying arresting aquiclude shale layer contains a vertical streak of highly reactive material, such as calcite, the acid could at most migrate 26 inches into this streak: 16 inches during a 60-year period of injection and an additional 10 inches for all eternity post-closure.
- Permeation through the arresting shale due to pressure buildup during injection is more important than shale-acid reactions in determining how far injected fluids can migrate into the overlying arresting aquiclude shale.

Therefore, interactions of the sequestered carbon dioxide and the formation fluids and materials are the most critical within the injection interval.

At the pressure and temperature conditions typical of carbon sequestration projects, carbon dioxide is soluble to a limited degree. The dissolved carbon dioxide transforms the native formation brine into a carbonic acid, such as:



The carbonic acid can react with and dissolve minerals in the matrix, which acts to neutralize the lower pH. The sequestration process includes both short- and long-term geochemical impacts. Short-term CO₂-water-rock interactions can affect injection over the operational time period (tens of years), such as dry-out and salt precipitation in the near-wellbore area from formation fluid evaporation. In addition, at first contact with CO₂ (*i.e.*, at the front of the CO₂ plume), carbonic acid is formed via CO₂ dissolution in the native formation brine. This triggers dissolution of carbonate minerals. This is not a reason for concern, because in the same process the carbonic acid is quickly neutralized, meaning that a new equilibrium is rapidly established between the elevated CO₂ concentration and the carbonate minerals. The new equilibrium is already established after only a small amount of carbonate dissolution, so that porosity and permeability changes are negligible. Behind the CO₂ plume front (where the formation brine is already neutralized) no further carbonate dissolution takes place. Long-term impacts and reactions can affect permanence of trapping of the carbon dioxide via mineral trapping. The long-term geochemical processes

consist of a combination of slow dissolution and precipitation reactions. Significant long-term dissolution without simultaneous co-precipitation is impossible because it would lead to unrealistic supersaturation levels in the formation brine. In most systems, precipitation dominates over dissolution resulting in a gradual decrease of porosity and permeability, and a gradual mineral trapping of CO₂.

The extent of secondary trapping mechanisms within the injection interval is highly site-specific and depends on the geology, structure, and hydrology of each reservoir. For instance, increasing pore fluid salinity decreases carbon dioxide solubility (Gunter et al., 1993). The purity of the injected carbon dioxide also affects the storage capacity of the reservoir (Talman, 2015). In such sedimentary settings, the injected carbon dioxide may remain mobile for centuries and trapping relies primarily on the impermeability of the overlying caprock and sealing faults. Large and extensive saline aquifers are essentially hydrodynamic traps, where the injected carbon dioxide is expected to move rapidly through the pore space, interacting with a larger volume of the reservoir. This interaction increases the extent of all secondary mechanisms (National Academies of Sciences Engineering Medicine, 2019).

The carbonic acid can readily react with calcium carbonate and hydroxide minerals, which also reduces the acidity of the formation brine. In addition to the precipitation of carbonates, a host of other fluid-rock reactions can take place within the injection zone. Silicate minerals in arkoses and shales display textures in experiments indicating that these minerals are reacting with carbonic acid (Kaszuba et al., 2002). Acid reacts with feldspars in a manner similar to its reaction with clays. However, the overall rate is slower with feldspars than with clays because in typical rock matrix, the feldspar is present as large particles, so the surface area available for feldspar to react is much smaller than for clay particles.

With silica, the silica can be solubilized by an acid as follows:



The rate of dissolution of silica is generally quite slow but becomes faster as the hydroxyl concentration increases. Note also that the rate is 10,000 times faster at a pH of 8.5 than at a pH of 3 (Iler, 1979).

Mineral compatibility from CO₂-brine-rock interaction experiments conducted in support of basin characterization projects under the Department of Energy suggests that feldspars (plagioclase and albite-K-spar system) are destabilized by the drop in pH associated with carbon dioxide dissolution in the formation brine water, favoring the formation of minerals such as kaolinite, muscovite, and paragonite (LBNL, 2014).

The principal effect of acid on clays is to leach metal ions from the clay lattice sites, leaving behind a silica framework. In experiments which monitored the x-ray diffraction pattern of the clays as the metal ions were leached out by acid, the pattern remained very similar to the original clay x-ray pattern even when 50% of the aluminum had been extracted from the mineral (Matthews et al., 1955). There are two types of sites in clays where metal ions can be located. The largest fraction of metal ions is located within the octahedral sites of the clay structure. These are part of the alumina sheet in the mineral structure and are coordinated to six oxygens. A smaller fraction of the metal ions occupies the tetrahedral sites. These are part of the silica sheet and are coordinated to four oxygens. Octahedrally coordinated aluminum is leached out at a faster rate than tetrahedrally coordinated aluminum (Turner, 1964).

At the Frio Brine Pilot Test (in the Texas Gulf Coast Region), following carbon dioxide breakthrough, samples from the monitoring well showed sharp drops in pH, pronounced increases in alkalinity and iron content, and significant shifts in the isotopic compositions of formation waters, dissolved inorganic carbon, and methane (Kharaka et al., 2006). Geochemical modeling of the Frio Brine Pilot indicates that brine pH would have dropped lower but was buffered by dissolution of carbonate and iron oxyhydroxides (Kharaka et al., 2006). The dissolution of minerals, especially iron oxyhydroxides and leaching of clays could mobilize metals and organic compounds in formations containing residual hydrocarbons or other organics (Kharaka et al., 2006).

The experimental and modeling analyses suggest that mineral precipitation and dissolution reactions (within the target formation) are not expected to lead to significant changes to the underground hydrologic system over time frames (approximately 30 years) typically relevant for injection operations.

2.7.3 Site Specific Geochemical Modeling

Injection of CO₂ into a reservoir leads to dissolution and dissociation of CO₂ in the formation water (FW), causing the pH to decline and changing the geochemical equilibrium. As a result, dissolution and precipitation of minerals will take place until a new geochemical equilibrium is reached. This process may take hundreds of years due to the slow rate at which some minerals react. Mineral reactions, speciation reactions, and gas dissolution reactions are quantified and coded in public geochemical databases (*e.g.*, Thermoddem developed by BRGM), which can be used by the simulation code PHREEQC to compute geochemical equilibria and kinetic rates. PHREEQ is a C and C++ model software designed to solve various aqueous calculations and is available as open-source code through the USGS.

Quantification of the reactions includes the dependency of the temperature, pressure, and composition of the FW. Since 2008, PHREEQC has been coupled to the Shell reservoir simulator MoReS (proprietary software), to enable simulation of gas and fluid flow together with geochemical reactions, also called reactive transport modelling (RTM). In this screening study, MoReS-PHREEQC and Thermoddem (adapted) are used to carry out batch geochemical modelling (0D, no transport) to quantify the impact of CO₂ injection for the St. Helena Parish site.

Shell carried out a geochemical screening study for the Shell St. Helena Parish site, to predict the impact of CO₂ storage on the mineralogy, formation water (FW), and potential generation of H₂S. Three aquifer formations were studied, Lower Tuscaloosa, Wilcox, and Frio, which have varying depth, pressure, temperature, and mineralogy.

The geologic matrix and initial conditions data for the three targeted reservoirs using has been provided through analogue and offset geologic data basis to provide the mineralogy, temperature, and pressures conditions outlined the prior sections. Porosity was set to 12 percent for all reservoirs. The composition of the formation fluids was only available for the Frio Formation. Data was provided from samples of the Lower Miocene (depths ~6,000 – 8,000 feet) from the Good Hope Field in St. Charles Parish.

Using the mineral and formation fluid data, Shell performed a reconciliation using OLI Studio and PHREEQC, hence defining and verifying a geochemical equilibrium state for all three aquifers.

MoReS-PHREEQC was then used to compute the impact of adding pure CO₂ gas (*i.e.*, without contaminants) on the geochemical equilibrium in one single grid cell. The latter is also called batch modelling and excludes transport effects.

The results show that CO₂ dissolves and dissociates in the formation water, causing the pH to decline. As a result, mineral dissolution and precipitation reactions occur. In general, the dissolution of chlorite, calcite, and illite is encountered, as well as precipitation of dolomite, kaolinite, siderite, and quartz. As minerals have different densities and react in various quantities, the porosity in the simulation decreased for all target reservoirs (Table 2-12).

In the two deepest formations, only very low amounts of H₂S in the gas phase are predicted by the model, up to 0.1 ppm in Lower Tuscaloosa and 0.02 ppm for Wilcox. Based on these relatively small numbers, a serious impact of H₂S generation due to CO₂ injection is considered to be low in these formations.

Results for Frio are uncertain as the simulations encountered numerical instabilities and depend on how the reaction of pyrite is treated in the model. A maximum of 14 ppm H₂S in the gas phase is computed during certain periods in the simulation, however we consider this a low reliability result due to the numerical instabilities. A much lower concentration (even below that predicted for the Wilcox), would be more in line with theoretical expectations (due to lower reservoir temperatures than in Wilcox), and in fact a very low concentration of 0.0001 ppm is observed during other periods in the Frio simulation. Nevertheless, due to the numerical instabilities we also cannot be 100% certain of this very low concentration prediction at this stage.

Further evaluation of the geochemical database, especially related to redox reactions and H₂S, is required to reduce model prediction uncertainties. It is recommended to carry out a follow-up study once more accurate data (mineralogical and formation fluid compositions) are obtained from the data acquisition of the injection wells. Such follow-up work should include a 1D and/or 2D modelling study to assess reactive transport effects of CO₂, uncertainty quantification (impact of physiochemical model input parameter uncertainties like mineral dissolution/precipitation kinetic rates), as well as the impact of contaminants in the reaction stream. The future geochemical modeling will also evaluate potential clogging of the near-well area, hence injectivity loss, due to

water evaporation (dry-out) in the injected CO₂ and salt precipitation. Salt accumulation can be enhanced as a result of capillary backflow of brine from the aquifer to the dry-out area.

The sampling program for the injectors has been designed to include fundamental testing to evaluate key geochemical parameters. Secondary trapping mechanisms include solubility trapping by dissolution of the injected carbon dioxide into the in-situ formation brine, residual gas trapping by capillary forces, and mineralization by chemical interactions between the injected carbon dioxide, formation fluids, and the rock matrix.

The sampling program that will be implemented during well construction has been designed to include sampling of relevant formation fluids and formation materials so that tests on both injection interval and caprock can be made (see the data acquisition plan in **Module D – Pre-Operational Testing and Logging**). The interactions between carbon dioxide, site-specific formation brines, and formation minerals (collected via core and cuttings) will be analyzed using geochemical and reactive transport models (as discussed above), to refine the current simulation model and provide a site-specific analysis of changes in formation water chemistry, mineral precipitation and dissolution reactions, and any potential resulting effects on formation porosity and permeability.

2.8 SITE SUITABILITY SUMMARY

The Shell St. Helena Parish site is suitable for injection of CO₂ as per 40 CFR 146.83 standards for the Confining and Injection Zones. The key factors driving site suitability are summarized:

- There is a minimum of artificial penetrations (legacy wells) in the leasehold area relative to the rest of Louisiana, reducing associated CO₂ containment risk.
- Sink depths are at 3,500-14,000 feet TVDSS, which is 1) favourable for supercritical CO₂ injection which increases site efficiency (injecting denser supercritical CO₂ means more can be stored in equivalent pore space) and 2) above the regional geopressured zone which reduces storage capacity as the reservoir is already near the fracture pressure threshold.
- The lease hold site is relatively structurally quiescent with minor or sub seismic faulting in the area.

- Structural dips are approximately 1.5 degrees which is low for onshore Louisiana and generally favorable for migration assisted CCS in a saline aquifer.
- There are three potential stacked injection zones Frio (primary), Wilcox (tertiary), Lower Tuscaloosa (secondary) in the storage complex thus improving site capacity and efficiency.
- The proposed storage complex at the Shell St. Helena Parish project site is capped by a thick (average ~370 ft TVT), regionally correlative primary confining zone above the Frio Injection Zone (Anahuac ‘Heterostegina’ limestones and shales and Lower Miocene shale) and contains thick secondary containment zones above the deeper injection zones (marine origin Midway Shale above the Wilcox Injection Zone and marine origin Eagle Ford/Tuscaloosa Marine shale above the Lower Tuscaloosa Injection Zone).

The Frio, Wilcox, and Lower Tuscaloosa Injection Zones are siliciclastic dominated packages. The heterogeneity and distribution of the sand and shale facies, as well as correlative intra-reservoir baffles and potential barriers, provide substantial local immobilization and containment of the proposed volumes of CO₂ to be injected. Along with the local trapping and immobilization of CO₂ by small and larger scale structural heterogeneity, substantial volumes of CO₂ can be trapped in the pore spaces by capillary forces and dissolved in the *in-situ* brine of the leasehold injection zones.

The low structural dips at the site result in lower rates of lateral migration. Any mobile CO₂ that moves to the top of the injection zone and along the base of the confining zone will travel more slowly, and thus allow for more time to be dissolved in the brine, trapped in the capillary pore spaces, or mineralized and thus reduce containment risk.

The mineralogy of the storage complex (geologic matrix) and formation water is not reactive with the injected CO₂ stream, which will be confirmed with data collected at the site during site appraisal. Injection and monitoring well materials that will be subject to the injected CO₂ stream have been chosen for their corrosion resistance and the well(s) design chosen to further reduce containment risk.

Injection wells have been sited at specified locations to maximum the offset to legacy wells and minor normal fault systems primarily interpretable in the deepest interval of interest (Lower Tuscaloosa) outside the AoR, thus, minimizing the risk of loss of containment. The rates of injection of CO₂ have been optimized to reduce risk of loss of containment of the mobile CO₂ as well as loss of containment of the *in-situ* injection zone formation fluids via pressure building up above defined threshold values.

The primary confining zone is a thick, low net to gross, heterolithic section of primarily carbonates and shale. A connected open fracture system in the carbonates, if present, could be a potential concern within the confining zone. This will be addressed by information gathered from whole core, borehole imaging and dynamic testing of the confining zone during appraisal of the leasehold site.

[REDACTED]

[REDACTED]

[REDACTED]

Injection is limited by potential pressure constraints associated with legacy artificial penetrations and known faults in the general area north and south of the Shell St. Helena Parish site. Site appraisal and monitoring activities are designed to better understand reservoir quality and hydraulic connectivity which drive the pressure behavior and associated site risks.

3.0 AOR AND CORRECTIVE ACTION PLAN

Shell has uploaded the “AOR and Corrective Action Plan” technical report [40 CFR 146.82(a) and 146.84(b)] via the EPA GS DT portal. The report contains the details of the computational modeling [40 CFR 146.84(c)], which includes pressure and plume maps at 5-year intervals for the simulated 25-year operation period. The report also includes a tabulation of all wells within the AoR [per 40 CFR 146.82(a)(4)]. A thorough evaluation of each of these wells, using well records, scout tickets, and logs was performed to determine if a corrective action plan is warranted. A reevaluation schedule for AoR delineation is set at 5-year intervals during injection operations.

This plan will be updated as the project is developed to be consistent with the data derived from the appraisal wells, injection wells, and collected through the operational and testing of the carbon sequestration project.

AoR and Corrective Action GS DT Submissions

GS DT Module: AoR and Corrective Action

Tab(s): All applicable tabs

Please use the checkbox(es) to verify the following information was submitted to the GS DT:

- Tabulation of all wells within AoR that penetrate confining zone **[40 CFR 146.82(a)(4)]**
- AoR and Corrective Action Plan **[40 CFR 146.82(a)(13) and 146.84(b)]**
- Computational modeling details **[40 CFR 146.84(c)]**

4.0 FINANCIAL RESPONSIBILITY

Shell has submitted a Financial Responsibility Demonstration (FRD) in accordance with 40 CFR 146.82(a) and 146.85. The submittal covers activities identified in the corrective action plan, injection plugging plan, post-injection site care and closure, and the emergency and remedial response plan. Additionally, it covers the monitoring and reporting activities during injection and closure operations.

Cost estimates for the activities were provided by independent third-party contractors and /or by knowledge of industry standards and practices per 40 CFR 146.85(c). The cost estimates include project management, administrative costs, overhead, and contingency and are presented in Table 4-1.

Cost estimates with supporting documentation have been uploaded on the “Cost Estimates” Tab in Module C of the GSDT Tool for this initial submittal of a permit application. Actual values may change due to inflation of costs or additional changes to the final project. If the cost estimate changes, Shell will adjust the value of the FRD, and it will be submitted to the authorized regulatory body for review and approval on an “as needed” basis. Detailed information and supporting documents have been submitted through the GSDT through “***Module C – Financial Responsibility Demonstration.***”

Financial Responsibility GSDT Submissions

GSDT Module: Financial Responsibility Demonstration

Tab(s): Cost Estimate tab and all applicable financial instrument tabs

Please use the checkbox(es) to verify the following information was submitted to the GSDT:

Demonstration of financial responsibility **[40 CFR 146.82(a)(14) and 146.85]**

5.0 INJECTION WELL CONSTRUCTION

Shell plans to operate a sequestration storage project in St. Helena Parish and is requesting a permit for two Class VI CO₂ Sequestration wells (Injection Wells Soterra IF 1-1 and Soterra IT 2-1) that will be completed for injection into the Frio and Lower Tuscaloosa Injection Intervals. The Soterra IF 1-1 will be plugged back to approximately 6,755 feet and completed for injection into the Frio reservoir. Both well(s) will be constructed in accordance with 40 CFR 146.86(b) standards for Class VI Injection Wells. Note, unless specified, all depths in this section are relative to True Measured depth (TMD).

The following sections address the procedures to drill, sample, complete, operate, and test the proposed wells, as well as specifications of the construction materials. Additionally, procedures for plugging and abandoning the wells are also provided. Specification of maximum instantaneous rate of injection; average rate of injection; and the total monthly and annual volumes requested are also included. All construction data meets the requirements for Class VI well in under 40 CFR 146.82(a)(9), (11), and (12).

All phases of well construction will be supervised by qualified individuals acting under the responsible charge of a licensed professional engineer who is knowledgeable and experienced in practical drilling engineering and who is familiar with the special conditions and requirements of Class VI CO₂ injection well construction.

5.1 PROPOSED STIMULATION PROGRAM [40 CFR 146.82(A)(9)]

A stimulation plan has been developed for the Soterra IF 1-1 and Soterra IT 2-1, which will be initially employed after the drilling and completion of the injection wells. The stimulation program will consist of an acidization and wellbore flowback (utilizing coiled tubing) to remove formation skin damage due to invasion of solids during drilling and any perforation damage. The acid treatment will consist of the following acids, with actual volumes to be determined prior to the time of placement:

- 15% Hydrochloric Acid (HCl)
- 7.5% HCl + 1.5% Hydrofluoric (HF) Acid

Best practices for recommended volumes for acid stimulations generally range from 50 to 100 gallons per foot, depending on the severity of near wellbore formation damage. Chemicals will be added to the acid blends to limit clay swelling, reduce emulsions, and inhibit reaction to the completion equipment and tubulars. The type and quantity of these chemicals will be determined based on formation characteristics determined from core and wireline log evaluation. All stimulations fluids that could be used will verify that there is no adverse reaction with confinement of the reservoir. Additional acids and diverter fluids may be considered at the time of placement. The acid fluids will be displaced from the wellbore using non-hazardous treating water or brine.

Additional stimulation treatment may be necessary if the injection performance of the well is unacceptable. Stimulation procedures will be submitted for approval prior to any additional stimulation work.

5.2 CONSTRUCTION DESIGN AND PROCEDURES [40 CFR 146.82(A)(12)]

The proposed Completion Schematics for the Injection Wells are included as Figure 5-1 and 5-2. The schematic includes well casing specifications and setting depths, cementing data, and completion details. The proposed Wellhead Schematics for each of the wells is included as Figure 5-3.

5.2.1 Casing String Details

Casing specifications for the proposed Injection Wells are detailed in Tables 5-1 and 5-2 respectively. Stress calculations for all well casing have been provided in Appendix D. All components of the surface and protection casings will be manufactured to API standards and are designed for the proposed life of the well, based on the materials of construction and the environment of use. The casing strings will consist of both carbon steel (non-CO₂ contact) and martensitic stainless steel (25CR for CO₂ contact usage) to ensure the longevity of the wellbore. Carbon steel for surface and intermediate casing and a mixed string of carbon steel and 25CR steel

for the completion casing. Additionally, all casing strings will be fully cemented to surface, which will provide additional isolation of the casing string from external formation fluids along the borehole path.

Prior to running the casing in the hole, each string will be visually inspected and drifted to ensure that no defects are present. The connections will be cleaned, and the manufacturer's recommended thread compound will be applied to the pin of each connection before make-up.

5.2.2 Centralizers

The number of centralizers needed depends upon pipe weight, mud weight, hole deviation and hole condition. Each casing string will be centralized per Shell policy, achieving at least 70% standoff throughout the string.

Casing strings will have a centralizer attached to the casing at intervals along the entire well path. Centralizers will be placed to maximize the casing standoff from the well bore to enhance the cementing of the wells. The centralizers will be placed as follows:

- 1 centralizer per joint for the bottom 500 feet of each casing string
- 1 centralizer per three joints from 500 feet above the shoe to surface

Actual placement of centralizers will be determined once the drilling of each well section is completed, and logs have been reviewed. Additional centralizers may be used as needed to provide the highest quality cementing job possible.

5.2.3 Annular Fluid

The annular fluid type will be designed for these wells with an annulus monitoring and pressurization system will maintain the annulus at least 100 psi pressure greater than the injection tubing pressure. Sodium chloride brine with inhibitors or base oil are both under consideration.

5.2.4 Cementing Details

Shell has designed the cement program (Table 5-3) using cement types and additives which will be compatible with the CO₂ stream and formation fluids over the lifetime of the project [per 40 CFR 146.86 (b)(5)]. All casing strings will be cemented to surface, and a cementing job summary indicating returns at surface will be provided to the UIC Program Director prior to authorization to inject [LAC §3617 (A)(2)(d)].

Expected downhole temperature is 168 °F at 6,400 feet TMD for the Soterra IF 1-1 and expected downhole temperature is 294 °F at 14,300 feet TMD which is not considered detrimental to the cement. The cement will increase in hardness over time and reach a value close to its maximum compressive strength soon after setting.

5.2.5 Tubing and Packer Details

Tubing specifications for the proposed Injection Wells are detailed in Table 5-4 and 5-5, respectively. Stress calculations for all well casing have been included in Appendix D. The well(s) will be completed tubing design deemed sufficient for resistance to corrosion. The tubing will extend from the surface to the injection packer, with a slip-and-seal assembly installed to provide engagement with the surface wellhead.

The proposed injection packer(s) will be set in the completion casing in the Frio Injection Zone for Soterra IF 1-1 at an approximate depth of 4,730 feet TMD, and in the Lower Tuscaloosa Injection Zone for the Soterra IT 2-1, at a depth of approximately 13,500 feet. The proposed packer will be designed such that all the parts that will be in contact with the injection stream (“wetted parts”) will have the same corrosion resistance capabilities as are deemed necessary for the tubing. The packer assembly will include a Polished Bore Receptacle (PBR) of sufficient length to account for potential tubing movement during well operation.

Prior to running the tubing in the hole, each string will be visually inspected and drifted to ensure that no defects are present. The connections will be cleaned, and the manufacturer’s recommended thread compound will be applied to the pin of each connection before make-up.

5.3 PROPOSED DRILLING PROGRAM

Normal plant and area safety rules and regulations will be in force during installation of the wells. Prior to well construction, the ground surface will be graded to level. An all-weather location will be installed, with additional reinforcement placed under the rig substructure area. The rig contractor will provide power for the rig and associated equipment. The construction site will be barricaded to prevent entry by unauthorized personnel. Normal handling of the wellbore solids and fluids is anticipated during the drilling phases of the work and completion phases of the work.

All phases of well construction will be supervised by qualified individuals acting under the responsible charge of a licensed professional engineer who is knowledgeable and experienced in practical drilling engineering and who is familiar with the special conditions and requirements of Class VI CO₂ injection well construction.

5.3.1 Soterra IF 1-1 Injection Well

The drilling program for the Soterra IF 1-1 (Frio Injector) at the St. Helena Parish site contains a conductor hole, surface hole, intermediate hole, and injection hole. All depths in the outlined procedure are referenced to the drill floor elevation (DFE), which is estimated at 32.5 feet above ground level. The ground level elevation (GLE) is 166.1 feet above MSL for the Soterra IF 1-1 well. All depths are specified as TMD from DFE unless otherwise indicated.

5.3.1.1 *Proposed Drilling Procedure*

The following is the drilling and completion procedure for drilling the Soterra IF 1-1:

Surface Hole

1. Spud well
2. Drill 17-1/2" hole to 2,900 ft TMD
3. CBU and POOH
4. Run electric line logs per program (per LAC §3617.B.1.b.i and §3617.B.3)
5. R/U and run 13-3/8" casing to ~2,900 ft TMD, refer to Table 5.1 – Well Casing Specifications for a detailed description of the casing.

6. Cement same with cement returns to surface. Refer to Well Cementing Program for details.
7. Install wellhead, test same per Shell requirements.
8. N/U BOP and test same (per LAC §111.F.2.d)
9. P/U BHA and RIH
10. Perform 1-hr casing test (per LAC §3617.A.3.a)
11. Drill-out shoe track

Intermediate Hole

1. Drill 12-1/4" hole to ~4,807 ft TMD (30 ft into Frio confining zone)
2. CBU, ensure well is stable and static
3. POOH
4. Run electric line logs per program (per LAC §3617.B.1.b.i and per LAC §3617.B.3)
5. Run cement bond log, variable density log, and temperature log (per LAC §3617.B.1.b.ii and c.ii) across 13-3/8" casing
6. R/U and run 9-5/8" casing to ~4,807 ft TMD, refer to Table 5.1 – Well Casing Specifications for a detailed description of the casing.
7. Cement same with full returns to surface. Refer to Well Cementing Program for details.
8. Wait 12 hours and cut casing and install the 'B' section, test same per Shell requirements.
9. Install BOP.
10. Test BOP (per LAC §111.F.2.d)
11. P/U BHA and RIH
12. Perform 1-hr casing test (per LAC §3617.A.3.a)
13. Drill-out shoe track

Injection Hole

1. Perform shoe test (per LAC §3617.A.3.b)
2. Drill 8-1/2" hole to ~6,805 ft TMD (200 ft below base of Frio), following core acquisition program.
3. CBU, ensure well is stable and static
4. POOH

5. Run electric line logs per program (per LAC §3617.B.1.b.i and §3617.B.3)
6. Run cement bond log, variable density log, and temperature log (per LAC §3617.B.1.b.ii and c.ii) across 9-5/8" casing
7. R/U and run 7" casing to ~6,805 ft TMD with 8.7" external casing packer set at 4,730 ft TMD. Refer to Table 5.1 – Well Casing Specifications for a detailed description of the casing.
8. Cement same with full returns to surface. Refer to Well Cementing Program for details.
9. Wait on cement 12 hours. Cut casing install the 'C' wellhead section, test same per Shell requirements.
10. Install the BOP.
11. Test BOPs (per LAC §111.F.2.d)
12. P/U BHA and RIH
13. Perform 1-hr casing test (per LAC §3617.A.3.a) and acquire casing test affidavit
14. Drill-out shoe track

Test Hole

1. Perform shoe test (per LAC§3617.A.3.b)
2. Drill 6" hole to TD, as deep as 14,781 ft TMD, 100 ft below the base of the Tuscaloosa
3. CBU, ensure well is stable and static
4. POOH
5. Run electric line logs per program (per LAC§3617.B.1.b.i and §3617.B.3)
6. Run cement bond log, variable density log, and temperature log (per LAC §3617.B.1.b.ii and c.ii) across 7" casing
7. P/U cement stinger and RIH
8. Spot cement across open hole and abandon same. Refer to Well Cementing Program for details.
9. Flow check and POOH
10. WOC
11. RIH and tag cement top, dress-off cement to leave 50 ft good cement inside the 7" shoe
12. (TOC 6,755 ft)

13. Displace well from drilling mud to clear fluid
14. POOH
15. Install and test tubing head spool
16. Release drilling rig

5.3.1.2 Drilling Contingency Plans

In the event that unforeseen events occur, detailed plans to remedy the specific problem will be implemented using best engineering practices and judgment based on facts. The following are general contingency plans to address specific problems.

Borehole Drilling Lost Circulation Plan

If circulation is lost (low probability) while drilling the boreholes, lost circulation material pills will be pumped to re-establish circulation. Depending upon the severity of lost circulation encountered, lost circulation material may need to be blended with the drilling fluid in concentrations dictated by hole conditions to maintain circulation to the surface casing point. Should lost circulation occur while drilling from the base of conductor to the surface casing point, paper, cottonseed hulls, or other forms of standard lost circulation material may be used to remedy the loss condition.

Borehole Drilling Over pressured Zone

If an overpressure zone is encountered (not expected) while drilling the surface hole, the drilling fluid pump rate down the drill pipe will be increased while the drill fluid density is increased. The increased pumping rate will continue until the well stops flowing. If a drilling influx is encountered while drilling any other hole section, the blow out preventer (BOP) will be closed-in, and the well will be secured. The influx will be circulated out of the well while maintaining constant bottom hole pressure using the choke to prevent additional influx. Finally, the mud weight will be increased to a density sufficient to overbalance the well while circulating through the choke to maintain constant bottom hole pressure throughout the circulation. Once kill weight mud has been circulated around the well is confirmed to not be flowing, drilling will recommence.

Borehole Deviation Issues

Take inclination surveys minimum every 100 to 200 feet and at the TD for the hole size to monitor the well path. A maximum allowable deviation from vertical is 3 degrees, and maximum allowable deviation between surveys is 1 degree. If the maximum recommended deviation is exceeded, an evaluation will be made to determine whether remedial action is necessary.

5.3.1.3 Proposed Completion Procedures

The completion procedure has been developed to utilize the Frio Formation for sequestration of the injected CO₂. It is anticipated that the full interval in the Frio Formation will be utilized in each well completion. The following is a proposed completion procedure for the Soterra IF 1-1.

1. MIRU WL equipment, rig up PCE on 7-1/16" 10k valves
2. Cement bond log, variable density log, and temperature log (per LAC §3617.B.1.b.ii and c.ii) completed at end of drilling phase
3. RU WL and RIH Perforate the **Frio formation**
4. POOH and rig down wireline
5. Install 7-1/16" 10k x 3-1/16" 10k adaptor cap and 3-1/16" 10k valve on wellhead
6. Pressure Test wellhead
7. RU and prepare for agreed upon perforation clean up.
8. RU high pressure pumps and ancillary equipment to wellhead
 - a. Pressure test all pumping equipment and TPW
9. Perform Injection step rate test and fall off with brine water down 7" 29# casing
 - a. Compatibility test performed with Injection brine
 - b. Total Injection Volume – 9,180 bbls
10. Evaluate results of the Injection test
11. RU WL and RIH and set cast iron bridge plug (CIBP)
12. POOH with WL
13. RU and RIH with WL Perforate the **Frio formation**
14. RU and prepare for agreed up perforation clean up.

15. RU high pressure pumps and ancillary equipment to wellhead
 - a. Pressure test all pumping equipment and TPW
16. Perform Injection step rate test and fall off with brine water down 7" 29# casing
 - a. Compatibility test performed with Injection brine
 - b. Total Injection Volume – 9,180 bbls
17. POOH and rig down wireline
18. Rig down high-pressure pumps and ancillary equipment
19. RIH set CIBP via WL above **Frio perforations**
20. Place 30 feet of cement on to of CIBP to Temporary Abandonment (TA)
21. POOH and allow cement to develop strength
22. Inflow or pressure test per requirements
23. Install tubing hanger and 3" BPV
24. Remove 7" working valves and install 7-1/16" 10k x 3-1/16" 10k adaptor and 3-1/16" MV on wellhead
25. Remove 3-1/16" BPV and install TWCV. Pressure test connection.
26. Remove TWCV and install BPV. Leave production tree as per diagram.

The final completion procedure has been developed to utilize the Frio Formation for sequestration of the injected CO₂. It is anticipated that the full interval in the Frio Formation will be utilized in each well completion. The following is a proposed final completion procedure for the Soterra IF 1-1.

1. Pick up a 6-inch bit and casing scraper for 7.0-inch casing and trip into the wellbore.
2. Confirm cement top and if necessary, drill out the cement and CIBP at $\pm 5,177$ and continue to $\pm 6,755$ feet (50 feet above the casing shoe), milling up the second plug.
3. Lower the workstring into the wellbore to the bottom of the protection casing and circulate solids from the wellbore.
4. Pick packer on workstring and lower into wellbore.
5. Set injection packer at approximately $\pm 4,730$ feet. Conduct preliminary pressure test to verify pressure integrity of the well annulus.

6. Retrieve the workstring from the wellbore.
7. Pick up the seal assembly on injection tubing and lower into the wellbore.
8. Circulate inhibitive packer fluid through wellbore until completion brine is fully displaced.
9. Land the tubing in the packer and wellhead and conduct preliminary annulus pressure test to verify pressure integrity.
10. Nipple down well control equipment and install tubing head adapter.
11. Rig down workover rig and demobilize from site.
12. Conduct mechanical integrity test and ambient pressure test
13. Return well to site for installation and connection of surface equipment and piping.

General Notes:

- *All depths referenced are approximate and are based on the expected log depth.*
- *Actual depths may vary based on lithology of local formations.*

5.3.1.4 Proposed Well Fluids Program

Lost circulation material (LCM) will be on location to treat for fluid losses in top hole sands. The fluid system will be pre-treated with LCM before encountering any known or suspected loss zones. High-viscosity sweeps will be used to assist hole cleaning. Sodium chloride (NaCl) is planned for use as the completion fluid. The fluid weight will be maintained to contain reservoir pressures without inducing flow to the wellbore. Table 5-6 is provided to show the proposed well fluids per hole.

5.3.1.5 Proposed Cementing Program

The surface and protection casing strings will be cemented using modern cementing technology and practices. Cementing standards and materials featured in as described in Section 5.2.4 will be used during the construction of the well.

Surface Casing

The following cementing program (Table 5-7) is proposed for installation of the surface casing string:

- 13-3/8-inch in 17-1/2-inch borehole at 2,900 feet
- Float shoe;
- Float Collar, 2 joints above the float shoe;
- Cement to surface;
- Cement volumes are estimated 50% excess over bit size in open hole interval;
- Actual volume to be calculated from caliper log plus 30% excess;
- In the event the hole diameter exceeds the scale of a 2-dimensional caliper, a minimum of 150 percent of the annular space between the casing and the maximum caliper reading will be used for calculating cement volume for that section of the wellbore.

Intermediate Casing

The following cementing program (Table 5-8) is proposed for installation of the intermediate casing string:

- 9-5/8-inch in 12-1/4-inch borehole at 4,807 feet
- Float shoe;
- Float Collar, 2 joints above the float shoe;
- Cement to surface;
- Cement volumes are estimated 30% excess over bit size in open hole interval;
- Actual volume to be calculated from caliper log plus 20% excess;
- In the event the hole diameter exceeds the scale of a 2-dimensional caliper, a minimum of 150 percent of the annular space between the casing and the maximum

caliper reading will be used for calculating cement volume for that section of the wellbore.

Completion Casing

The following cementing program (Table 5-9) is proposed for installation of the protection casing string:

- 7.0-inch in 8-1/2-inch hole at 6,805 feet;
- Float shoe;
- Float Collar, 2 joints above the float shoe;
- Stage tool and external casing packer at 4,730 ft
- cement to surface;
- estimated 30% excess over bit size in open hole sections only;
- actual volume to be calculated from caliper log plus 20% excess; and
- In the event the hole diameter exceeds the scale of a 2-dimensional caliper, a minimum of 150 percent of the annular space between the casing and the maximum caliper reading will be used for calculating cement volume for that section of the wellbore.
- 50 bbls of excess cement in the second stage in cased hole

5.3.1.6 Well Logging, Coring, and Testing Program

Details on the proposed logging program are contained in the “*Pre-Operational Testing and Logging Plan*” submitted in **Module D** – Pre-Operational Testing. All tools will be run on a wireline and will be compatible with open hole and cased hole diameters, allowing for successful testing runs.

5.3.2 Soterra IT 2-1 Injection Well

The drilling program for the Soterra IT 2-1 (Lower Tuscaloosa Injector) at the St. Helena Parish site contains a conductor hole, surface hole, intermediate hole, and injection hole. All depths in

the outlined procedure are referenced to the DFE, which is estimated at 32.5 feet above ground level. The ground level elevation is 108.2 ft above MSL for the Soterra IT 2-1 well. All depths are specified as TMD from drill floor elevation DFE unless otherwise indicated.

5.3.2.1 Proposed Drilling Procedures

The following is the drilling and completion procedure for drilling the Soterra IT 2-1:

Surface Hole

1. Spud well
2. Drill 17-1/2" hole to 3,000 ft TMD
3. CBU and POOH
4. Run electric line logs per program (per LAC §3617.B.1.b.i and §3617.B.3)
5. R/U and run 13-3/8" casing to ~3,000 ft TMD, refer to Table 5.2 – Well Casing Specifications for a detailed description of the casing.
6. Cement same with cement returns to surface. Refer to Well Cementing Program for details.
7. Install wellhead, test same per Shell requirements.
8. N/U BOP and test same (per §111.F.2.d)
9. P/U BHA and RIH
10. Perform 1-hr casing test (per LAC §3617.A.3.a)
11. Drill-out shoe track

Intermediate Hole

1. Drill 12-1/4" hole to ~13,550 ft TMD (50 ft below the base of the Austin Chalk)
2. CBU, ensure well is stable and static
3. POOH
4. Run electric line logs per program (per LAC §3617.B.1.b.i and §3617.B.3)
5. Run cement bond log, variable density log, and temperature log (per LAC §3617.B.1.b.ii and c.ii) across 13-3/8" casing
6. R/U and run 9-5/8" casing to ~13,550 ft TMD, refer to Table 5.2 – Well Casing Specifications for a detailed description of the casing.

7. Cement same with full returns to surface. Refer to Well Cementing Program for details.
8. Wait 12 hours and cut casing and install the ‘B’ section, test same per Shell requirements.
9. Install BOP.
10. Test BOP (per §111.F.2.d)
11. P/U BHA and RIH
12. Perform 1-hr casing test (per LAC §3617.A.3.a)
13. Drill-out shoe track

Protection Hole

1. Perform shoe test (per LAC §3617.A.3.b)
2. Drill 8-½” hole to ~14,721 ft TMD (150 ft below base of the Lower Tuscaloosa Formation), following core acquisition program.
3. CBU, ensure well is stable and static
4. POOH
5. Run electric line logs per program (per LAC §3617.B.1.b.i and §3617.B.3)
6. Run cement bond log, variable density log, and temperature log (per LAC §3617.B.1.b.ii and c.ii) across 9-5/8” casing
7. R/U and run 7” casing to ~14,721 ft TMD with 8.7” external casing packer set at 13,500 ft TMD. Refer to Table 5.2 – Well Casing Specifications for a detailed description of the casing strings.
8. Cement same with full returns to surface. Refer to Well Cementing Program for details.
9. Wait on cement 12 hours. Cut casing install the ‘C’ wellhead section, test same per Shell requirements.
10. Perform 1-hr casing test (per LAC §3617.A.3.a) and acquire casing test affidavit
11. Run cement bond log, variable density log, and temperature log (per LAC §3617.B.1.b.ii and c.ii) across 7” casing
12. Displace well from drilling mud to clear fluid
13. POOH
14. Install and test tubing head spool
15. Release drilling rig

5.3.2.2 Drilling Contingency Plans

Borehole Drilling Lost Circulation Plan

If circulation is lost (low probability) while drilling the boreholes, lost circulation material pills will be pumped to re-establish circulation. Depending upon the severity of lost circulation encountered, lost circulation material may need to be blended with the drilling fluid in concentrations dictated by hole conditions to maintain circulation to the surface casing point. Should lost circulation occur while drilling from the base of conductor to the surface casing point, paper, cottonseed hulls, or other forms of standard lost circulation material may be used to remedy the loss condition.

Borehole Drilling Over pressured Zone

If an overpressure zone is encountered (not expected) while drilling the surface hole, the drilling fluid pump rate down the drill pipe will be increased while the drill fluid density is increased. The increased pumping rate will continue until the well stops flowing. If a drilling influx is encountered while drilling any other hole section, the blow out preventer (BOP) will be closed-in, and the well will be secured. The influx will be circulated out of the well while maintaining constant bottom hole pressure using the choke to prevent additional influx. Finally, the mud weight will be increased to a density sufficient to overbalance the well while circulating through the choke to maintain constant bottom hole pressure throughout the circulation. Once kill weight mud has been circulated around the well is confirmed to not be flowing, drilling will recommence.

Borehole Deviation Issues

Take inclination surveys minimum every 500 feet and at the TD for the hole size to monitor the well path. A maximum allowable deviation from vertical is 3 degrees, and maximum allowable deviation between surveys is 1 degree. If the maximum recommended deviation is exceeded, an evaluation will be made to determine whether remedial action is necessary.

5.3.2.3 Proposed Completion Procedures

The completion procedure has been developed to utilize the Lower Tuscaloosa Formation for sequestration of the injected CO₂. It is anticipated that the full interval in the Lower Tuscaloosa Formation will be utilized in each well completion. The following is a proposed completion procedure for the Soterra IT 2-1.

1. MIRU WL equipment, rig up PCE on 7-1/16" 10k valves
2. Run GR-CBL and other logs if necessary
3. RU WL and RIH Perforate the **Lower Tuscaloosa formation**
4. POOH and rig down wireline
5. Install 7-1/16" 10k x 3-1/16" 10k adaptor cap and 3-1/16" 10k valve on wellhead
6. Pressure Test wellhead
7. RU and prepare for agreed upon perforation clean up.
8. RU high pressure pumps and ancillary equipment to wellhead
 - a. Pressure tests all pumping equipment and TPW
9. Perform Injection step rate test and fall off with brine water down 7" 29# casing
 - a. Compatibility test performed with Injection brine
 - b. Total Injection Volume – 9,180 bbls
10. Evaluate results of the Injection test
11. POOH and rig down wireline
12. Rig down high-pressure pumps and ancillary equipment
13. RIH set CIBP via WL above **Lower Tuscaloosa perforations**
14. Place 30 feet of cement on top of CIBP to Temporary Abandonment (TA).
15. Inflow or pressure test per requirements
16. Install tubing hanger and 3" BPV
17. Remove 7" working valves and install 7-1/16" 10k x 3-1/16" 10k adaptor and 3-1/16" MV on wellhead
18. Remove 3-1/16" BPV and install TWCV. Pressure test connection.

19. Remove TWCV and install BPV. Leave production tree as per diagram

The final completion procedure has been developed to utilize the Lower Tuscaloosa Formation for sequestration of the injected CO₂. It is anticipated that the full interval in the Lower Tuscaloosa Formation will be utilized in each well completion. The following is a proposed final completion procedure for the Soterra IT 2-1.

1. Pick up a 6-inch bit and casing scraper for 7.0-inch casing and trip into the wellbore.
2. Confirm cement top and if necessary, drill out the cement and CIBP at $\pm 14,296$ and continue to $\pm 14,671$ feet (50 feet above the casing shoe).
(Note: Perforating depths are approximate and will be determined after review of open hole logs.)
3. Lower the workstring into the wellbore to the bottom of the protection casing and circulate solids from the wellbore.
4. Pick up injection packer on workstring and lower into wellbore.
5. Set injection packer at approximately $\pm 13,500$ feet. Conduct preliminary pressure test to verify pressure integrity of the well annulus.
6. Retrieve the workstring from the wellbore.
7. Pick up the seal assembly on injection tubing and lower into the wellbore. Externally pressure test each connection.
8. Circulate inhibitive packer fluid through wellbore until completion brine is fully displaced.
9. Land the tubing in the packer and wellhead and conduct preliminary annulus pressure test to verify pressure integrity.
10. Nipple down well control equipment and install tubing head adapter.
11. Rig down drilling rig and demobilize from site.
12. Rig up coiled tubing and nitrogen equipment. Conduct formation backflow with nitrogen to develop well and collect native formation brine samples. An acid stimulation treatment may also be required and may be followed by either a wellbore flowback to remove drilling/completion solids from near-wellbore interval or displacement of the acid into the formation.

13. Conduct mechanical integrity test and ambient pressure test per Section VI.A.9 – Well Logging, Coring, and Testing.
14. Return well to site for installation and connection of surface equipment and piping.

General Notes:

- *All depths referenced are approximate and are based on the expected log depth.*
- *Actual depths may vary based on lithology of local formations.*

5.3.2.4 Proposed Well Fluids Program

Lost circulation material (LCM) will be on location to treat for fluid losses in top hole sands. The fluid system will be pre-treated with LCM before encountering any known or suspected loss zones. High-viscosity sweeps will be used to assist hole cleaning. Sodium chloride (NaCl) is planned for use as the completion fluid. The fluid weight will be maintained to contain reservoir pressures without inducing flow to the wellbore. Table 5-10 is provided to show the proposed well fluids per hole.

5.3.2.5 Proposed Cementing Program

The surface and protection casing strings will be cemented using model cementing technology and practices. Cementing standards featured in Section 5.2.4 will be used during the construction of the well.

Surface Casing

The following cementing program (Table 5-11) is proposed for installation of the surface casing string:

- 13-3/8-inch in 17-1/2-inch borehole at 3,000 feet
- Float shoe;
- Float Collar, 2 joints above the float shoe;
- Cement to surface;

- Cement volumes are estimated 50% excess over bit size in open hole interval;
- Actual volume to be calculated from caliper log plus 30% excess; and,
- In the event the hole diameter exceeds the scale of a 2-dimensional caliper, a minimum of 150 percent of the annular space between the casing and the maximum caliper reading will be used for calculating cement volume for that section of the wellbore.

Intermediate Casing

The following cementing program (Table 5-12) is proposed for installation of the intermediate casing string:

- 9-5/8-inch in 12-1/4-inch borehole at 13,550 feet; with 12.45" external casing packer and stage tool set at 7,400 feet;
- Float shoe;
- Float Collar, 2 joints above the float shoe;
- Cement to surface;
- Cement volumes are estimated 30% excess over bit size in open hole interval;
- Actual volume to be calculated from caliper log plus 20% excess; and,
- In the event the hole diameter exceeds the scale of a 2-dimensional caliper, a minimum of 150 percent of the annular space between the casing and the maximum caliper reading will be used for calculating cement volume for that section of the wellbore.

Protection Casing

The following cementing program (Table 5-13) is proposed for installation of the protection casing string:

- 7.0-inch in 8-1/2-inch hole at 14,721 feet, with 8.7" external casing packer and stage tool set at 13,500 feet;
- Float shoe;

- Float Collar, two joints above the float shoe;
- cement to surface;
- estimated 30% excess over bit size in open hole sections only;
- actual volume to be calculated from caliper log plus 20% excess; and
- In the event the hole diameter exceeds the scale of a 2-dimensional caliper, a minimum of 150 percent of the annular space between the casing and the maximum caliper reading will be used for calculating cement volume for that section of the wellbore.
- 50 bbls of excess cement in the second stage in cased hole

5.3.2.6 Well Logging, Coring, and Testing Plan

Details on the proposed logging program are contained in the “*Pre-Operational Testing and Logging Plan*” submitted in **Module D** – Pre-Operational Testing. All tools will be run on a wireline and will be compatible with open hole and cased hole diameters, allowing for successful testing runs.

5.3.3 Wellhead Schematics

The final wellheads for each of the aforementioned wells will be similar with trim that is resistant to the CO₂ stream and its impurities. All wellheads are per API standards. The tubing spool and master valves shown are from the previous injection test and will be replaced prior to CO₂ injection. Wellhead Schematics are contained in Figure 5-3 for both injection wells.

6.0 PRE-OPERATIONAL LOGGING AND TESTING

Shell has designed the sequestration project using 2 injection wells. These wells will be completed into one or more of the project Injection Zones described above. All injection wells will follow the 40 CFR §146.87(a), (b), (c), and (d) and standards for logging and testing requirements. Coring will be adaptive and based upon well spatial variability, wellbore conditions, core recovery, and core quality as each project well is drilled. All wells will demonstrate mechanical integrity prior to receiving authorization to inject.

The data obtained in this plan will be used to validate and update, if necessary, the “*Area of Review and Corrective Action Plan*” (submitted in **Module B**), to define and reduce uncertainties with the site characterization, revise the “*E.1-Testing and Monitoring Plan*” (submitted in **Module E**), and determine final operational procedures and limits.

This plan has been uploaded in **Module D**:

“*D. Pre-Operations Testing and Logging Plan (Rev. 0 – November 2022)*”

Pre-Operational Logging and Testing GSDT Submissions

GSDT Module: Pre-Operational Testing

Tab(s): Welcome tab

Please use the checkbox(es) to verify the following information was submitted to the GSDT:

Proposed pre-operational testing program [**40 CFR 146.82(a)(8) and 146.87**]

7.0 WELL OPERATION

Shell will operate the Injection Wells at the St. Helena Parish Site per the operating requirements in accordance with 40 CFR 146.82(a)(7) and (10). No injection operations will occur between the outermost casing and the USDW per 40 CFR 146.88 (a). Operating the well in this fashion will prevent the movement of fluids that could result in the pollution of a USDW and will prevent leaks from any of the subject injection wells into unauthorized zones.

During injection operations, continuous measurements will be taken at the wellhead for injection pressure, rate, volume, and temperature of the CO₂ stream [40 CFR 146.88(e)(1)]. The maximum injection pressure is governed by the fracture gradient. Operating injection pressures are set at 80 percent below the calculated values (see Section 2.4.4 for value determination) when possible but will always remain below 90 percent. Site specific in-situ fracture gradients will be determined during the drilling and testing of the Class VI Injection Wells.

If there are major changes to the operational stream (density changes, composition, etc.) or a new source, Shell may reevaluate and adjust the operating pressures with approval from the UIC Program Director. Under routine operations, injection pressures that approach the limits shown below will trigger reduced injection or a full system shutdown. Well conditions will then be monitored to decide on steps to return to full rate injection. In cases where return to full injection is not possible, additional troubleshooting steps may be required. Values in Tables 7-1 and 7-2 will be updated after drilling the appraisal wells and will be finalized after the completion of the approved injection wells.

Shell will provide an analysis of the chemical and physical characteristics of the CO₂ stream prior to injection operations [40 CFR 146.82(a)(7)(iv)]. The source(s) of the final stream will also be provided in accordance with 40 CFR 146.82(a)(7)(iii).

During operations, Shell will analyze the composite carbon dioxide stream to yield data representative of its chemical and physical characteristics and to meet the requirements of 40 CFR §146.90(a) and LAC §3625.A.1 (State of Louisiana) as present in the E.1 - Testing and Monitoring Plan – submitted in **Module E**.

8.0 TESTING AND MONITORING

In accordance with USEPA 40 CFR §146.90, Shell has developed a testing and monitoring plan for the lifetime of injection operations. In addition to demonstrating that the injection wells will be operating as expected, that the carbon dioxide plume and pressure front are moving as predicted, and there is no endangerment to USDWs, the monitoring data will be used to validate and guide any required adjustments to the geologic and dynamic models used to predict the distribution of carbon dioxide within the storage complex, supporting AoR evaluations and a non-endangerment demonstration. Additionally, the testing and monitoring components include a leak detection plan to monitor and account for any movement of the carbon dioxide outside of the storage complex.

Shell has designed the program with two Above Confining Zone Monitoring (ACZM) wells which will be located on the well pads in close proximity to the Injection Wells. The initial ACZ monitoring zone for the sequestration project will be a permeable sandstone (directly overlying the Confining Zone) within the Lower Miocene Formation (exact sand will be identified following appraisal drilling). Each of the ACZM wells is planned to be located near the point of carbon dioxide injection, where elevated formation pressure within the storage project is expected to be the greatest. The ACZM wells will be completed with a real-time, continuously recording downhole pressure/temperature gauge.

Direct in-zone monitoring at the injection wells will confirm that the wells are performing as intended; delivering the carbon dioxide to the subsurface storage intervals only (Injection Zones), do not exceed safe injection pressures, and measure the pressure response in the reservoir intervals (a key model match parameter). Downhole pressure gauges and injection logging in the constructed injection wells will be used for data collection.

An additional In-Zone pressure (IZ) monitoring well, located updip from the injection wells, will validate the dynamic model, calibrating both the growth of sequestered carbon dioxide plume and pressure front over time. Downhole pressure gauges and injection logging in the constructed IZ monitoring well will be used to collect real-time, continuous data. The IZ monitor well will be located initially outside of the carbon dioxide plume and will primarily monitor the pressure changes due to the developing pressure front.

The TMP has been uploaded in **Module E** – Project Plan Submission as Report:

“E.1 – Testing and Monitoring Plan (Rev. 0 – November 2022)”

A Quality Assurance and Surveillance Plan (QASP) for all testing and monitoring activities, required pursuant to §146.90(k), is provided in Appendix 1 – Quality Assurance and Surveillance Plan (QASP) to the Testing and Monitoring Plan.

Testing and Monitoring GSDT Submissions

GSDT Module: Project Plan Submissions

Tab(s): Testing and Monitoring tab

Please use the checkbox(es) to verify the following information was submitted to the GSDT:

Testing and Monitoring Plan *[40 CFR 146.82(a)(15) and 146.90]*

9.0 INJECTION WELL PLUGGING

The Injection Well Plugging Plan has been developed using the GSĐT Template and meets the requirements under 40 CFR 146.92(b). It contains testing prior to closure and plugging plans and schematics for each injection well in this application. It has been uploaded in **Module E** – Project Plan Submission as Report:

“E.2 – Injection Well Plugging Plan (Rev. 0 – November 2022)”

This plan will be updated as the project is developed to be consistent with the Injection Well “as built” after construction.

Injection Well Plugging GSĐT Submissions

GSĐT Module: Project Plan Submissions

Tab(s): Injection Well Plugging tab

Please use the checkbox(es) to verify the following information was submitted to the GSĐT:

Injection Well Plugging Plan [**40 CFR 146.82(a)(16) and 146.92(b)**]

10.0 POST INJECTION SITE CARE (PISC) AND SITE CLOSURE

The Post Injection Site Care (PISC) and Site Closure Plan has been developed using the GSDT Template and meets the requirements under 40 CFR 146.9. It has been uploaded in **Module E** – Project Plan Submission as Report:

“E.3 – Post Injection Site Care and Closure Plan (Rev. 0 – November 2022)”

Shell plans to implement a PISC over a 50-year timeframe to demonstrate conformance and containment. Data will be gathered to track the position of the CO₂ plume, declining pressure front and to demonstrate that the USDW is not endangered, using an adaptive, sustainable, risk-based monitoring approach. Figures representing the pressure differentials in each injection zone, as well as figures projecting the plume extent, both at the end of the 50-year observation period are included.

Depending on project performance during the project life cycle, Shell may request an alternative PISC timeframe based upon modeling results and AoR reevaluations. Prior to authorization for site closure, Shell will demonstrate that no additional monitoring is needed to ensure that the geologic sequestration project does not pose an endangerment to USDWs as per 40 CFR 146.93(b)(3).

PISC and Site Closure GSDT Submissions

GSDT Module: Project Plan Submissions

Tab(s): PISC and Site Closure tab

Please use the checkbox(es) to verify the following information was submitted to the GSDT:

PISC and Site Closure Plan [**40 CFR 146.82(a)(17) and 146.93(a)**]

11.0 EMERGENCY AND REMEDIAL RESPONSE

The Emergency and Remedial Response Plan (ERRP) has been developed using the GSĐT Template and meets the requirements under 40 CFR 146.94(a). It has been uploaded in **Module E** – Project Plan Submission as Report:

“E.4 – Emergency and Remedial Response Plan (Rev. 0 – November 2022)”

The EERRP Plan will be updated and further developed to meet the project's needs throughout three phases of development: 1) Construction; 2) Operation; and 3) Post-Injection Site Closure. Revisions will be drafted and notated with date of submittal. Detailed information is contained in the Emergency and Remedial Response Plan [40 CFR 146.94(a)] submitted within **Module E** – Project Plan Submission through the GSĐT Tool.

Emergency and Remedial Response GSĐT Submissions

GSĐT Module: Project Plan Submissions

Tab(s): Emergency and Remedial Response tab

Please use the checkbox(es) to verify the following information was submitted to the GSĐT:

Emergency and Remedial Response Plan [**40 CFR 146.82(a)(19) and 146.94(a)**]

12.0 INJECTION DEPTH WAIVER AND AQUIFER EXEMPTION

EXPANSION

Shell is not requesting an Injection Depth Waiver or an Aquifer Exemption Expansion. Therefore, this section is not applicable.

13.0 OPTIONAL ADDITIONAL PROJECT INFORMATION

Shell has not identified any current Federal laws that may impact injection at the St. Helena Parish site. However, Shell will apply for a Class VI Injection well permit (in addition to the federal request) to the State of Louisiana, through the LDNR. This well permit application is a requirement for all Class VI wells that are to be drilled in the state, regardless of primacy status.

14.0 OTHER RELEVANT INFORMATION

No additional information or documents have been requested by the UIC Program Director to date for this Class VI Permit Application for the St. Helena Parish site.

However, Shell has performed an initial assessment using the Environmental Justice Screening and Mapping Tool (EJScreen Tool) in November 2022. Reports applicable to the project are contained in Appendix E to this Project Narrative.

REFERENCES

Adkins, W. S., 1933, The Mesozoic systems in Texas, The geology of Texas; v. 1, Stratigraphy; University of Texas Bulletin 3232 p. 239-517

Ambrose, W. A., Loucks, R. G. and Dutton, S. P., 2015, Sequence stratigraphy and depositional controls on reservoir quality in lowstand incised-valley-fill and highstand shallow marine systems in the Upper Cretaceous Cenomanian Tuscaloosa Formation, Louisiana, U. S. A: Gulf Coast Association of Geological Societies Journal, v. 4, p. 43-66

Archie, G. E., 1942, The electrical resistivity log as an aid in determining some reservoir characteristics, Petroleum Transactions of the AIME, v. 146, p. 54-62.

Aronow, S. and Wesselman, J. B., 1971, Groundwater Resources of Chambers and Jefferson Counties, Texas: Texas Water Development Board Report No. 133.

Aumman, H. H., 1966, Experimental study of the effect of stress on the creep in shales: Exxon Production Research Report, (private communication to R. E. Collins, DuPont consultant)

Baria, L. R., Stoudt, D. L., Victoria, P. M. and Crevello, P. D., 1982, Upper Jurassic reefs of Smackover Formation, United States Gulf Coast: Am. Assoc. Petroleum Geologists Bull., v. 66, n. 10, p. 1449-1482.

Bebout, D. G. and Gutierrez, D. R., 1983, Regional Cross Section – Louisiana Gulf Coast, Eastern Part, Louisiana Geological Survey, Folio Series No. 6

Bentley, C. B., 1983, Preliminary Report of the Geohydrology Near Cypress Creek and Richton Salt Domes, Perry County, Mississippi: Water-Resources Investigations Report 83-4169, U. S. G. S., Jackson, MS.

Berg, R. B. and Cook, B. C., 1968, Petrography and origin of Lower Tuscaloosa sandstones, Mallalieu Field, Lincoln County, Mississippi: Gulf Coast Association of Geological Societies Transactions, v. 18, 242-255.

Bethke, C. M., Harrison, W. J., Upson, C. and Altaner, S. P., 1988, Supercomputer analysis of sedimentary basins: Science, v. 239, Washington, D. C.

Bornhauser, M., 1960, Depositional and structural history of Northeast Hartburg field, Newton County, Texas: AAPG Bulletin, v. 44, no. 4, p. 458-470

Bowden, R. K., and Curran J. H., 1984, Time dependent behavior of joints in shale: Proc. 25th Symposium of Rock Mechanics, Northwestern University, Evanston, Illinois, published by American Institute of Mechanical Engineers, New York, New York, pp. 320328

Brantly, J. A., Seanor, R. C., and McCoy, K. L. 2002, “Louisiana groundwater map No. 13, hydrogeology and potentiometric surface of the Sparta aquifer in, northern Louisiana,

October 1996.” Water-Resources Investigations Rep. No. 02-4053, U.S. Geological Survey, Denver

Bredehoeft, J.D., & Pinder, G.F., 1970, Digital Analysis of Areal Flow in Multiaquifer Groundwater Systems: A Quasi Three-Dimensional Model. *Water Resources Research*, 6, 883-888.

Brendsdal, A.O.E., 2017, The capacity of creeping shale to form an annular barrier, Master Thesis, Norwegian University of Science and Technology, Department of Geoscience and Petroleum.

Brown, G. F., Foster, V. M., Adams, R. W., Reed, E. W. and Padgett, H. D., 1944, Geology and groundwater resources of the coastal area in Mississippi: Mississippi State Geological Survey, Bulletin 60, 232 [0110092].

Byerly, G. R., 1991, Igneous activity, in Salvador, A., The Gulf of Mexico Basin: Boulder,

Chang, C. and Zoback, M.D., 2009, Viscous creep in room-dried unconsolidated Gulf of Mexico shale (I): Experimental results. *Journal of Petroleum Science and Engineering*, 69, 239-246

Chasteen, H. R., 1983, Reevaluation of the lower Tuscaloosa and Dantzler Formations Mid-Cretaceous with emphasis on depositional environments and time-stratigraphic

Chen-Charpentier, B. and Herrera I.R., 1982, Numerical Treatment of Leaky Aquifers in the Short Time Range. *Water Resources Research*. 18. 557-562

Clark, J. E., 1987, Groundwater flow in deep saline aquifers: Special Session on the Hydrologic and Geochemical Processes Involved in Deep Injection of Liquid Wastes, Groundwater Committee of the American Geophysical Union and the International Association of Hydrogeologists, Baltimore, Maryland.

Clark, J. E., 1988, Groundwater flow in deep saline aquifers: Special Session on the Hydrologic and Geochemical Processes Involved in Deep Injection of Liquid Wastes, Groundwater Committee of the American Geophysical Union and the International Association of Hydrogeologists, Baltimore, Maryland.

Clark, J. E., Howard, M. R., and Sparks, D. K., 1987, Factors that can Cause Abandoned Wells to Leak as Verified by Case Histories from Class II injection, Texas Railroad Commission files: International Symposium on Subsurface Injection of Oilfield Brines, Underground Injection Practices Council, New Orleans, LA., p. 166-223.

Clark J. E., Bonura, D. K., Papadeas, P. W., McGowen, R., 2005, Gulf Coast Borehole-Closure-Test Well Near Orange, Texas: Developments in Water Science, v. 52, p. 157-166.

Clark, W. J., 1995, Depositional environments, diagenesis, and porosity of Upper Cretaceous volcanic-rich Tokio sandstone reservoirs, Haynesville field, Claiborne Parish Louisiana: Transactions—Gulf Coast Association of Geological Societies, v. 45, p. 127–134.

Clifford, H. J., 1973, Hydrodynamics of the Mt. Simon Sandstone, Ohio, and Adjacent Areas: in Underground Waste Management and Artificial Recharge Vol. 1, American Association of Petroleum Geologists, Tulsa, OK.

Clifford, H. J., 1975, Subsurface Liquid Waste Injection in Ohio: Ohio Geological Survey Information Circ., n. 43.

Collier, A.L. and Sargent, B.P., 2015, Water Use in Louisiana, 2015, Department of Transportation and Development, Water Resources Special Report No. 18

Collins, R. E., 1986, Potential Breaches in the Confining Layer Near Injections Wells on the Gulf Coastal Plain. Report to E.I. du Pont de Nemours & Co. Inc.

Cox, R. T. and Van Arsdale, R. B., 2002, The Mississippi Embayment, North America: a first order continental structure generated by Cretaceous superplume event: Journal of Geodynamics, v. 34, p. 163-176

Davis, K. E., 1986, Factors Effecting the Area of Review for Hazardous Waste Disposal Wells: Proceedings of the International Symposium on Subsurface Injection of Liquid Wastes, New Orleans, National Water Well Association, Dublin, OH, p. 148-194.

Dawson, W. C. and Reaser, D. F., 1990, Trace fossils and paleoenvironments of lower and middle Austin Chalk Upper Cretaceous, north-central Texas: Transactions— Gulf Coast Association of Geological Societies, v. 40, p. 161–173.

Dawson, W. C., Katz, B. and Robison, V. D., 1995, Austin Chalk (!) petroleum system Upper Cretaceous, southeastern Texas: a case study: Transactions—Gulf Coast Association of Geological Societies, v. 45, p. 157–163.

Dawson, W. C., 2000, Shale Microfacies; Eagle Ford Group Cenomanian-Turonian North-Central Texas Outcrops and Subsurface Equivalents, Gulf Coast Association of Geological Transactions, v. 50, p. 607-627

Decade of North American Geology 1991

Devery, D. M., 1980, The Lower Tuscaloosa of Southern Mississippi: Mississippi Geology, Vol 1, Number 2 December 1980

Dockery, D. T., 1977, Mollusca of the Moodys Branch Formation, Mississippi. Mississippi Geological, Economic and Topographical Survey, Bulletin 120,

Donovan, A. and Staerker, T. S., 2010, Sequence Stratigraphy of the Eagle Ford Boquillas Formation in the Subsurface of South Texas and Outcrops of West Texas, Gulf Coast

Association of Geologic Societies Transactions, v. 60, p. 861-899

Drumm, T. and Nunn, J. A., 2012, Geothermal and Geopressure Assessment with Implications for Carbon Dioxide Sequestration, Lower Tuscaloosa Formation, Louisiana, Gulf Coast Association of Geological Societies Transactions, pp 39-55.

Dutton, S.P., Loucks, R.G., 2014, Reservoir quality and porosity-permeability trends in on shore Wilcox sandstones, Texas, and Louisiana Gulf Coast: Application to deep Wilcox plays, offshore Gulf of Mexico. GCAGS Journal 3, 33-40.

Eaton, B. A., 1969, Fracture Gradient Prediction And its Application In Oilfield Operations, Journal of Petroleum Technology, October 1353 – 1360.

Eaton, B. A., 1972, The effect of overburden stress on geopressure prediction from well logs, Journal Petroleum Technology, v. 24, 929 – 934.

Esker, G. C., 1968, Biostratigraphy of the Cretaceous-Tertiary Boundary in the East Texas Embayment Based on Planktonic Foraminifera, LSU Historical Dissertations and These. 1484.

Everett, A. G., Anderson, J. J. and Shakoor, A., 1986, Factors Affecting the Integrity of Confining Beds for Injected Waste Reservoirs: A Review: Underground Injection Committee Modeling Work Group, Chemical Manufacturers Association, Inc., Vol. II, pp 1-60.

Ewing, T. E. and Lopez, J. A., 1991, Principal structural features, Gulf of Mexico basin: in A. Salvador, ed., The Gulf of Mexico Basin: The Geological Society of America, The Geology of North America, v. J., plate 2, 1 sheet.

Ewing, T. E. and Galloway, W. E., 2019, Evolution of the Northern Gulf of Mexico Sedimentary Basin, in Miall, A. D., ed., Sedimentary Basins of the United States and Canada, Second Edition: The Netherlands, Elsevier, p. 627-694

Ewing, T. E., 2009, The Ups and Downs of the Sabine Uplift and Northern Gulf of Mexico Basin; Jurassic Basement Blocks, Cretaceous Therman Upfits and Cenozoic Flexure: Gulf Coast Association of Geological Societies Transactions, v. 59, p. 253-269

Fendick, R.B., Jr., 2007, Generalized Potentiometric Surface of the Amite Aquifer and the “2-800-Foot” Sand of the Baton Rouge Area in the Southeastern Louisiana, June-August 2006: U.S. Geological Survey Scientific Investigations Map 2984, 1 sheet

Fjær, E., Holt, R. M., Raaen, A., 2008, Petroleum related rock mechanics, 2nd edition. Elsevier, Amsterdam Fjær E, Stenebråten, J. F., Bakheim S, 2018, Laboratory test for studies on shale barrier formation. In: 52nd U. S. Rock mechanics/ geomechanics symposium proceedings. American Rock Mechanics Association

Fogg, G. E. and Kreitler, C. W., 1982, Groundwater hydraulics and hydrochemical facies in Eocene aquifers of the East Texas Basin: University of Texas at Austin, Bureau of Economic Geology Report of Investigations No. 127, 75 p.

Fogg, G. E., Seni, S. J. and Kreitler, C. W., 1983, Three-dimensional ground-water modeling in depositional systems, Wilcox Group, Oakwood Salt Dome area, East Texas: Texas Bureau of Economic Geology Report of Investigations 133, Austin, 55 p.

Folk, R. L., 1959, Practical petrographic classification of limestones: American Association of Petroleum Geologists Bulletin, v. 43, p. 1–38.

Foote, R.Q., 1984, Open-File Report Vol. 1984 (84-339), Summary report on the regional geology, petroleum potential, environmental consideration for development, and estimates of undiscovered recoverable oil and gas resources of the United States Gulf of Mexico Continental Margin in the area of proposed oil and gas lease sales nos. 81 and 84. US Geological Survey Open-File Report 84-339, p. 1-193.

Galloway, W. E., 1968, Depositional systems of the lower Wilcox Group, north-central Gulf Coast Basin: Gulf Coast Association of Geological Societies Transactions, v. 18, p. 275–289.

Galloway, W. E., 1989, Genetic stratigraphic sequences in basin analysis I: Architecture and genesis of flooding surface bounded depositional units: The American Association of Petroleum Geologists Bulletin, v. 73, no. 2, p. 125–142.

Galloway, W. E., 2008, Depositional evolution of the Gulf of Mexico sedimentary basin, in Hsü, K. J., ed., Sedimentary basins of the world, Volume 5, The sedimentary basins of the United States and Canada, Miall, A. D., ed.: The Netherlands, Elsevier, p. 505–549.

Galloway, W. E., Hobday, D. K. and Magara, K., 1982(a), Frio Formation of the Texas Gulf of Mexico Basin-depositional systems, structural framework and hydrocarbon origin, migration, distribution, and exploration potential: Bureau of Economic Geology, Report of Investigations No. 122, The University of Texas at Austin, Austin, Texas, p. 78.

Galloway, W. E., Henry, C. G. and Smith, G. E., 1982(b), Depositional framework, hydrostratigraphy and uranium mineralization of the Oakville sandstone Miocene Texas Coastal Plain: Bureau of Economic Geology, Report of Investigations No. 113, The University of Texas at Austin, Austin, Texas, 59 p.

Galloway, W. E., Ganey-Curry, P. E., Li, X. and Buffler, R. T., 2000, Cenozoic depositional history of the Gulf of Mexico basin: AAPG Bulletin, v. 84, no. 11, p. 1743-1774.

Galloway, W. E., Whiteaker, T. L. and Ganey-Curry, P., 2011, History if Cenozoic North American Drainage basin evolution, sediment yield and accumulation in the Gulf of Mexico Basin, Geosphere, August 211; v. 7; no. 4; p. 938-973

Glawe, L. N. and Bell, D. E., 2014, A Substitute Reference Section for the Wilcox Group, Paleocene-Eocene, from Northwestern Louisiana, GCAGS, Lafayette, Louisiana.

Gray, G. R., H. C. H. Darley, and W. F. Rodgers, 1980, Composition and Properties of Oil Well Drilling Fluids: Gulf Publishing Company, Houston, Texas.

Griffith, J.M., 2003, West-east hydrogeologic section I-I', Southeastern Louisiana – Plate 11: Louisiana Department of Transportation and Development, Water Resources Technical Report 72

Gunter, W., Perkins, E. and McCann, T., 1993, Aquifer disposal of CO₂-rich gases: Reaction design for added capacity: Energy Conversion and Management. 34. 941-948.

Han, H. X., 2021, Effects of transient borehole deformation on rock stress and rock properties analysis: University of Waterloo Doctoral Thesis

Hantush, M. S., 1964, Hydraulics of Wells: Advances in Hydroscience," Vol. 1, Ed.: V. T. Chow, Academic Press, New York, pp. 281–432.

Hart, B. S., Flemings, P. B., & Deshpande, A., 1995, Porosity and pressure: Role of compaction disequilibrium in the development of geopressures in a Gulf Coast Pleistocene basin. *Geology*, 23(1), 45-48.

Hearne, J. H. and Lock, B. E., 1985, Diagenesis of the Lower Tuscaloosa as seen in the du Pont de Nemours No. 1 Lester Earnest, Harrison County, Mississippi: Gulf Coast Association of Geological Societies Transactions, v 35, 387-393.

Hiland, P., 2010, Generic Issue 199 GI-199, Implications of updated probabilistic seismic hazard estimates in central and eastern United States on existing plants, Safety Risk Assessment: Nuclear Regulatory Commission

Holt, R.M., Larsen, I., Fjær, E. and Stenebraten, J.F., 2020, Comparing mechanical and ultrasonic behaviour of a brittle and a ductile shale: Relevance to prediction of borehole stability and verification of shale barriers, *J. of Petroleum Science and Engineering*, 187, 106746.

Hosford, W. F., 2005, Mechanical Behaviour of Materials, Cambridge: Cambridge University Press, The Edinburgh building.

Hosman, R. L., 1996, Regional Stratigraphy and subsurface geology of Cenozoic deposits. Gulf Coastal Plain, South-Central United States: U. S. Geological Survey professional paper; 1416-G

Hosman, R.L., Long, A.T., Lambert, T.W., and others, 1968, Tertiary aquifers in the Mississippi embayment, with discussions of quality of the water, by Jeffery, H.G.: U.S. Geological Survey Professional Paper 448-D, 29 p.

Hosseini, S. A., Lashgari, H., Nicot, J. P., Hovorka, S. D., Lu J., Kordi, M., Chang, K. W., 2012, Site characterization and reservoir history matching for geological CO₂ sequestration at the S3 site: 11th Annual Carbon Capture, Utilization and Sequestration Conference, Pittsburgh, PA

Hovorka, S. D. and Nance, H. S., 1994, Dynamic depositional and early diagenetic processes in a deep-water shelf setting, Upper Cretaceous Austin Chalk, north Texas: Transactions—Gulf Coast Association of Geological Societies, v. 44, p. 269–276.

Hovorka, Susan D., and Jiemin Lu. 2019. “Field Observations of Geochemical Response to CO₂ Injection at the Reservoir Scale.” In *Science of Carbon Storage in Deep Saline Formations*, 33–61. Elsevier.

Howe, H. J., 1962, Subsurface geology of St. Helena, Tangipahoa, Washington and St. Tammany Parishes, Louisiana: GCAGS Trans., v. 12, p. 121-155.

Iler, R. K., 1979, *The chemistry of silica*: New York, Wiley, p. 866.

Jackson, M. P. A. and Galloway, W. E., 1984, Structural and depositional styles of Gulf Coast Tertiary continental margins: Application to hydrocarbon exploration: Am. Assoc. Petroleum Geologists, Continuing Education Course Note Series No. 25, p. 226.

John, C.J., Jones, B.L., Moncrief, J.E., Bourgeois, R., Harder, B.J., 1997. An Unproven Unconventional Seven Billion Barrel Oil Resource-The Tuscaloosa Marine Shale. BRI Bulletin. V. 7, pp. 1-22

Johnston, O. C. and Greene, C. J., 1979, Investigation of Artificial Penetrations in the Vicinity of Subsurface Disposal Wells: Texas Department of Water Resources.

Johnston, O. C., and Knape, 1986, Pressure effects of the static mud column in abandoned wells: Texas Water Commission LP 86-06, 106 p.

Jones, T. A. and Haimson, J. S., 1986, Demonstration of Confinement: An Assessment of Class 1 Wells in the Great Lakes and Gulf Coast Regions: *Journal of the Underground Injection Practices Council*, Number 1, pp. 279-317.

Kaszuba, J.P., Janecky, D.R. and Snow, M., 2002, October. Experimental evaluation of mixed fluid reactions between supercritical carbon dioxide and a NaCl brine: relevance to geologic aquifer carbon sequestration. In *2002 Geological Society of America annual meeting, session* (Vol. 135, No. 3, pp. 27-30).

Kehle, R. O., 1971, Origin of the Gulf of Mexico: University of Texas at Austin, Geology Library, unpublished report, unpaginated.

Kestin, Khalifa, E. H., Correia, R. J., 1981, Tables of the Dynamic and Kinematic Viscosity of Aqueous NaCl Solutions in the Temperature Range 20-150 °C and the Pressure Range 0. 1-35 MPa: *J. Phy~. Chem. Ref. Data.* Vol. 10. No. 1.

Kharaka Y.K., Cole D.R., Hovorka S.D., Gunter W.D., Knauss K.G., Freifeld B.M. (2006) Gas–water–rock interactions in Frio Formation following CO₂ injection: implications for the storage of greenhouse gases in sedimentary basins. *Geology* 34(7):577–580

Kidwell, A. L., 1951, Mesozoic igneous activity in the northern Gulf Coastal Plain: GCAGS Trans., v. 1, p. 182-199.

Kordi, M., Hovorka, S., Milliken, K., Trevino, R. and Lu, J., 2010. Diagenesis and reservoir heterogeneity in the Lower Tuscaloosa Formation at Cranfield Field, Mississippi. *GCCC Digital Publication Series*, pp.10-13.

Kose, S. G., 2013, Crustal Architecture, Cretaceous Rise and Igneous Activity of Sabine, Monroe and Jackson Uplifts, Northern Gulf of Mexico Basin, Master's Thesis, University of Houston

Kristiansen, T.G., Dyngeland, T., Kinn, S., Flatebø, R. and Aarseth, N.A., 2018, Activating shale to form well barriers: Theory and field examples, SPE-191607-MS.

Kreitler, C. W., 1986, Hydrogeology of sedimentary basins as it relates to deep-well injection of chemical wastes, Proceedings of the International Symposium on Subsurface Injection of Liquid Wastes, New Orleans, National Water Well Assoc., Dublin, Ohio, pp. 398-416.

Kreitler, C. W. and Richter, B.C. 1986, Hydrochemical Characterization of Saline Aquifers of the Texas Gulf Coast Used for the Disposal of industrial Waste: The University of Texas at Austin. Bureau of Economic Geology. contract report to the U.S. Environmental Protection Agency. Contract No. R-812785-01-0. 164 p.

Kreitler, C. W., Akhter, M. S., Donnelly, A. C. A. and Wood, W. T., 1988, Hydrogeology of formations used for deep-well injection, Texas Gulf Coast: Prepared for the U. S. Environmental Protection Agency under Cooperative Agreement ID No. CR812786-01-0, The University of Texas at Austin, Bureau of Economic Geology Austin, Texas, 215 p.

Krutak, P. R. and Beron, P., 1993, Heterostegina zone carbonates, Southeastern Louisiana-offshore Mississippi: petrography, seismic stratigraphy, hydrocarbon potential: Gulf Coast Association of Geological Societies Transactions, v. 43, p. 183-194

Land, L.S., & Fisher, R.S., 1987, Wilcox sandstone diagenesis, Texas Gulf Coast: a regional isotopic comparison with the Frio Formation. *Geological Society, London, Special Publications*, 36, 219 - 235.

Lawless, P. N. and Hart, G. F., 1990, The LaSalle Arch and its Effects on Lower Paleogene Genetic Sequence Stratigraphy, Nebo-Hemphill Field, LaSalle Parish, Louisiana. Gulf Coast Association of Geological Societies Transactions, v. 40, p. 459-473

LBNL, 2014, Final report on experimental and numerical modeling activities for the Newark Basin: Lawrence Berkeley National Laboratory, Berkeley California, 130 p.

Ledger, E. B., Tieh, T. T. and Rowe, M. W., 1984, An evaluation of the Catahoula Formation as a uranium source rock in East Texas: Gulf Coast Association of Geologists Society. Transactions, v. 34, pp. 99108.

Leeds, D. J., 1989, Seismicity--natural and induced, DeLisle Plant, Mississippi.

Leeds and Associates, 1989, Seismic Effects/DuPont Sabine River Works, DuPont Sabine River Works HWDIR Exemption Petition.

Loizzo, M., Lecampion B., Mogilevskaya S., 2017, The role of geological barriers in achieving robust well integrity. Energy Procedia

Loucks, R. G., Dodge, M. M. and Galloway, W. E., 1986, Controls on porosity and permeability of hydrocarbon reservoirs in lower Tertiary sandstones along the Texas Gulf Coast: Bureau of Economic Geology, Report of Investigations No. 149.

Louisiana Department of Environmental Quality, 2003. Chicot Aquifer Summary Baseline Monitoring Program, FY 2002. Appendix 10 of the 2003 Triennial Summary Report of the Environmental Evaluation Division of the LDEQ.

Louisiana Department of Environmental Quality, 2008, Environmental Regulatory Code, Title 33, Part IX, Subpart 1: Baton Rouge, Louisiana Department of Environmental Quality.

Louisiana Department of Natural Resources, 2016, Strategic Online Natural Resources Information System, SONRIS, Louisiana Department of Natural Resources database.

Louisiana Department of Natural Resources ASSET Aquifer Summaries 2012 - Sparta Aquifer <https://deq.louisiana.gov/page/asset-aquifer-summaries-2012>

Lovelace, J. K., Fontenot, J. W., Frederick, C. P., 2004. Withdrawals, Water Levels and Specific Conductance in the Chicot Aquifer System in Southwestern Louisiana, 2000-03. U. S. Geological Survey, Scientific Investigations Report 2004-5212, p. 61.

Lowry, P., 1988, Stratigraphic Framework and Sedimentary Facies of a Clastic Shelf Margin: Wilcox Group Paleocene-Eocene, Central Louisiana; Louisiana State University and Agricultural and Mechanical College, PhD Dissertation

Lu., J., Kordi, M., Hovorka, S. D., Meckel, T. A. and Christopher, C. A., 2013, Reservoir characterization and complications for trapping mechanisms at Cranfield CO₂ injection site: International Journal of Greenhouse Gas Control, v. 18, pp. 361-374.

Lund Snee, J. E., & Zoback, M. D. (2016). State of stress in Texas: Implications for induced seismicity. *Geophysical Research Letters*, 43(19), 10-208.

Lund Snee, J. E. and Zoback, M. D., 2020(a), Impacts of the state of stress on development of unconventional energy resources in North America: AAPG Bulletin.

Lund Snee, J. E. and Zoback, M. D., 2020(b), Multiscale variations of the crustal stress field throughout North America: Nature Communications.

Mancini, E. A., Mink, R. M., Bearden, B. L. and Wilkerson, R. P., 1985, Norphlet Formation Upper Jurassic of southwestern and offshore Alabama: environments of deposition and petroleum geology: Am. Assoc. Petroleum Geologists Bull., v. 69, n. 6, p. 881-889.

Mancini, E. A., Mink, R. M., Payton, J. W. and Bearden, B. L., 1987, Environments of deposition and petroleum geology of Tuscaloosa Group Upper Cretaceous, South Carlton and Pollard Fields, Southwestern Alabama: American Association of Petroleum Geologists Bulletin, v. 71, 1128-1142.

Martin, A. T., 2014, Depositional History and Stratigraphic Framework of Upper Cretaceous Campanian to Maastrichtian Strata in the Minerva-Rockdale Oil Field of Milam County and Adjacent Counties, Texas, Graduate Theses and Dissertations, University of Arkansas, Fayetteville

Martin, A. Jr and Whiteman, C.D., Jr. 1985, Generalized Potentiometric Surface of Aquifers of Pleistocene Age, Southern Louisiana, 1980.S. Geological Survey Water-Resources Investigation Report 84-4331, Sheet

Matthews, A. C., Weed, S. B., Coleman, N. T. 1955, The Effect of Acid and Heat Treatment on Montmorillonite: National Academy of Sciences, Washington DC.

Matthews, W. R. and Kelly, J., 1967, How to predict formation pressure and fracture gradient from electric and sonic logs: The Oil and Gas Journal, Figure 3, ADT 21

McGee, B.D. and Brantly, J.A., 2015, Potentiometric surface, 2012, and water-level differences, 2005–12, of the Sparta Aquifer in north-central Louisiana: U.S. Geological Survey Scientific Investigations Map 3313, 2 sheets

McGlothlin, T., 1944, General Geology of Mississippi: Bulletin of the American Association of Petroleum Geologists Vol. 28, No. 1 January 1944 PP 29-62

McGuire, V.L., Seanor, R.C., Asquith, W.H, Kress, W.H., and Strauch, K.R., 2019, Potentiometric Surface, Mississippi River Valley Alluvial (MRVA) Aquifer, Spring 2016 and Associated Groundwater and Surface Water Control Points: U.S. Geological Survey Scientific Investigations Map 3439, 5 sheets

Meckel, T. A., Hovorka, S. D., 2009, Results from continuous downhole monitoring, PDG, at a field-scale CO₂ demonstration project, Cranfield, MS. Soc. Pet. Eng. SPE 127087, p. 8

Meckel, T.A., Nicholson, A.J., and Trevino, R.H., 2017, Capillary Aspects of Fault-Seal Capacity for CO₂ Storage, Lower Miocene, Texas Gulf of Mexico”, in Geological CO₂ Sequestration Atlas of Miocene Strata, Offshore Texas State Waters, Bureau of Economic Geology, 2017.

Miller, C., Hales C., Clark, J. E. and Collins, G., 1989, Density drive flow near salt domes: Underground Injection Practices Council Winter Meeting, San Antonio, Texas.

Moody, C. L., 1949, Mesozoic igneous rocks of the Northern Gulf Coastal Plain; American Associated of Petroleum Geologists Bulletin, v. 33, p 1410-1428

Murray, 1957, Hydrocarbons in Gulf Coastal Province of the United States: Gulf Coast Association of Geological Societies, Transactions, Vol. VII, and p. 254.

National Academies of Sciences, Engineering, and Medicine, 2019, Negative Emissions Technologies and Reliable Sequestration: A Research Agenda. Washington, DC: The National Academies Press. <https://doi.org/10.17226/25259>

Nealon, D. J., 1982, A Hydrological Simulation of Hazardous Waste Injection in Mt. Simon, Ohio: Master's Thesis, Ohio University.

Neuman, S. P. and Witherspoon, P. A., 1969a, Theory of flow in a confined two aquifer system, Water Resources. Res., 5, 4, 803-816.

Neuman, S. P. and Witherspoon, P. A., 1969b, Applicability of current theories of flow in leaky aquifers, Water Resources. Res., 5, 4, 817-829.

Neuzil, C. E., 1986, Groundwater flow in low permeability environments: Water Resources Research, v. 22, no. 8, p. 1163-1195

Nichols, P. H., Peterson, G. E. and Wuestner, C. E., 1968, Summary of subsurface geology of northeast Texas, in Beebe, B. W. and Curtis, B. F., eds., Natural gases of North American: American Associated of Petroleum Geologists, Memoir 9, v. 1, p. 982-1004

Nicholson, A., J., 2012, Empirical Analysis of Fault Seal Capacity for CO2 sequestration, Lower Miocene, Texas Gulf Coast: Master's Thesis, The University of Texas at Austin, 100 p.

Nyman, D.J. and L.D. Fayard, 1978, Groundwater resources of Tangipahoa and St. Tammany Parishes, southeastern Louisiana: State of LA, Office of Public Works, Water Resources Technical Report No. 15, 76 p.

Nyman, D. J., 1984, The occurrence of high concentrations of chloride in the Chicot aquifer system in southwestern Louisiana, 200 03: US Geological Survey Scientific Investigations Report 2004-5212, 56 p.

Nyman, D. J., 1989. Quality of Water in Freshwater Aquifers in Southwestern Louisiana. Louisiana Department of Transportation and Development, Water Resources Technical Report 42, p. 29.

Ostermeier, R. M. 2001, Compaction effects on porosity and permeability: Deepwater Gulf of Mexico turbidite. Journal of Petroleum Technology, 53(02), 68-74.

Paine, W. R., 1968, Stratigraphy and sedimentation of subsurface Hackberry wedge and associated beds of southwestern Louisiana: AAPG Bulletin, v. 52, no. 2, p. 322-342

Payne, J.N., 1968, Hydrologic significance of the lithofacies of the Sparta Sand in Arkansas, Louisiana, Mississippi, and Texas: U.S. Geological Survey Professional Paper 569-A, 17

p.

Pair, J. D., 2017 The Tuscaloosa Marine Shale: Geologic History, Depositional Analysis and Exploration Potential: Electronic Theses and Dissertations. 68

Pan, P., Wu, Z., Feng, X. and Yan, F., 2016, Geomechanical modeling of CO₂ geological storage: A review, *J. of Rock Mechanics, and Geotechnical Engineering*, 8, 936-947

Paulson, O. L., 1972, Various factors influence Wilcox deposits in the “Golden Triangle”: *Oil and Gas Journal*, 86-87.

Payne, J. N., 1972, Hydrogeologic significance of lithofacies of the Cane River Formation or equivalents of Arkansas, Louisiana, Mississippi, and Texas: *Geological Survey Professional Paper 569-C*, 17 p

Porter, W. M. and Newsom, S. W., 1987, Shale Porosity and Permeability,

Poulsen, S. E., Nielsen, S. B., Balling, N., 2012, Estimating the equilibrium formation temperature in the presence of bore fluid invasion, *Geophysical Journal International*, vol. 190, Issue 3, pp. 1551–1561.

Prakken, L. B., 2004, Generalized Potentiometric Surface of the Kentwood Aquifer System and the “1,500-foot” and “1,700-foot” Sands of the Baton Rouge Area in Southeastern Louisiana, March-April 2003: U.S. Geological Survey Scientific Investigations Map 2862, 2 sheets

Prakken, L., White, V., and Lovelace, J. 2014, Water resources of Sabine Parish, Louisiana. Reston, VA: U. S. Geological Survey, Reston, VA, United States. [doi:10.3133/fs20143040](https://doi.org/10.3133/fs20143040)

Rainwater, E., H., 1962, Geological history and oil and gas possibilities of Mississippi: *Geologic Research Papers – 1962*, Mississippi Geological Survey Bulletin 97, pp. 77–105.

Rainwater, E. H., 1964, Regional stratigraphy of the Gulf Coast Miocene: *GCAGS Trans.*, v. 14, p. 81-124.

Rainwater, E. H., 1964(a), Regional Stratigraphy of the Midway and Wilcox in Mississippi: *Mississippi Geological Economic and Topographical Survey, Bulletin No. 102*, 9-31 pp.

Rainwater, E. H., 1964(b), Stratigraphy Gulf Coast Miocene: *Gulf Coast Association of Geological Societies Transactions*, v. 14, 76-77.

Rouse, W. A., Enomoto, C. B. and Gianoutsos, N. J., 2018, Correlation of the Tuscaloosa marine shale in Mississippi, Louisiana and East Texas, U. S. A

Rollo, J.R., 1960, Ground water in Louisiana: Louisiana Department of Conservation and Department of Public Works, *Water Resources Bulletin* 1, 84 p.

Rutqvist, J., Wu, Y. S., Tsang, C. F. and Bodvarsson, G., 2002, A modeling approach for analysis

of coupled multiphase fluid flow, heat transfer, and deformation in fractured porous rock: International Journal of Rock Mechanics and Mining Sciences, v. 39, no. 4, p. 429–442

Salvador, A., 1991, Triassic–Jurassic, in A. Salvador, ed., The Gulf of Mexico basin: Boulder, Colorado, Geological Society of America, The Geology of North America, v. J, p. 131–180.

Sargent, B. P., 2011, Water use in Louisiana, 2010: Louisiana Department of Transportation and Development Water Resources Special Report no. 17, 135 p.

Schlumberger, 1979, Log Interpretation Charts: Schlumberger Well Surveying Corporation, 97 p.

Schlumberger, 1987, Log Interpretation Principles/Applications, Schlumberger Educational Services, Houston, Texas, p. 198.

Schlumberger, 1988, Archie’s Law: Electrical Conduction in Clean, Water-bearing Rock, The Technical Review, v. 36, n. 3, Schlumberger Educational Services, Houston, Texas, pp. 4–13.

Shirley, K., 1987, Trend spins seismic success story: American Association of Petroleum Geologists Explorer, v. 8, No. 10, 14.

Skoumal, R. J., Ries, R., Brudzinski, M., Barbour, A., & Currie, B. 2018, Earthquakes induced by hydraulic fracturing are pervasive in Oklahoma. *Journal of Geophysical Research*, **123**, 10,918– 10,935

Skoumal, R. J., Kaven J. O., Barbour A. J., Wicks, C., Brudzinski M. R., Cochran E. S., Rubinstein, J. L., The Induced Mw 5. 0 March 2020 West Texas Seismic Sequence: JGR Solid Earth, Volume 126, Issue 1, January 2021

Smoot, C.W., 1988, Louisiana hydraulic atlas map No. 3: Altitude of the base of the Freshwater in Louisiana: U.S. Geological Survey Water-Resources Investigation Report 86-4314, 1 sheet, <http://pubs.er.usgs.gov/publication/wri864314>

Slaughter, G. M., 1981, An Analysis of Ground Water Flow Times Near Seven Interior Salt Domes: Dept. of Energy for Battelle Memorial Institute Office of Nuclear Waste Isolation.

Sneddon, J. W., Virdell, J., Whiteaker, T. L. and Ganey-Curry, P., 2016, A basin-scale perspective on Cenomanian-Turonian Cretaceous depositional systems, greater Gulf of Mexico USA: Interpretation Journal, v. 1, p. SC1-SC22

Sone, H. and Zoback, M., 2013, Mechanical properties of shale-gas reservoir rocks — Part 2: Ductile creep, brittle strength, and their relation to the elastic modulus. Geophysics, Vol. 78, No. 5 Sept-Oct; p. D393–D402.

Spooner, H. V., 1964, Basal Tuscaloosa sediments, east-central Louisiana: American Association of Petroleum Geologist Bulletin, v. 48, p. 1-21

Stancliffe, R. J. and Adams, R. E. 1986, Lower Tuscaloosa fluvial channel styles at Liberty Field, Amite County, Mississippi: Gulf Coast Association of Geological Societies Transactions., v. 36, 305-313

Stephens, B.P., 2009, Basement controls on subsurface geologic patterns and coastal geomorphology across the northern Gulf of Mexico: Implications for subsidence studies and coastal restoration: Gulf Coast Association of Geological Societies Transactions, v. 59, p. 729-751.

Stevenson, D., and Agnew J. D., 1988, Lake Charles, Louisiana, Earthquake of 16 October 1983: Bulletin of the Seismological Society of America, Vol. 78, No. 4, pp. 1463-1474

Stevenson, D. A., and R. P. McCulloh (2001). Earthquakes in Louisiana, Louisiana Geol. Surv. Public Information Series No. 7, 8 pp

Stuart, C. G., Knochenmus, D. D., & McGee, B. D., 1994, Guide to Louisiana's ground-water resources (Vol. 94, No. 4085). US Geological Survey.

Sun, M., 1950, A Petrographic Study of the Eocene Jackson Group of Mississippi and adjacent Areas, LSU Historical Dissertations and Theses. 7954

Swanson, S. M. & Karlsen, A. W., 2009, PS USGS Assessment of Undiscovered Oil and Gas Resources for the Oligocene Frio and Anahuac Formations, Onshore Gulf of Mexico Basin, USA.

Swanson, S. M., Karlsen, A. W. and Valentine, B. J., 2013, Geologic Assessment of undiscovered oil and gas resources – Oligocene Frio and Anahuac Formations, United States Gulf of Mexico coastal plane and State waters: U. S. Geological Survey Open-File Report 2013-1257, 66 p.

Talman, S., 2015, Subsurface geochemical fate and effects of impurities contained in a CO₂ stream injected into a deep saline aquifer: What is known: International Journal of Greenhouse Gas Control p. 40.

Todd, E. G. and Mitchum, R. M., 1977, Seismic sequences and global changes in sea level, part 8: Identification of Upper Triassic, Jurassic, and Lower Cretaceous seismic sequences in Gulf of Mexico and offshore West Africa: in Payton, C. E., ed., Seismic

Tomaszewski, D.J., 1988, Ground-water hydrology of Livingston, St. Helena, and parts of Ascension and Tangipahoa Parishes, southeastern Louisiana: Louisiana Department of Transportation and Development Water Resources Technical Report no. 43, 54 p

Tomaszewski, D.J., 2011, Water-Level surface in the Chicot Equivalent Aquifer System in Southeastern Louisiana, 2009: U.S. Geological Survey Scientific Investigations Map 3173, 2 sheets

Turner, R., 1964, Kinetic studies of Acid Dissolution of Montmorillonite and Kaolinite: Ph.D. thesis, Univ. of Calif. Davis.

Vail, P. R., Mitchum, R. M. and Thompson, S., 1977, Seismic stratigraphy and global changes in sea-level, Part 4: global cycles of relative changes in sea-level, in Payton, C. E., ed., Seismic stratigraphy-applications to hydrocarbon exploration: American Association of Petroleum Geologists Memoir 26, 82-97.

Warner, D. L., 1988, Abandoned oil and gas industry wells and their environmental implications: prepared for the American Petroleum Institute.

Warner, D. L. and Syed, T., 1986, Confining layer study-supplemental report: prepared for U. S. EPA Region V, Chicago, Illinois.

Weingarten, M., Ge S., Godt, J. W., Bekins B. A. and Rubinstein, J. L., 2015, High-rate injection is associated with the increase in U. S. mid-continent seismicity: *Science* 348, 6241, 1336-1340

Wesson, R. L., and C. Nicholson, 1987, Earthquake hazard associated with deep well injection: U.S. Geological Survey Open-File Report 87-331, 72

White, V.E., 2017, Water resources of the Southern Hills regional aquifer system, southeastern Louisiana: U.S. Geological Survey Fact Sheet 2017-3010, 6 p., <https://doi.org/10.3133/fs20173010>

White, V.E., and Prakken, L.B., 2016, Water resources of St. Helena Parish, Louisiana: U.S. Geological Survey Fact Sheet 2016-3047, 6 p., <http://dx.doi.org/10.3133/fs20163047>

White, V.E., and Prakken, L.B., 2017, Water resources of Calcasieu Parish, Louisiana: U.S. Geological Survey Fact Sheet 2016-3066, 6 p., <http://dx.doi.org/10.3133/fs20163066>.

Williams S., Carlsen T., Constable K., Guldahl A., 2009, Identification and qualification of shale annular barriers using wireline logs

Wood, D. H. and Guerva, E. H., 1981, Regional Structural cross sections and general stratigraphy, East Texas basin: University of Texas at Austin, Bureau of Economic Geology, 21 p.

Woolf, K. S., 2012, Regional Character of the Lower Tuscaloosa Formation Depositional Systems and Trends in Reservoir Quality, Dissertations, University of Texas at Austin

Yuma Energy, 2014 <https://www.slideshare.net/Companyspotlight/yuma-energy-inc-october-2014-corporate-presentation>.

Zhang, J. and Roegiers, J. C., 2010, Integrating borehole-breakout dimensions, strength criteria and leak-off test results, to constrain the state of stress across the Chelungpu Fault, Taiwan. *Tectonophysics*, 24921-4, p. 295-8.

Zoback, M.L. and Zoback, M., 1980, States of Stress in the Conterminous United States. *Journal of Geophysical Research*, v. 85, no. B11, 6113-6156 pp.

